Bit Error Rate Performance of Wireless CDMA Communications Systems: with and without Filters

A Thesis Submitted to the College of
Graduate Studies and Research
in Partial Fulfillment of the Requirements
for the Degree of
Master of Science
in the Department of Electrical Engineering
University of Saskatchewan
Saskatoon, Saskatchewan, Canada

by

Abdulfattah M. Shamiss

June 1998

Permission To Use

In presenting this thesis in partial fulfilment of the requirements for a Master of Science degree from the University of Saskatchewan, I agree that the libraries of this University may make it freely available for inspection. I further agree that permission for copying of this thesis in any manner, in whole or in part for scholarly purpose may be granted by professor who supervised this thesis work or, in his absence, by the Head of Department or the Dean of the College in which this thesis work was done. It is understood that any copying or publication or use of this thesis or parts therefor for financial gain shall not be allowed without my written permission. It is also understood that due to recognition shall be given to me and to the University of Saskatchewan in any scholarly use which may be made of any material in this thesis.

Request for permission to copy or to make other use material in this thesis in whole or part should be addressed to:

Head of the Department of Electrical Engineering,
University of Saskatchewan,
saskatoon, Saskatchewan,
Canada, S7N 0W0.

Abstract

Code-division multiple- access (CDMA) implemented with direct-sequence spread spectrum (DS/SS) signaling is expected to play a key role in the wireless telecommunications services such as personal communications, mobile telephony, and wireless networks. To gain insight and understanding of DS/CDMA system performance without actually building it first requires both analysis and simulations. In this thesis, DS/CDMA system performance analysis and simulations are addressed.

Calculating the bit error probability for DS/CDMA systems is analytically difficult and computationally intensive. A simple and accurate approximation technique is applied to the calculation of DS/CDMA bit error probability under the assumption of infinite RF bandwidth. The bit error probability, expressed as a real function of a random variable, is simplified by using a technique that expands the function in Taylor series. As well, an architecture for DS/CDMA system with filters is developed and its performance measures, signal to noise ratio (SNR) and bit error rate (BER), are analyzed. This analysis investigates the effect of filtering on the performance of DS/CDMA systems using correlator receiver. Computer simulations of the system are also performed in this thesis.

Simulation results of BER show a reasonable agreement with the BER obtained from analysis. This agreement justifies the approximation used in the analysis. It is also concluded from the simulations that filters with a bandwidth equivalent to twice the data rate provide a good BER results for a DS/CDMA system compared to the BER performance of DS/CDMA system without filters (in which an infinite bandwidth is assumed).

Acknowledgments

I express my sincere gratitude and appreciation to my research supervisor Professor Surinder Kumar for his supervision, guidance, and constant encouragement during the course of this work. His invaluable advice and kind assistance in the preparation of this thesis is gratefully acknowledged. Thanks are due to Professor J. Eric Salt for his assistance and useful suggestions. I am also grateful to all faculty members that I have come in contact with during my course work at University of Saskatchewan for the knowledge I have acquired from them.

I am indebted to my parents and wife for their encouragement, the many sacrifices they made, and moral support during the period of this research work. I also wish to thank my fellow graduate students for their discussion, suggestions, and assistance. Particular thanks are due to F. Djoemadi, N. S. Sandhu, and B. Abolhassani.

I gratefully acknowledge the financial and moral support provided by Waha Oil Company and I thank the staff of Umm Al-Jawaby Oil Services Co. Ltd. for their continuos assistance during my stay in Canada. Finally, I wish to thank the management and staff of Telecommunication Research Labs, Saskatoon, Canada, for allowing me to use their computer facilities.

Table of Contents

Dedication

This thesis is dedicated to my wife and my parents for their patience, support, and kindness, and also to my children, Ahmed and Arwa.

List of Tables

List of Figures

List of Abbreviations

AMPS	Advanced Mobile Phone Services
AWGN	Additive White Gaussian Noise
BER	Bit Error Rate
BLFSR	Binary Linear Feedback Shift Register
BPSK	Binary Phase Shift Keying
BW	Bandwidth
bps	Bit Per Second
CDMA	Code Division Multiple Access
DPSK	Differential Phase Shift Keying
DS	Direct Sequence
FDMA	Frequency Division Multiple Access
FH	Frequency Hopping
FIR	Finite Impulse Response
FM	Frequency Modulation
GMSK	Gaussian Minimum Shift Keying
Hz	Hertz
IGA	Improved Gaussian Approximation
IIR	Infinite Impulse Response
IS	Interim Standard
ISI	Intersymbol Interference
MA	Multiple Access
MAI	Multiple Access Interference
MHz	Mega Hertz
MLSRS	Maximal Length Shift Register Sequence
MSK	Minimum Shift Keying
PG	Processing Gain
PN	Pseodo-Noise
PSD	Power Spectral Density
QPSK	Quadrature Phase Shift Keying
RF	Radio Frequency
Rx	Receiver

SGA	Standard Gaussian Approximation
SNR	Signal to Noise Ratio
SS	Spread Spectrum
TDMA	Time Division Multiple Access
TIA	Telecommunication Industry Association
Tx	Transmitter
XOR	Exclusive-OR

1. Introduction

1.1 Background

Wireless communications are widely used around the world as a convenient means for accessing telecommunications networks. Over the last decade, the annual increase of cellular subscribers in the world has averaged about 40 percent [1]. In some countries, more than 25 percent of population use mobile communications [2]. According to the current market trends and available forecasts, there will be more than 590 million subscribers worldwide by the end of year 2001 [1]. The ultimate goal of wireless communication is to allow a user access to the capabilities of the global network at any time without regard to location or mobility.

According to the current popularity of cellular telecommunications services, it is apparent that there will be a greater demand in the future for wireless communications. To satisfy the increased need for wireless communications, more bandwidth will be required for wireless communication services. However, bandwidth is a limited natural resource, and hence, it has to be shared properly and used efficiently. The efficient use of the spectrum is the obligation of communications system designers and represents a great challenge since no single solution is appropriate for all applications .

Digital modulation approach (these are classified as second generation wireless communications systems) is one of the solutions for offering lower power consumption, smaller, and light-weight equipment compared to analog systems (first generation of wireless communications systems). The other most outstanding design decision is the choice of a Multiple Access (MA) schemes. Multiple access schemes allow many users to share simultaneously a finite amount of radio spectrum. The sharing of spectrum is required

to achieve high capacity by simultaneously allocating the available bandwidth (or available amount of channels) to multiple users. For high quality communications, this must be done without severe degradation in the performance of the system [3].

1.2 Multiple Access Schemes

Wireless multiple access schemes may be broadly classified into three categories:

- **Frequency Division Multiple Access (FDMA):** In FDMA, an individual channels are assigned to individual users. Each user is allocated a unique frequency band or channel. These channels are assigned on demand to users who request service. While a channel is being used, no other user can share the same frequency band. Advanced Mobile Phone Service (AMPS), the first generation of mobile radio services, is an example of a system that employs FDMA.

- **Time Division Multiple Access (TDMA):** TDMA systems divide the radio spectrum into time slots, and in each slot only one user is allowed to either transmit or receive. Each user occupies a cyclically repeating time slot, so a channel may be thought of as particular time slot that reoccurs every frame, where N time slots form a frame [3]. TDMA systems transmit data in a buffer-and-burst method and the transmission for any user is noncontinuous. This implies that, unlike FDMA systems which accommodate analog FM, digital data and digital modulation must be used with TDMA [2]. The second generation of mobile radio services based on Interim Standard 54 (IS-54) employs TDMA.

- **Code Division Multiple Access (CDMA):** This system is more commonly known as spread spectrum multiple access. In this system all the users are permitted to transmit simultaneously, operate at the same nominal frequency, and use the entire bandwidth [4]. Unique codes are used by

transmitters to spread the information signal over a large frequency range. Receivers use a synchronized version of these codes to de-spread the information signal.

Over the past several years, there has been much interest in application of Code Division Multiple Access (CDMA) in cellular and wireless communications. One of the reasons for interest is its possibility for achieving a greater capacity per unit bandwidth than other multiple access schemes (TDMA and FDMA) [5].That is because CDMA capacity is only interference limited (unlike FDMA and TDMA capacities which are primarily bandwidth limited), and thus any reduction in interference converts directly and linearly into an increase in capacity. The choice of CDMA is attractive because of potential capacity increase, low power requirement, privacy, and the capability to avoid multipath fading [6]. Recently, the Telecommunication Industry Association (TIA) developed a standard, IS-95, for mobile cellular spread spectrum communication systems based on CDMA technology [7].

1.3 Spread Spectrum (SS) Technique

Spread Spectrum is defined as a communication technique in which the intended signal is spread over a bandwidth in excess of the minimum bandwidth required to transmit the signal [4]. The spreading is achieved by means of a code which is independent of data. At the receiver, a synchronized reception with this code is performed for de-spreading and subsequent data recovery [8].

Spread Spectrum signals are designed to provide negligible interference to other users. In this modulation technique, a spread spectrum receiver spreads the spectrum of the interfering signal and hence reduces the interference so that it does not noticeably degrade system performance. However, if more than a given number of users access the channel simultaneously, the noise level and the error rate increases. Signals from other simultaneous users of the channel appear as an additive interference, known as Multiple Access Interference (MAI). The level of this interference varies depending on the number

of users at any given time.

There are primarily two spread spectrum techniques: Direct Sequence (DS) and Frequency Hopping (FH). Direct Sequence is also called Code Division Multiple Access (CDMA). In a DS, an information bearing signal is modulated by a very high frequency spreading waveform or spreading code. The spreading code is a Pseudo Noise (PN) sequence having the value ±1 during a duration of time interval T_c. Each pulse of duration T_c is called a chip; therefore, $1/T_c$ is the chip rate. This spreading code is pseudo-random because the receiver in a practical SS system needs a time synchronized replica of the spreading code used at the transmitter, which is impossible with truly random spreading codes. Therefore, the spreading code is really periodic and deterministically generated to have randomness properties. However, for simplicity, analysis usually assume that the spreading code is truly random [9]. The FH technique allows the information signal band to "hop" over a very wide range of frequencies. This is accomplished by changing the carrier frequency once each T_h seconds. The carrier frequency used each T_h seconds is chosen pseudo-randomly from a specified set of frequencies. This pseudo-random hopping pattern service the same purpose as the spreading code in the DS case [9].

DS/CDMA performance is best assessed from field trials and measurements of actual systems. However, to gain insights of system performance without actually building it first requires both analysis and simulation. Therefore, analysis and simulation of the performance measures of a DS/CDMA system are considered in this thesis.

The calculation of the data bit error probability (Bit-Error-Rate, or BER) for DS/CDMA has in the past been analytically difficult and computationally intensive. Therefore, an approximation approach must be used to calculate the data bit error probability. The Standard Gaussian Approximation (SGA) is one of the earliest and simplest approximations for DS/CDMA bit error probability. In the SGA, the MAI due to other users is handled as Additive White Gaussian Noise (AWGN) and then the probability of error is easily computed as a function of the signal-to-noise ratio (SNR). The SGA is inaccurate for small numbers of simultaneous users of the channel because of the

inapplicability of the central limit theorem (on which the SGA is based) for this case [9]. Another method, results from further analysis of the SGA, was derived for the bit error probability. This approximation is the Improved Gaussian Approximation (IGA). The difference between standard Gaussian approximation and the improved Gaussian approximation is in the distribution function of the MAI. In the standard Gaussian approximation the MAI is assumed to have unconditional Gaussian distribution whereas in the improved Gaussian approximation MAI is assumed to have a conditionally Gaussian approximation [8].

An analysis of bit error probability of Binary Phase Shift Keying (BPSK) DS/CDMA in a single path channel has been presented by Simpson [9]. In Simpson's Dissertation, an accurate and simplified method to assess the bit error probability for DS/CDMA has been given. The bit error probability, expressed as a real function of a random variable, is simplified by using a technique that expands the function in Taylor series. The first and second moments of the random variable, instead of the probability density function, are the only parameters that required in this technique. A simulation verification of this analysis is addressed in this thesis.

1.4 Filtering

Virtually every communication system includes filters for the purpose of saving a spectrum or separating an information signal from unwanted signals such as interference, noise, and distortion products. In practical wireless systems, the presence of a transmitter filter is essential to shape the in-band portion of the spectrum in order to reduce the interference and save spectrum as much as possible. The purpose of a receiver filter is to reject the out-of-band spectrum for the benefit of increasing the signal-to-noise ratio (SNR). One of the objectives of this thesis is to consider the effects of filters on the performance of DS/CDMA systems.

1.5 Thesis Objectives

A considerable literature can be found on the performance measures of DS/CDMA communication systems [9, 22, 24, 27] and [30]. Pursley in [24] presented an analysis of a phase-coded CDMA communication system in a single path channel. A simple and accurate computational approximation for DS/CDMA data bit error probability, under the assumption of infinite RF bandwidth, has been derived in [9]. The effects of filtering on the performance of DS/CDMA systems have also been considered in [30]. The objectives of this thesis are the following:

1. Simulate a Binary Phase Shift Keying (BPSK) DS/CDMA communication system in a wireless channel, using Monte-Carlo method, for verifying the BER performance analyzed in [9].

2. Analyze the effect of filtering on the performance of BPSK modulation in DS spread spectrum using a correlator receiver. The system performance measures, in this analysis, are the signal-to-noise ratio (SNR) and the bit error probability (or BER).

3. Develop simulation programs using Monte-Carlo method to evaluate BER performance of DS/CDMA receiver, including filters, for investigating the effect of filters on the BER performance.

1.6 Thesis Organization

This thesis consists of six chapters, including this introductory chapter. The second chapter describes Code Division Multiple Access (CDMA) communication system. System model is described in order to introduce the related parameters. In the third chapter, the performance of BPSK DS/CDMA communications system is discussed. Then some practical filter types are described in chapter four. This is followed by performance measure analysis of BPSK DS/CDMA systems in the presence of filters. Chapter five provides the BER performance simulation results of the BPSK DS/CDMA communication

system (with and without filters). A results discussion is also presented in chapter five. Finally, conclusions and directions for future work are given in chapter six.

2. Code Division Multiple Access Systems (CDMA)

2.1 Introduction

As mentioned in chapter one, CDMA is a promising multiplexing technique for wireless communications. In this chapter, digital modulation and spread spectrum concepts are briefly discussed. This discussion is followed by an explanation of spreading codes used for DS/CDMA and their correlation properties. Finally, DS/CDMA system model and correlator receiver are also considered.

2.2 Digital Modulation Techniques

Digital modulation is the process by which digital symbols are transformed into signal waveforms that are compatible with the characteristic of the channel. In the case of baseband modulation, these waveforms are pulses. In the case of bandpass modulation, the information signal modulates a sinusoidal signal waveform called a carrier [8].

Digital modulation techniques may be broadly classified as linear and non-linear [3]. In linear modulation techniques, the amplitude of transmitted signal varies linearly with the modulating digital signal (the information signal). Binary Phase Shift Keying (BPSK), Differential Phase Shift Keying (DPSK), and Quadrature Phase Shift Keying (QPSK) are examples of linear modulation techniques. In contrast, the amplitude of the carrier in non-linear modulation techniques is constant regardless of the variation in the modulating signals. Minimum Shift Keying (MSK) and Gaussian Minimum Shift Keying (GMSK) are examples of non-linear modulation techniques. Linear modulation techniques are bandwidth efficient and hence are very attractive for use in wireless communications systems where there is an increasing demand to accommodate more users within a limited spectrum [3].

Two types of digital modulation techniques that are relevant to the DS/CDMA system study in this thesis are Spread Spectrum (SS) modulation and Binary Phase Shift Keying (BPSK) modulation. Next subsection is about BPSK. SS modulation is considered in section 2.3.

2.2.1 Binary Phase Shift Keying (BPSK)

Binary phase shift keying is the simplest modulation scheme for wireless communication systems. A BPSK carrier signal can be expressed as [10]

$$\begin{aligned} S_T(t) &= A\cos(2\pi f_o t+\theta_D(t)) \\ &= A\cos(\theta_D(t))\cos(2\pi f_o t)-A\sin(\theta_D(t))\sin(2\pi f_o t) \\ &= u_I(t)\cos(2\pi f_o t)-u_Q(t)\sin(2\pi f_o t), \end{aligned} \tag{2.1}$$

where A is the amplitude of the modulated signal, f_o is the carrier frequency, $\theta_D(t)$ is the phase, and

$$\begin{aligned} u_I(t) &= A\cos(\theta_D(t)) \\ u_Q(t) &= A\sin(\theta_D(t)). \end{aligned} \tag{2.2}$$

The carrier phase $\theta_D(t)$ is modulated according to the digital source bit as $\theta_D(t)=0$ when the digital source bit is 1, and $\theta_D(t)=\pi$ when the digital source bit is 0. Thus for a binary bit of duration T, the BPSK modulated carrier signal, $S_T(t)$, can be simplified as

$$S_T(t)=u_I(t)\cos(2\pi f_o t) \tag{2.3}$$

for $0\le t\le T$ (Notice $u_Q(t)$ is always 0 in the case of BPSK).

In the BPSK modulator, $u_I(t)=1$ corresponds to $\theta_D(t)=0$ and $u_I(t)=-1$ corresponds to $\theta_D(t)=\pi$, and $\theta_D(t)$ is changed every T second (assuming that the digital source bit is

transmitted every T second). Figure 2.1 shows a typical BPSK waveform with its abrupt phase changes at bit transitions. This figure illustrated the situation when the modulating data stream is 1001 with bit duration T. At the receiver the signal arrives with an arbitrary initial phase. A receiver known as coherent receiver when the phase of the RF carrier is recovered and then used for the detection process, while the process is referred to as non-coherent detection if the receiver does not utilize such phase information.

2.3 Spread Spectrum (SS) Modulation Technique

Spread spectrum modulation has become an increasingly popular technique in communication systems over the years. The initial application of the SS technique was in military guidance communication systems. The concept of SS was first documented in the late 1940s and early 1950s by Rogoff [11] in terms of a transmission of signals using noise-like waveforms experiments. The experiments successfully demonstrated the possibility of conveying information hidden in noise-like signals. This idea was then applied into the development of SS communication systems around 1955 [12]. Recently, some of the potential of SS in commercial applications, such as mobile and indoor communications, has been realized [13,14].

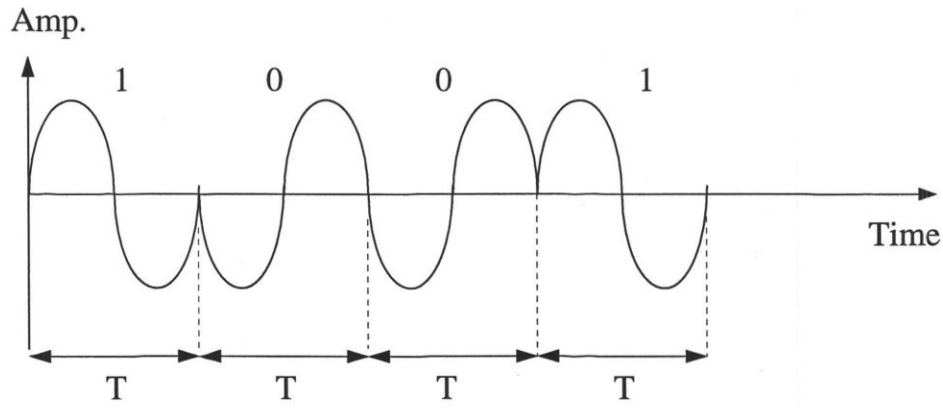

Figure 2.1 Binary Phase Shift Keying (BPSK) modulation

As stated in chapter one, spread spectrum techniques employ a transmission bandwidth that is several orders of magnitude greater than the minimum required signal bandwidth. This is illustrated in figure 2.2. The ratio W_{ss} / B is called the processing gain and typically 10-30 dB [15]. Although this system is very bandwidth inefficient for a single user, the advantage of spread spectrum is that many users can simultaneously use the same bandwidth without significantly interfering with one another. In other words, if different users employ different codes to spread the information signal, spread signals from all these users can co-exist in the same bandwidth (this technique is referred to as Code Division Multiple Access (CDMA)). In a multiple user, multiple access interference (MAI) environment, spread spectrum systems become very bandwidth efficient [3]. Apart from occupying a very large bandwidth, spread spectrum signals are pseudorandom and have noise-like properties when compared with the digital information data. In SS, the spreading

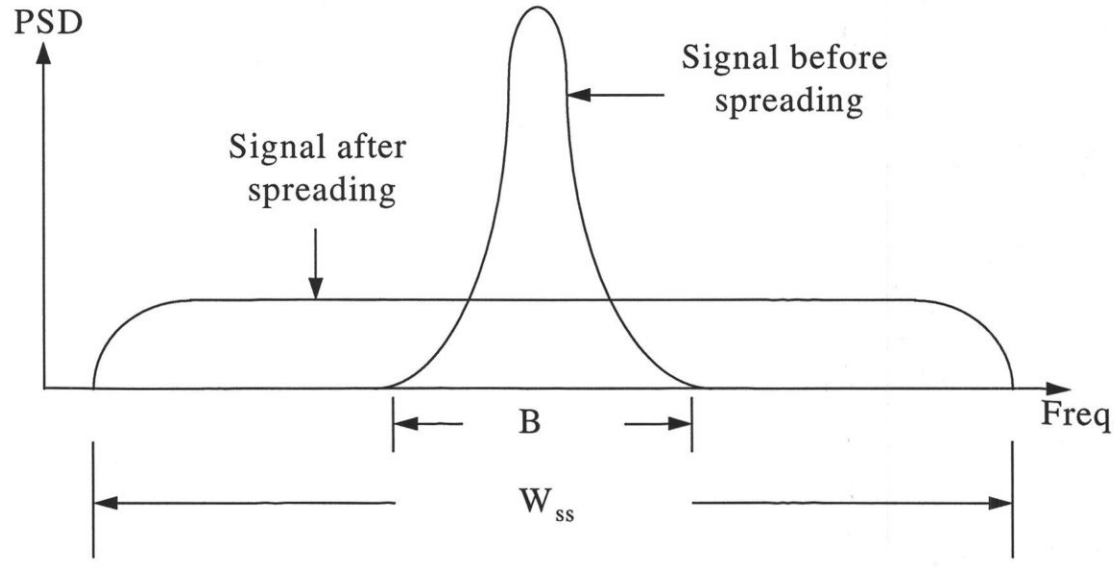

Figure 2.2 Spectra of signal before and after spreading.

waveform is controlled by a pseudo-noise (PN) sequence or pseudo-noise code (this will be explained in more detail in section 2.4), which is a binary sequence that appears random but can be reproduced in a deterministic manner by intended receivers. At the receiver, spread spectrum signals are demodulated through crosscorrelation with a locally-generated version of the pseudorandom carrier. Crosscorelation with the correct PN sequence de-spreads the spread spectrum signal and restores the modulated message in the same narrow band as the original data, whereas cross-correlating the signal from an undesired user results in a very small amount of wide-band noise at the receiver output [3].

The most important advantage, that makes SS well-suited for use in wireless communications environment, is its inherent interference rejection capability. This is based on the fact that the receiver can separate each user based on their approximate orthogonal codes, even though they occupy the same spectrum at all times. This implies that, up to a certain number of users, interference between spread spectrum signals using the same frequency is negligible.

2.3.1 Direct-Sequence Spread Spectrum (DS/SS)

A direct sequence spread spectrum (DS-SS) system spreads the bipolar information signal $b(t)$ by directly multiplying the information signal bits with a bipolar pseudo-noise (PN) spreading code, $a(t)$. The code sequence waveform, $a(t)$, may be thought of as being pseudorandomly generated so that the sequence can change (with probability of 0.5) every T_c seconds, where T_c is the code chip duration. Figure 2.3 shows time waveforms involved in generating direct sequence signal. In a typical DS-SS, the spreading operation is followed by BPSK carrier modulation resulting in the transmitted signal given by [3]

$$S_{ss}(t)=\sqrt{2P}\ b(t)a(t)\cos(2\pi f_o t+\theta), \qquad (2.4)$$

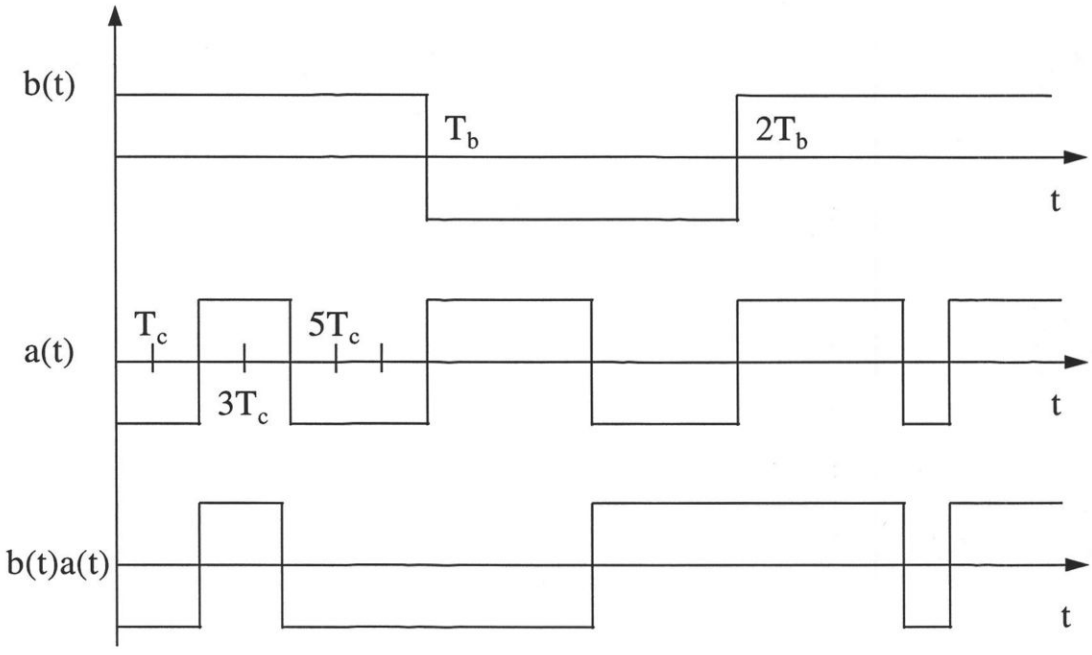

Figure 2.3 Direct sequence spread spectrum signal

where P is the power of the carrier signal, f_o is the carrier frequency, and θ is the carrier phase angle at t=0. This process is illustrated in Figure 2.4. The bandwidth of the transmitted signal $S_{ss}(t)$ is much larger than the minimum bandwidth required to transmit the information signal $b(t)$ (assuming that the bandwidth of the spreading signal $a(t)$ is much larger than the bandwidth of $b(t)$). The processing gain (PG) in a direct sequence spread spectrum is expressed as the ratio of the bandwidth of the spread spectrum waveform to that of the data; i.e [16]

$$PG = \frac{W_{ss}}{B} = \frac{T_b}{T_c} = N, \tag{2.5}$$

where, W_{ss} is the bandwidth in Hertz of the spread spectrum signal, B is the minimum

bandwidth that would be required to send the information signal if one did not use spread spectrum modulation technique, T_b is the data bit duration, T_c is the chip duration, and N is the number of chips per one data bit.

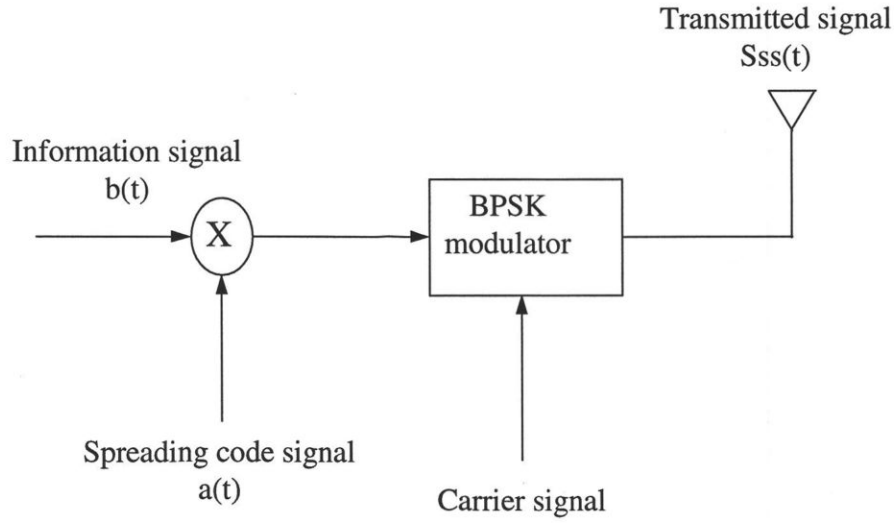

Figure 2.4 Simplified block diagram of DS-SS transmitter

The received signal of a DS-SS contains the desired signal, the interference caused by co-users in the system, and the white Gaussian noise. With a transmission delay of t_d, the received signal can be written as [8]

$$r(t) = A\sqrt{2P}\ b(t-t_d)a(t-t_d)\cos[2\pi f_o(t-t_d)+\psi] + \textit{interference} + n(t), \qquad (2.6)$$

where A represents the attenuation in the channel, and $n(t)$ represents the white Gaussian noise. Assuming that code synchronization has been achieved at the receiver, the received signal is multiplied by a carrier $\cos(2\pi f_o t+\varphi)$, where φ is an estimate of $t_d+\psi$. It is then filtered and de-spread by correlating with a replica of the spreading code $a(t-\hat{t}_d)$, where $\hat{t}_d$

is an estimate of t_d . Figure 2.5 illustrates this process. De-spreading also results in separation of the desired signal from other user signals. The de-spreading operation is then followed by BPSK data demodulation. The output signal is equal to $A\{[2P]^{1/2}\}\ b(t-t_d)$, the transmitted information signal with a scaling factor (assume that $\hat{t}_d = t_d$ and $\varphi=t_d+\psi$).

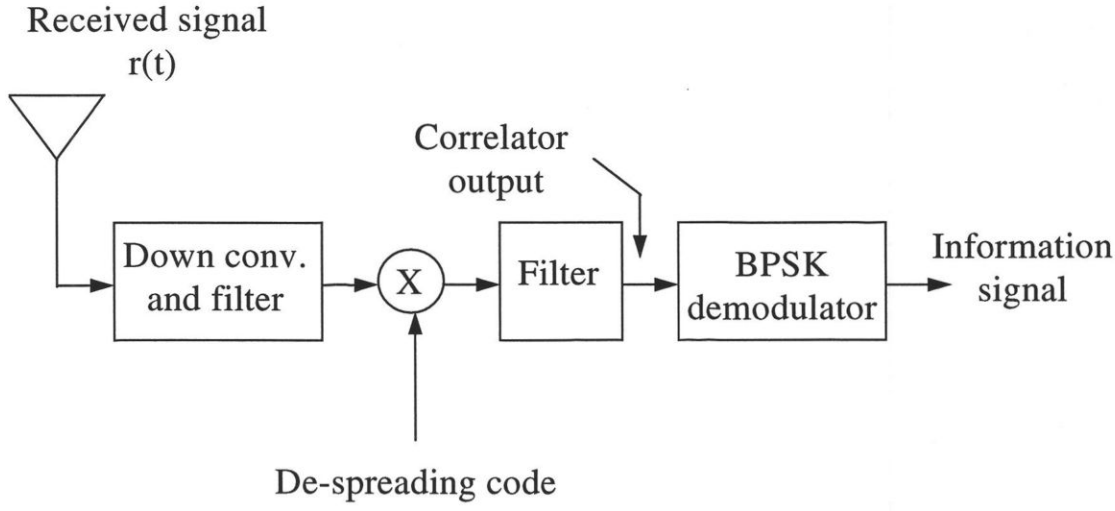

Figure 2.5 A simplified block diagram of DS-SS receiver

2.3.2 Code Division Multiple Access (CDMA)

Resource-sharing can be a very efficient way of achieving high capacity in any communication network. As far as wireless communication systems are concerned, the resource is the bandwidth. As mentioned in the introductory chapter, frequency division multiple access (FDMA), time division multiple access (TDMA), and code division multiple access (CDMA) are the three major access techniques used to share the available bandwidth in a wireless communication systems.

CDMA is a multiple technique that exploits the properties of Spread Spectrum (SS) modulation to allow more than one user to simultaneously share a common channel bandwidth. In CDMA systems, the narrowband message signal is multiplied by a very large

bandwidth signal called the spreading signal or spreading code. As seen from Figure 2.6 [3], the same carrier frequency, in a CDMA system, can be used by all users and hence they may transmit simultaneously. The simultaneous transmission is possible because each user has its own pseudorandom codeword which is approximately orthogonal to all other codewords. All other codewords appear as noise due to de-correlation. The cumulative interference of all the non-referenced users on the reference user is referred to as the multiple access interference (MAI). In order to detect the message signal, the receiver needs to know the codeword used by the transmitter. Each user operates independently with no knowledge of the other users.

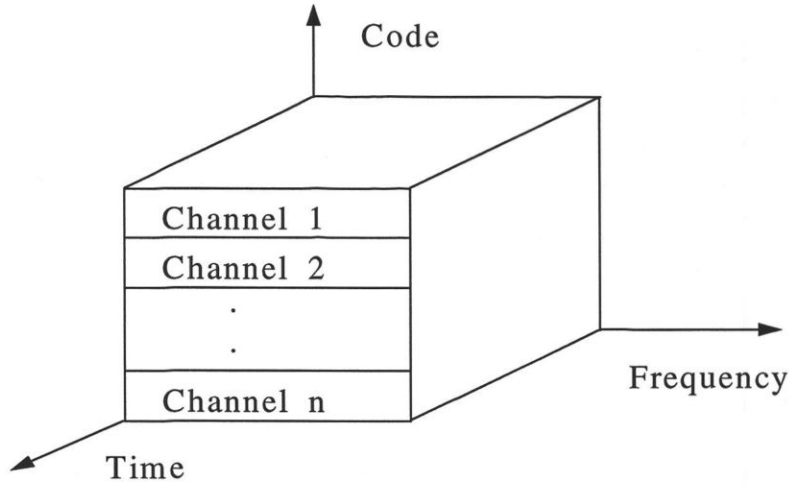

Figure 2.6 CDMA in which each channel is assigned a unique PN code

A CDMA system configuration is shown in Figure 2.7 [9]. An attractive feature of CDMA is that, unlike TDMA or FDMA, CDMA has a soft capacity limit. Increasing the number of users in a CDMA system raises the noise floor in a linear manner. Thus, there is no absolute limit on the number of users in CDMA. Rather, the system performance gradually degrades for all users as the number of users is increased and improves as the number of users is decreased. Accordingly, the system can tolerate significant amounts of

overload if users are willing to tolerate poorer performance. Another feature of CDMA is the capability of rejecting an external interference. A multipath nature of the channel, other users, or jamming signals may cause this interference.

An important concern in CDMA is the number of users that can be accommodated simultaneously. This is dependent on the cross-correlation properties (degree of orthogonality) of the PN codes used by different users for spreading their information signal bandwidth. In the next section, more information about PN codes is presented to bring out the importance of this aspect of CDMA systems.

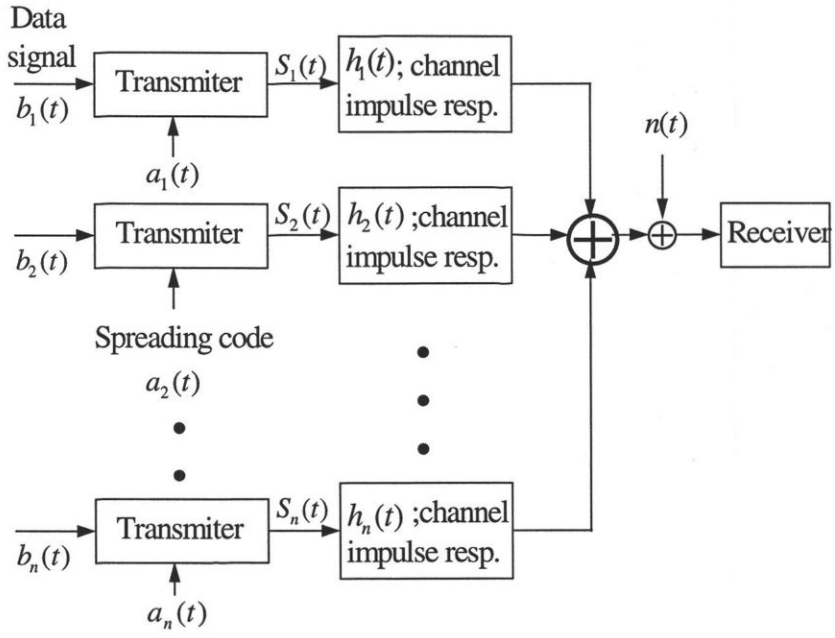

Figure 2.7 CDMA system with direct sequence spread spectrum

2.4 Codes for Spectrum Spreading

The key part of any spread spectrum system is the spreading sequences needed to spread and de-spread the information signal. Purely random sequences are ideal in spread

spectrum modulation to spread the signal spectrum. Unfortunately, in order to de-spread the signal, the receiver needs a replica of the transmitted sequence. In practice, therefore, there is a need for signals which are deterministic and have statistical properties of white noise which are purely random. These deterministic signals are usually a binary sequence generated with shift registers. In the case of CDMA communication system, a set of a group of binary sequences or spreading codes is needed. For efficient operation, this binary sequences are required to satisfy the following properties [16, 8]:

1. Easy to generate.
2. The sequence is periodic. The period depends on system requirements.
3. The sequences are difficult to reconstruct from a short segment.
4. Each sequence in the set is easy to distinguish from a time shifted version of itself and from every other spreading code in the set.

Property (4) reflects two important properties of the code sequences: autocorrelation function and cross-correlation function which both are of interest in communication system design. To explain these two functions, let $f(t)$ and $g(t)$ be two different sequence signals of period $T = NT_c$, where N is the number of chips per period, and T_c is one chip duration. Autocorrelation function, in general, is defined as the integral [17]

$$\theta_{ff}(\tau)=\frac{1}{T}\int_0^T f(t)f(t-\tau)dt, \tag{2.7}$$

where τ is a time interval $\in(0,T)$. This function is a measure of the similarity between a sequence and a phase-shifted replica of itself. Cross-correlation is the measure of similarity between two different code sequences. The only difference between auto-correlation and cross-correlation is that in autocorrelation a different term is substituted for the general integral. Cross-correlation function is defined as [17]

$$\theta_{f,g}(\tau)=\frac{1}{T}\int_{0}^{T} f(t)g(t-\tau)dt. \qquad (2.8)$$

For periodic sequences, autocorrelation and cross-correlation functions are also periodic.

The most well known class of code sequences is called Maximal Length Shift Register Sequences (MLSRS) or m-sequences. "Maximal length codes are, by definition, the longest codes that can be generated by a given shift register or a delay element of a given length." These basic sequences are discussed in the next subsection. Another type of code sequences, known as Gold code and can be generated by a combination of maximal sequences, is discussed in subsection 2.4.2.

2.4.1 M-Sequences

M-sequences are generated by using Binary Linear Feedback Shift Register (BLFSR). A shift register sequence generator consists of a shift register working in conjunction with appropriate logic, which feeds back a logical combination of the state of two or more of its stages to its input. The output of a sequence generator, and the contents of its n stages at any sample (clock) time, is a function of the outputs of the stages fed back at the preceding sample time. For an n-stage linear feedback shift register sequence the m-sequence has a repetition period (maximum sequence length) of $N = 2^n-1$, where n is equal to the length of the shift register and corresponds to primitive polynomials degree . Primitive polynomials of degree n exist for every n.

Figure 2.8 is an example of a m-sequence generator which uses a 5-bit shift register. The generator shown is called a (3,5) generator, which means feedback taps are taken after the third and fifth stages. The rate of the m-sequence is determine by a stream of clock pulses where each code symbol (chip) interval, T_c, is equivalent to the clock period. The content in each stage of the register shifts one stage to the right every time the generator

clocks. Furthermore, the contents of stages 3 and 5 are modulo-2 added, and the result is fed back to the input of stage 1. The m-sequence, in this example, is taken from the output of the last stage and is shown in Figure 2.9 [12]. Although, the sequence has a random appearance, it repeats after a period of 31 chips and hence its a maximum length is (2^5-1).

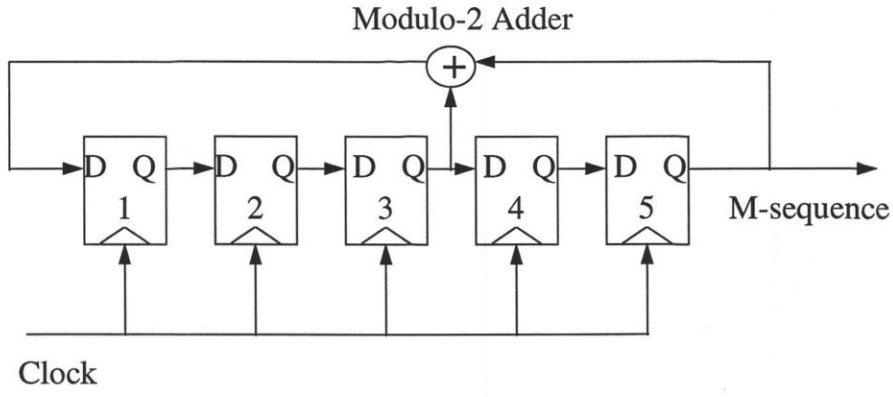

Figure 2.8 M-sequence generator (n = 5).

When the length of a m-sequence is less than 2^5-1 the sequence is classified as a non-maximal length sequence.

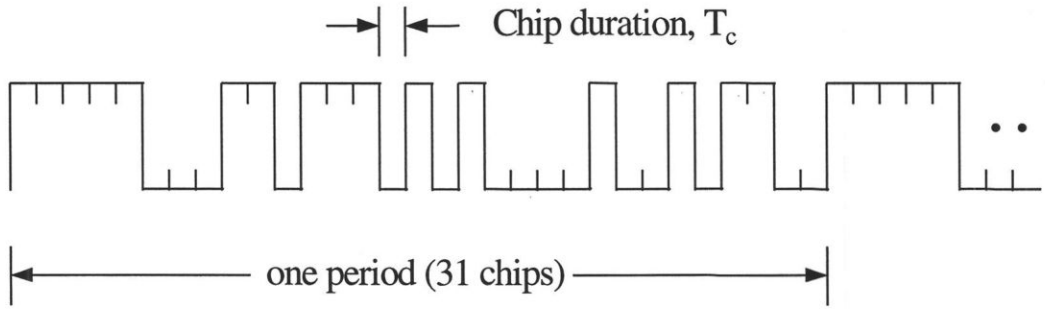

Figure 2.9 Maximum length m-sequence

If one has a maximum length sequence, then this sequence will have basic randomness properties. Properties 1, 2, and 3 of the following are very useful in their application to spread spectrum systems [17, 18].

1. *Balance property*: The number of ones "1" in a sequence equals the number of zeros "0" in each period of the sequence (i.e the number of ones = 1/2 $(N+1)$, where N is the length of the sequence).

2. *Run property*: Define a run as a sequence of a single type of binary digits. The appearance of alternate digit in a sequence starts a new run. Then, for any m-sequence, it is desirable that about one-half of the runs of each type (ones or zeros) are of length one, about one-fourth are of length 2, one-eighth are of length 3, and so on.

3. *Correlation property*: If a full period of the sequence is compared chip by chip with any cyclic shift of itself, the number of agreements and disagreements differ by not more than one count.

4. *Shift and add property*: A modulo-2 addition of an m-sequence and a phase-shifted replica of itself results in another replica with a phase shift different from either of the originals.

It should be pointed out here that the usefulness of the m-sequences in spread spectrum communications depends in large part on their correlation properties. In CDMA, cross-correlation properties of code sequences are as important as auto-correlation properties because of cross-correlation properties influence on the degree of Multiple Access Interference (MAI).

To analyze the correlation properties of such m-sequence, it is helpful to define basic concepts. Since all of the spreading codes to be discussed are periodic sequences of ones and zeros with period N, the output sequences may be expressed as $a_i = a_{N+i}$ for any i [18]. The spreading waveform $a(t)$ derived from this sequence is periodic with period

$T = NT_c$ and is specified by [18]

$$a(t) = \sum_{i=-\infty}^{+\infty} a_i \, p(t-iT_c), \tag{2.9}$$

where $a_i = \pm 1$ and $p(t)$ is the shaping signal over the duration from 0 to T_c.

The discrete periodic auto-correlation function of a sequence of period N may be written as [18]

$$\theta_a(k) = \frac{1}{N}\sum_{i=0}^{N-1} a_i \, a_{i+k} \, , \tag{2.10}$$

for k=0,±1,±2,±3,..... For an m-sequence the periodic autocorrelation function $\Theta_a(k)$ is two valued and is given by [18]

$$\Theta_a(k) = \begin{cases} 1 & k=iN \\ -1/N & k \neq iN, \end{cases} \tag{2.11}$$

where i is any integer and N is the sequence period. The autocorrelation function of the waveform, $R_a(\tau)$, is given by [18]

$$R_a(\tau) = \left(1 - \frac{\tau_\epsilon}{T_c} \right) \theta_a(k) + \frac{\tau_\epsilon}{T_c} \, \theta_a(k+1), \tag{2.12}$$

where $0 \leq \tau_\epsilon \leq T_c$.

The discrete cross-correlation between two m-sequences a and b can be defined as [18]

$$\theta_{a,b}(k) = \frac{1}{N}\sum_{i=0}^{N-1} a_i \, b_{i+k} \tag{2.13}$$

for k=0,±1,±2,±3,.... Similarly, the continuous cross-correlation function of the waveform, $R_{a,b}(\tau)$, is given by

$$R_{a,b}(\tau) = \left(1-\frac{\tau_\epsilon}{T_c} \right) \theta_{a,b}(k) + \frac{\tau_\epsilon}{T_c} \theta_{a,b}(k+1). \tag{2.14}$$

The periodic cross-correlation function between any pair of m-sequences of the same period can have relatively large peaks [19] (Such high values of cross-correlation are unacceptable in the CDMA systems). That might lead to a possibility of selecting a small subset of m-sequences for a given length of register that have smaller cross-correlation peak values. However, this limited number in the m-sequence set is usually too small for CDMA applications. Sequences used by different users in CDMA should be mutually orthogonal in order to keep the level of multiple access interference (MAI) of system minimum, (i.e the magnitude of the cross-correlation function is minimum).

In 1967, Robert Gold proposed a PN sequences with better periodic cross-correlation properties than the m-sequence [20]. These codes, which referred to as Gold codes, are discussed in the next subsection.

2.4.2 Gold Codes

The Gold codes were invented at the Magnavox Corporation specifically for

multiple- access applications of spread spectrum [18]. They are derived from certain pairs of m-sequences of length $N = 2^n - 1$. These certain pairs of m-sequences exhibit a three valued cross-correlation function with values $\left\{ -\frac{1}{N},\ -\frac{1}{N}t(n),\ \frac{1}{N}[t(n) - 2] \right\}$ where

$$t(n) = \begin{cases} 1 + 2^{(n+1)/2} & \textit{for odd values of } n \\ 1 + 2^{(n+2)/2} & \textit{for even values of } n. \end{cases} \tag{2.15}$$

Such m-sequences are referred to as the preferred sequences.

The Gold codes are generated by a modulo-2 addition of specific relative phases of a preferred pair of m-sequence: **a** and **b** for instance . The preferred pair added chip-by-chip by synchronous clocking. Thus the two code generators maintain the same phase relationship, and the codes generated are the same length as the two base codes which are added together but are non-maximal. A specific example is shown in Figure 2.10 to illustrate Gold code generation. The corresponding preferred pair, in this example, are described by the following polynomials

$$\begin{aligned} h_1(x) &= 1 + x^2 + x^5 && \textit{for the generator } [5,2] \\ h_2(x) &= 1 + x^2 + x^3 + x^4 + x^5 && \textit{for the generator } [5,4,3,2]. \end{aligned} \tag{2.16}$$

In CDMA system, Gold code sequences are more attractive than m-sequence codes. This is because of their low cross-correlation property which result in reducing MUI .

2.5 DS/CDMA System Model

The DS/CDMA system model for asynchronous use of the common channel bandwidth by K users is shown in Figure 2.11. This model was given in [9], and has also been used in [21, 22]. In Figure 2.11, the data signal $b_k(t)$ is a binary sequence of unit amplitude and rectangular pulses of duration T_b that represents the k^{th} user's information sequence. A code waveform, $a_k(t)$, is assigned to the k^{th} user for spreading purposes. This

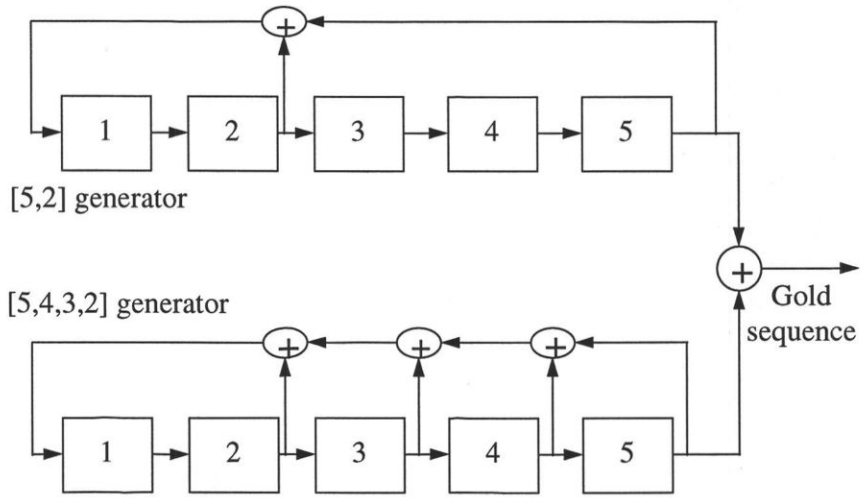

Figure 2.10 Generation of Gold codes of length N=31

code is a periodic sequence (signature sequence) of unit amplitude and rectangular pulses of duration T_c (chips), such that $T_c \ll T_b$. For simplicity, Binary Phase Shift Keying (BPSK) carrier modulation will be considered throughout this thesis.

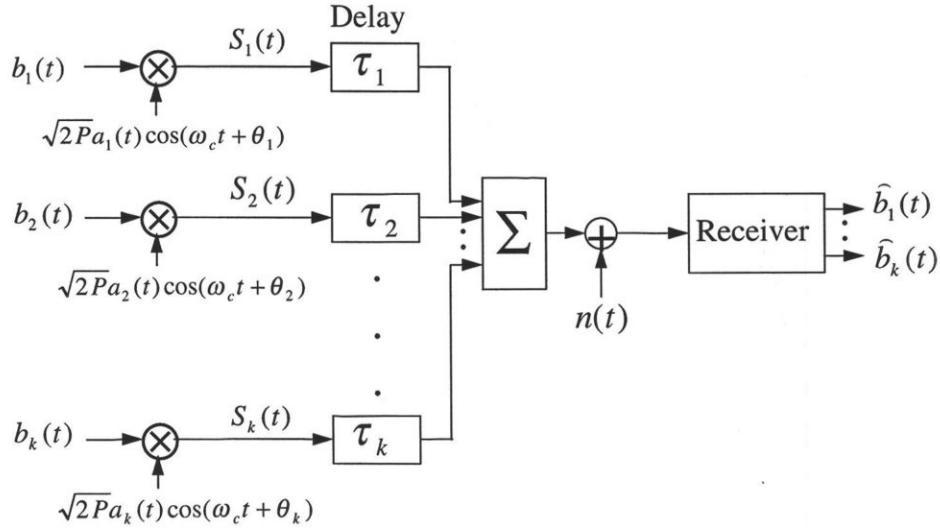

Figure 2.11 A BPSK DS/CDMA system model

The k^{th} transmitted signal for a DS/CDMA system with BPSK modulation and arbitrary spreading waveform can be expressed as [9] (assuming a 1 Ohm system resistance)

$$S_k(t-\tau_k) = \sqrt{2P}\, b_k(t-\tau_k)\, a_k(t-\tau_k) \cos(\omega_o t + \theta_k - \omega_o \tau_k), \tag{2.17}$$

where

$$a_k(t) = \sum_{j=-\infty}^{\infty} a_j^{(k)}\, p_{T_c}(t-jT_c) \tag{2.18}$$

is the spreading waveform, where $a_j^{(k)} \in \{-1, +1\}$ is the j^{th} chip of the k^{th} user's signature sequence, and the rectangular pulse $p_{T_c}(t)$ is given by

$$p_{T_c} = \begin{cases} 1 & for\ 0 \le t \le T_c \\ 0 & otherwise. \end{cases} \tag{2.19}$$

Similarly, the data signal $b_k(t)$ may be written as

$$b_k(t) = \sum_{i=-\infty}^{\infty} b_i^{(k)}\, p_{T_b}(t-iT_b), \tag{2.20}$$

where $b_i^{(k)} \in \{-1, +1\}$ is the i^{th} data bit in the binary information sequence for user k. As stated in [9], the information sequence is modeled as an independent and identically (iid) sequence of random variables $b_i^{(k)}$ with equal probabilities of being +1 or -1. Random signature sequence is also assumed, so that $\{a_j^{(k)},\ 0 \le j \le (N-1),\ where\ N=T_b/T_c\}$ form a set of iid random variables with equal probabilities of being +1, -1.

The rest of the elements of equation (2.17) are defined as

P = The received signal power.

$\omega_c = 2\pi f_c$ is the common carrier radian frequency.

θ_k = The relative (to a reference user) phase of the carrier for the k^{th} user.

τ_k = The k^{th} user's relative time delay that is used to account for propagation delays and asynchronous transmission.

For asynchronous systems the received signal $r(t)$ in Figure 2.11 is given by [9]

$$r(t) = \sum_{k=1}^{K} \sqrt{2P}\ b_k(t-\tau_k)\ a_k(t-\tau_k)\ \cos\ (\omega_o t + \phi_k)\ +\ n(t), \qquad (2.21)$$

where $\phi_k = \theta_k - \omega_c \tau$ and $n(t)$ is the receiver front-end noise modeled as an Additive White Gaussian Noise (AWGN) process with two-sided power spectral density of $N_o/2$ (W/Hz).

In order to reconstruct the original information signal (demodulation process), $r(t)$ is passed through a correlation receiver matched to a reference user signature sequence. The principle of operation of CDMA correlator receiver is described in the next subsection.

2.5.1 Correlator Receiver

The majority of direct sequence spread spectrum systems employ correlator receivers because they are relatively simple to implement. However, this type of receivers is considered as suboptimal in a multiuser environment [23]. A structure of a DS/CDMA correlator receiver is shown in Figure 2.12. As shown in this figure, the received signal $r(t)$ is initially down converted and then de-spread by multiplying it with synchronized transmitter spreading code. Furthermore, the de-spread signal is integrated over a symbol duration to obtain the decision variable to detect the information data. The correlator is aligned with the first or the strongest path signal received. Better performance is obtained by aligning the correlator to the strongest path. This alignment requires a complex multipath tracking circuit.

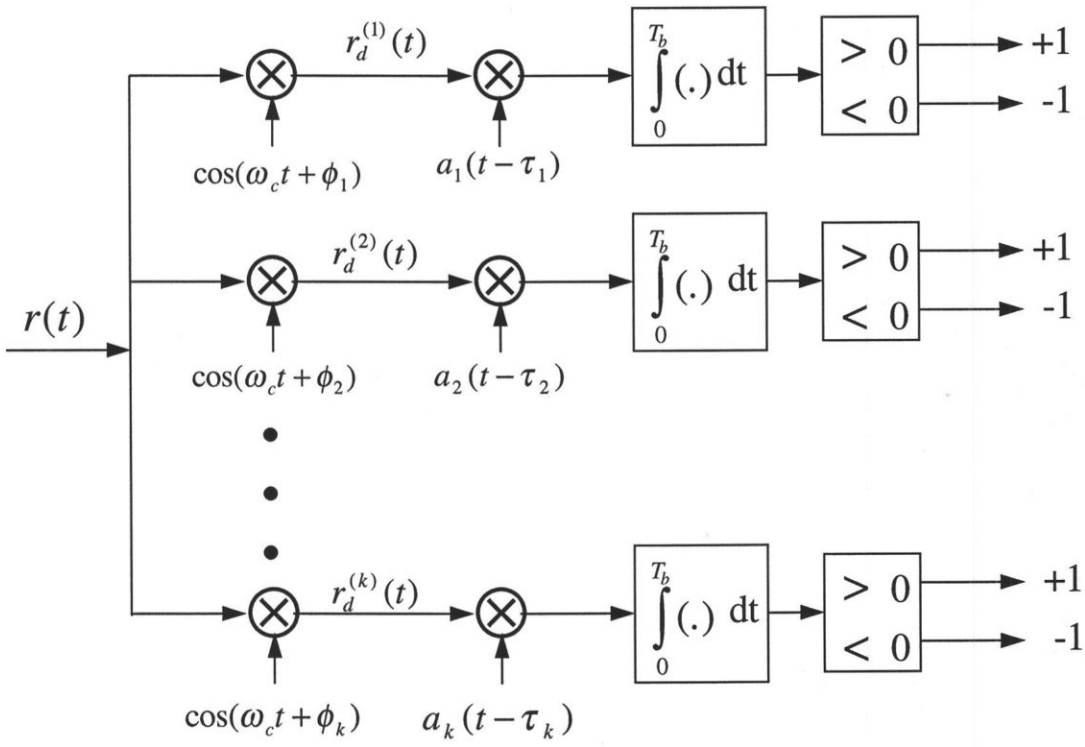

Figure 2.12 Structure of DS/CDMA correlator receiver

3. Performance of BPSK DS/CDMA Communications Systems

3.1 Introduction

In the previous chapter, CDMA wireless communications systems were described. CDMA was shown to hold promise in solving the bandwidth efficiency problem. However, it is observed that co-users signals are a source of interference, which depends on the orthogonality of users' spreading sequences.

The performance of a DS/CDMA communications system can be expressed in terms of the bit error probability (it is also called bit error rate or BER), P_e, or the signal to noise ratio (SNR) of the decision variable. In this chapter, an analysis of a bit error probability for this system is presented. A simple and accurate approximation is used to calculate a bit error probability for the DS/CDMA. The bit error probability, expressed as a real function of a random variable, is simplified by using a technique that expands the function in Taylor series. The technique only requires first and second moments of the random variable, instead of the probability density function.

As mentioned in the introductory chapter, one of the objectives of this thesis is to simulate a BPSK DS/CDMA communications system for verifying the BER performance analysis given in [9]. The analysis reported in this chapter closely follows that in [9].

3.2 Bit Error Probability Analysis

Consider a simple BPSK DS/CDMA communications system shown in Figures 2.11 and 2.12 to compute the performance in the form of the bit error probability. As explained in section 2.5, the k^{th} transmitted signal for a DS/CDMA system with BPSK modulation and arbitrary spreading waveform is of the form [9]

$$S_k(t-\tau_k) = \sqrt{2P}\ b_k(t-\tau_k)\ a_k(t-\tau_k)\ \cos(\omega_o t + \theta_k - \omega_o \tau_k), \tag{3.1}$$

and the received signal $r(t)$ is given by

$$r(t)=\sum_{k=1}^{K} \sqrt{2P}\ b_k(t-\tau_k)\ a_k(t-\tau_k)\ \cos\ (\omega_o t+\phi_k)\ +\ n(t). \tag{3.2}$$

For demodulation, $r(t)$ is passed through a correlator receiver (see Figure 2.12) matched to a reference user signature sequence (user 1 can be assumed as a reference user). Since only the relative delays and phases are of concern, τ_1 and ϕ_1 are assumed to be known (consider them as a reference; $\tau_1=\phi_1=0$), with $0\le\tau_k\le T_b$ and $0\le\phi_k\le 2\pi$ for $k>1$.

The calculation of the bit error probability starts with the equation for the output of a correlation receiver matched to $a_1(t)$ (the reference user) as [9]

$$D_1=\int_0^{T_b} r(t)\ a_1(t)\ \cos(\omega_o t)\ dt. \tag{3.3}$$

Using the fact that the condition $\omega_o \gg T_b^{-1}$ is always satisfied in a practical SS communication system and ignoring the double frequency component in $r(t)\ \cos(\omega_o t)$ yields [21]

$$D_1 = T_b \left(\frac{P}{2}\right)^{1/2} \left[b_0^{(1)} + \sum_{k=2}^{K} I_{k,1}(\underline{b_k}, \tau_k, \phi_k)\right] + \eta, \tag{3.4}$$

where

$$I_{k,1}(\underline{b_k},\ \tau_k,\ \phi_k)=T_b^{-1}[B_{k,1}(\underline{b_k},\ \tau)]\cos(\phi_k)\,, \tag{3.5}$$

and

$$B_{k,1}(\underline{b_k},\ \tau)=b_{-1}^{(k)}R_{k,1}(\tau)+b_0^{(k)}\hat{R}_{k,1}(\tau). \tag{3.6}$$

The random variable η is a Gaussian random variable with zero mean and variance $N_oT_b/4$, where $N_o/2$ is the two-sided spectral density of the white Gaussian noise and T_b is the data bit duration. The vector $\underline{b_k}=(b_{-1}^{(k)},\ b_0^{(k)})$ represents a pair of consecutive data bits for the k[th] signal. The functions $R_{k,m}(\tau)$ and $\hat{R}_{k,m}(\tau)$ are the continuous-time partial cross correlation functions of the k[th] and m[th] spreading waveform defined as [24]

$$R_{k,m}(\tau)=\int_0^{\tau} a_k(t-\tau)\ a_m(t)\ dt, \tag{3.7}$$

$$\hat{R}_{k,m}(\tau)=\int_{\tau}^{T_b} a_k(t-\tau)\ a_m(t)\ dt, \tag{3.8}$$

for $0\le\tau\le T_b$. For $0\le lT_c\le\tau\le(l+1)T_c\le T_b$, these two cross-correlation functions, $R_{k,m}(\tau)$ and $\hat{R}_{k,m}(\tau)$, can be written as [9] (assuming rectangular pulse shape for the chip waveform)

$$R_{k,m}(\tau)\ =\ C_{k,m}(l-N)T_c+\ [C_{k,m}(l+1-N)\ -\ C_{k,m}(l-N)](\tau-lT_c), \tag{3.9}$$

$$\hat{R}_{k,m}(\tau) = C_{k,m}(l)T_c + [C_{k,m}(l+1) - C_{k,m}(l)](\tau - lT_c), \tag{3.10}$$

where $l = \lfloor \tau_k / T_c \rfloor$ and the discrete aperiodic cross-correlation function $C_{k,m}$ for the signature sequences of user k and m is defined as [9]

$$C_{k,m}(l) = \begin{cases} \sum_{j=0}^{N-1-l} a_j^{(k)} a_{j+l}^{(m)} & for\ 0 \le l \le (N-1), \\ \sum_{j=0}^{N-1+l} a_j^{(m)} a_{j-l}^{(k)} & for\ (1-N) \le l < 0, \\ 0 & for\ |l| \ge N, \end{cases} \tag{3.11}$$

when the reference user is considered (i.e., m=1).

Assuming a perfect power control, with all signals at received power P=2, and the referenced data bit $b_o^{(1)} = 1$, the decision statistics for the reference user, normalized with respect to the chip duration $T_c = 1$, is obtained by substituting (3.6) and (3.5) into (3.4) to get [9]

$$D_1 = \zeta + N + \sum_{k=2}^{K} W_k \cos\varphi_k, \tag{3.12}$$

where N is the number of chips per one data bit, ζ is a Gaussian random variable with variance $N(N_o/4)$, $\sum_{k=2}^{K} W_k \cos\varphi_k$ represents MAI, and W_k (see (A.10) in appendix A) is given by

$$W_k = L_k S_k + Q_k(1 - S_k) + X_k + Y_k(1 - 2S_k), \tag{3.13}$$

with $0 \le S_k < T_c = 1$. The kth interfering user has time offset to the nearest chip given by $S_k = \tau_k - lT_c$ (assuming that τ_k is uniformly distributed on $[0, T_b]$ and l is uniformly

distributed on $\{0,1,...,(N-1)\}$) and carrier phase φ_k relative to the desired signal. The random variables L_k and Q_k are uniform on $\{-1,1\}$ and X_k and Y_k have densities [25]

$$\Gamma_{X_k}(i)=\begin{pmatrix} A \\ \frac{i+A}{2} \end{pmatrix} 2^{-A} \; ; \quad i\in\{-A,-A+2,...,A-2,A\} \tag{3.14}$$

and

$$\Gamma_{Y_k}(j)=\begin{pmatrix} B \\ \frac{j+B}{2} \end{pmatrix} 2^{-B} \; ; \quad j\in\{-B,-B+2,...,B-2,B\}. \tag{3.15}$$

The quantities A and B are related to $C=C_{1,1}(1)$, the discrete aperiodic autocorrelation of the signature sequence of receiver 1, offset by one chip, by [25]

$$A=\frac{N-1+C}{2} \tag{3.16}$$

and

$$B=\frac{N-1-C}{2} \; . \tag{3.17}$$

The random variable C may be expressed as [25]

$$C=\sum_{j=0}^{N-2} a_j^{(1)} a_{j+1}^{(1)}, \tag{3.18}$$

where $a_j^{(k)}$ is denoted as the jth chip in the signature sequence of signal k. Equation (3.18) represents the sum of N-1 symmetric Bernoulli random variables, where the density of C

is given by [25]

$$\Gamma_C(j)=\begin{pmatrix} N \\ \frac{j+N-1}{2} \end{pmatrix} 2^{1-N} \; ; \quad j\in\{1-N,3-N,...,N-3,N-1\}. \tag{3.19}$$

Notice that since the random variables L_k, Q_k, X_k, and Y_k of (3.12) are composed of disjoint set of symmetric Bernoulli trials for a particular desired signature sequence, they are conditionally independent given C.

The relationship between the quantity B and C, which is the discrete aperiodic auto-correlation of the signature sequence of receiver 1, is well explained in [25] as: "A signature sequence of length N has N-1 chip boundaries, at which the sequence may or may not change to a different value. The quantity B represents the number of chip boundaries at which a transition to a different value occurs. As a consequence, B can be treated as a measure of the amount of "Spreading" given to the desired signal. For example, B is minimized when C takes on its maximum value of N-1, which is equivalent to a signature sequence of all ones (minimum spreading). Conversely, when B is maximized, C is at its minimum value of -(N-1), meaning that the signature sequence is composed entirely of chips alternating between +1 and -1 (maximum spreading) ."

To calculate the bit error probability, starting from (3.12), one needs first to calculate the variance of the MAI. This calculation is done in the next subsection.

3.2.1 Variance of the Multiple-Access Interference (MAI)

The MAI term in (3.12) is a function of the random variables C (or B), $S_k, k=2,3,...,K$, and $\varphi_k, k=2,3,...,K$. For convenience, let $\underline{S}=(S_2,...,S_K)$ and $\underline{\varphi}=(\varphi_2,...,\varphi_K)$ be the delays and phases of all the interfering signals (N and K are assumed fixed). The MAI term has zero mean since the component random variables, L_k, Q_k, X_k, and Y_k in (3.13) are zero mean. Also, $\{W_k\cos(\varphi_k)\}$ are conditionally independent given B. By using the fact

that the variance of the sum of zero-mean, independent random variables is the sum of their second moments and by conditioning on B, S_k , and φ_k, the conditional variance $\Psi = Var[MAI|S,\varphi,B]$ of the MAI is given by [9]

$$\begin{aligned}\Psi &= E\left[\left(\sum_{k=2}^{K} W_k \cos\varphi_k\right)^2 \middle| S_k,\varphi_k,B\right] \\ &= \sum_{k=2}^{K} E[W_k^2|S_k,B]\ E[\cos^2\varphi_k|\varphi_k] \\ &= \sum_{k=2}^{K}\left[\frac{1+\cos(2\varphi_k)}{2}\right] Var[W_k|S_k,B].\end{aligned} \tag{3.20}$$

The conditional variance of W_k given S_k and B (or C) is given by

$$\begin{aligned}Var[W_k|S_k,B] &= E[L_k^2 S_k^2|S_k] + E[Q_k^2(1-S_k^2)|S_k] \\ &\quad + E[X_k^2|B] + E[Y_k^2(1-2S_k)^2|S_k,B].\end{aligned} \tag{3.21}$$

Since L_k and Q_k are uniform on $\{-1,1\}$, their variances are equal 1. The variance of X_k given B can be calculated by (see appendix A) [25]

$$Var[X_k|B] = \sum_{j=1}^{N-B-1} Var[b_j] = N-B-1. \tag{3.22}$$

Similarly,

$$Var[Y_k(1-2S_k)|S_k,B] = B(1-2S_k)^2. \tag{3.23}$$

Combining (3.22), (3.23) and the fact that $Var[P_k] = Var[Q_k] = 1$ in (3.21) yields

$$Var[W_k|S_k,B] = 2[(1+2B)(S_k^2 - S_k)] + N. \tag{3.24}$$

Substituting (3.24) in (3.20) yields [9]

$$\begin{aligned}\Psi &= \sum_{k=2}^{k} [1+\cos(2\varphi_k)][(S_k^2 - S_k)(1+2B)+N/2] \\ &= \sum_{k=2}^{K} Z_k,\end{aligned} \tag{3.25}$$

where Z_k are conditionally independent (given B) and identically distributed random variables specified by $Z_k = U_k V_k$, with

$$U_k = 1+\cos(2\varphi_k) \tag{3.26}$$

and

$$V_k = (S_k^2 - S_k)(1+2B)+N/2. \tag{3.27}$$

In the following subsections a calculation of bit error probability using SGA and IGA is given.

3.2.2 Bit error probability using SGA

To find the probability of data bit error using the SGA for MAI, D_1 from (3.12) can be treated as a Gaussian random variable. Then the average probability of data bit error, can be found as $Q_f(\overline{SNR})$, where $\overline{SNR}$ is the average signal -to- noise ratio and given by

$$\overline{SNR} = \frac{E[D_1]}{\sqrt{E[\Psi]}} \tag{3.28}$$

and

$$Q_f(x) = \frac{1}{\sqrt{2\pi}} \int_x^{\infty} e^{-t^2/2} dt. \tag{3.29}$$

Then, it can be shown from (3.12) that, $E[D_1]$ is simply N. Assuming that the interferers and the reference user are not chip and phase synchronous, the expected value of $S_k^2 - S_k = -1/6$; since S_k is uniformly distributed on [0, 1) and $E[\cos(2\varphi_k)]$ is 0 as φ_k is uniformly distributed on $[0, 2\pi)$. Using $Z_k = U_k V_k$ and equations (3.26) and (3.27), $E[Z_k|B]$ becomes [25]

$$E[Z_k|B] = \frac{3N - 2B - 1}{6}. \tag{3.30}$$

If the desired sequence is random, then $E[C] = 0$ and as a result of this $E[B] = (N-1)/2$, which yield

$$E[Z_k] = E\left[E[Z_k|B]\right] = \frac{N}{3}. \tag{3.31}$$

Finally, $E[\Psi]$ can be expressed as [9]

$$\begin{aligned} E[\Psi] &= E\left[\sum_{k=2}^{K} Z_k\right] \\ &= \sum_{k=2}^{K} E[Z_k] \\ &= (K-1)\frac{N}{3}. \end{aligned} \tag{3.32}$$

Therefore, $\overline{SNR}$ becomes

$$\overline{SNR} = \frac{N}{\sqrt{(K - 1)N/3}} . \tag{3.33}$$

The average data bit error probability, P_b, is then approximated by

$$P_b = Q_f\left(\sqrt{\frac{3N}{K - 1}}\right) , \tag{3.34}$$

where K is the total number of users and N is the number of chips per data bit.

The previous result, (3.34), considers only the noise due to the interference from co-users. If one assume that AWGN with two-sided spectral density of $N_o/2$ is added to the sum of the k spread spectrum signals. Then, (3.34) is modified to [26]

$$P_b = Q_f\left(\left[\frac{k - 1}{3N} + \frac{N_o}{2E_b}\right]^{-0.5}\right) , \tag{3.35}$$

where E_b is the energy per bit.

3.2.3 Bit error probability using IGA

As shown in [25], the Improved Gaussian Approximation resulted from noting that the conditional MAI variance Ψ is a function of the delays and phases (S_k and φ_k) of all interfering signals and of the desired sequence structure expressed through the quantity B. In addition, the conditional data bit error probability, P_b, can be written as

$$Q_f\left(N/\sqrt{\Psi}\right) . \tag{3.36}$$

Therefore, the average data bit error probability can be calculated by

$$\begin{aligned}\hat{P}_b &= E\left[Q_f\left(N/\sqrt{\Psi}\right)\right] \\ &= \int_0^\infty Q_f\left(N/\sqrt{\Psi}\right) f_\Psi(\psi)\, d\psi,\end{aligned} \tag{3.37}$$

where $f_\Psi(\psi) = E[f_{Z|B}(z) * ..... * f_{Z|B}(z)]$ is the density function of the total MAI variance, Ψ, with K-2 convolutions being performed. The function $f_{Z|B}(z)$ is the conditional density of Z_k=Z (Since Z_k identically distributed) given B and * denotes convolution [9].

A technique that does not require convolutions or the conditional density function $f_{Z|B}(z)$ to calculate the average data bit probability will be described in the next subsection.

3.2.4 An Approximation Technique for Calculating the Expected Value of a Real Function of a Random Variable

Assuming a real function h of a random variable ξ with mean μ_ξ and variance σ_ξ and the existence of the function derivatives, $h(\xi)$ may be expanded in a Talyor series [27]

$$h(\xi) = h(\mu_\xi) + (\xi - \mu_\xi) h'(\mu_\xi) + \frac{1}{2}(\xi - \mu_\xi)^2 h''(\mu_\xi) + ... \tag{3.38}$$

By taking the expected value of the above expansion, it can be shown that

$$E[h(\xi)] \cong h(\mu_\xi) + \frac{1}{2}\sigma_\xi^2 h''(\mu_\xi), \tag{3.39}$$

and

$$Var[h(\xi)] \cong \sigma_\xi^2 \left(h'(\mu_\xi)\right)^2. \tag{3.40}$$

As shown in [27], an expansion in differences instead of derivatives for the function $h(\xi)$ can be used. Consider $h(\xi)$ expanded using central differences, i.e.,

$$h(\xi) = h(\mu_\xi) + (\xi - \mu_\xi)\frac{h(\mu_\xi + \Delta) - h(\mu_\xi - \Delta)}{2\Delta} + \frac{1}{2}(\xi - \mu_\xi)^2 \frac{h(\mu_\xi + \Delta) - 2h(\mu_\xi) + h(\mu_\xi - \Delta)}{\Delta^2} + \ldots. \tag{3.41}$$

The following result can be obtained by taking the expectation of (3.41) [27]

$$E[h(\xi)] \cong h(\mu_\xi) + \frac{1}{2}\sigma_\xi^2 \left[\frac{h(\mu_\xi + \Delta) - 2h(\mu_\xi) + h(\mu_\xi - \Delta)}{\Delta^2}\right]. \tag{3.42}$$

The difference $\Delta = \sqrt{3}\,\sigma_\xi$ is shown in [27] to be exact for fifth degree polynomials $h(.)$, and ξ normally distributed. Therefore, for this case, $E[h(\xi)]$ becomes

$$E[h(\xi)] \cong h(\mu_\xi) + \frac{h(\mu_\xi + \sqrt{3}\,\sigma_\xi) - 2h(\mu_\xi) + h(\mu_\xi - \sqrt{3}\,\sigma_\xi)}{6}. \tag{3.43}$$

Now, for a reference user, it is the average bit error probability that one is able to calculate using (3.42). Notice that since (3.37) is the expectation of a real function of the random variable Ψ, (3.42) can be directly applied. This was done in [26]. Let μ and σ^2 be the mean and variance of Ψ, respectively. Based on (3.25) and the information in appendix C, μ and σ^2 can be expressed as (assuming $Z = Z_k$) [9]

$$\mu = (K-1)E[Z], \tag{3.44}$$

and

$$\sigma^2 = (K-1)\left[E[Z^2] - E^2[Z] + (K-2)\,Cov(Z_j, Z_k)\right] \quad for\ j \neq k. \tag{3.45}$$

From (3.31)

$$E[Z] = N/3 \tag{3.46}$$

and as shown in appendix C

$$E[Z^2] = \frac{7N^2 + 2N - 2}{40} \tag{3.47}$$

and

$$Cov(Z_j, Z_k) = \frac{N-1}{36} \quad for\ j \neq k. \tag{3.48}$$

As a result of the above, a simple approximation for the average data bit error probability in (3.37) becomes [26]

$$\hat{P}_b \cong \frac{2}{3} Q_f\left(\sqrt{3\frac{N}{(K-1)}}\right) + \frac{1}{6} Q_f\left(\frac{N}{\sqrt{(K-1)N/3 + \sqrt{3}\sigma}}\right) + \frac{1}{6} Q_f\left(\frac{N}{\sqrt{(K-1)N/3 - \sqrt{3}\sigma}}\right) \tag{3.49}$$

where

$$\sigma^2 = (K-1)\left[\frac{23}{360}N^2 + N\left(\frac{1}{20} + \frac{K-2}{36}\right) - \frac{1}{20} - \frac{K-2}{36}\right]. \tag{3.50}$$

The result in (3.49) is only for the noise due to the interference from other users. Assuming that AWGN is added to the sum of the k spread-spectrum signals, (3.49) may be rewritten as [27]

$$\hat{P}_b \cong \frac{2}{3}Q_f\left(\left[\frac{k-1}{3N}+\frac{N_o}{E_b}\right]^{(-0.5)}\right)+\frac{1}{6}Q_f\left(\left[\frac{(K-1)N/3+\sqrt{3}\sigma}{N^2}+\frac{N_o}{2E_b}\right]^{(-0.5)}\right)+ \frac{1}{6}Q_f\left(\left[\frac{(K-1)N/3-\sqrt{3}\sigma}{N^2}+\frac{N_o}{2E_b}\right]^{(-0.5)}\right), \tag{3.51}$$

where E_b is the energy per bit.

3.3 Computed Results

Using the analysis developed in the above sections, the bit error rate performance results were computed as a function of the bit energy to noise spectral density ratio. The spreading gain, N, and the number of users, K, were used as the variable parameters for computing these results. Further, both the standard Gaussian approximation (SGA) and improved Gaussian approximation (IGA) were used to bring out comparison between these two approximation methods. The computed bit error results are presented in Figures 3.1-3.3. From these Figures, it may be seen that the standard Gaussian approximation provides optimistic bit error rate for the number of users K < 5 when N=7, for K < 10 when N=31, and for K < 13 when N=63. The agreement with analytical results is much better for improved Gaussian approximation in these cases. This optimistic nature of the results is not unexpected because the standard Gaussian approximation was base on the applicability of the central limit theorem. This theorem which predicts the Gaussian behavior of a random variable obtained by summing a number of random variables. It is well known that the accuracy of this theorem depends on the number of variables being added. For lower values of K the application of this theorem in the standard Gaussian approximation makes results in error. The error due to this assumption depends on the processing gain N as the overall impact of mutiuser interference is reduced by the higher processing gain.

Another noteworthy result in Figures 3.1-3.3 is the improvement in the bit error rate as N increases: this is once again expected as the multiuser interference is spread out over a wider bandwidth when the processing gain increases. This improvement, however, is obtained at the price of higher spreading bandwidth for the system. For an example of 10 users (K=10), the bit error rate P_e improves from 6×10^{-2} to 10^{-5} when N increases from & to 63. The effect of the additive white Gaussian noise is shown in Figures 3.4 - 3.7. These Figures are based on (3.35) and (3.51). It is clear from the Figures 3.4-3.7 that a better P_e results as E_b/N_o increases. For a fixed E_b/N_o , the P_e performance degrades as the number of users increase. In practice, some improvement in P_e can be obtained by increasing E_b/N_o if the number of users increases; for example, (consider IGA), to keep P_e at a level of 10^{-3}, E_b/N_o should be increased by approximately 3dB where K increases from 3 to 6. It may be noticed that the standard Gaussian approximation provides very optimistic P_e performance at high values of E_b/N_o with K=3 and N=31 as in Figure 3.4. As the number of users increases the difference between the two P_es values using the SGA and the IGA reduces considerably, as shown in Figures 3.5-3.7.

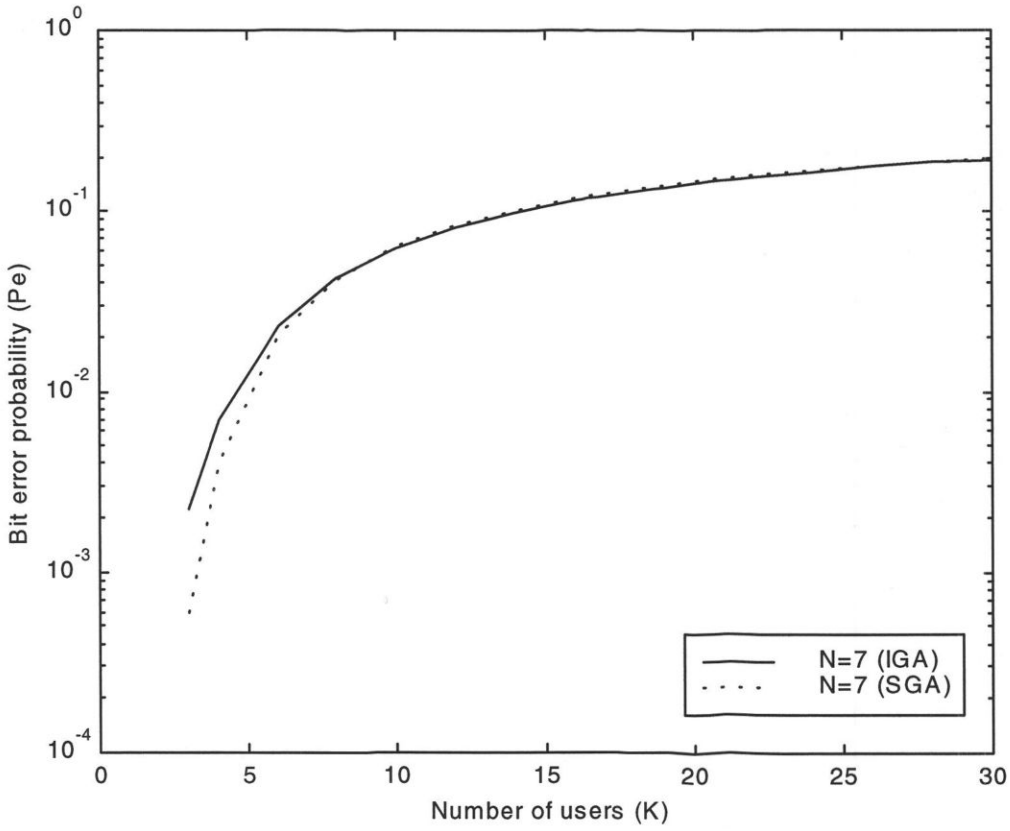

Figure 3.1 Probability of data bit error (Pe) as a function of number of users K (Spreading sequence length N =7)

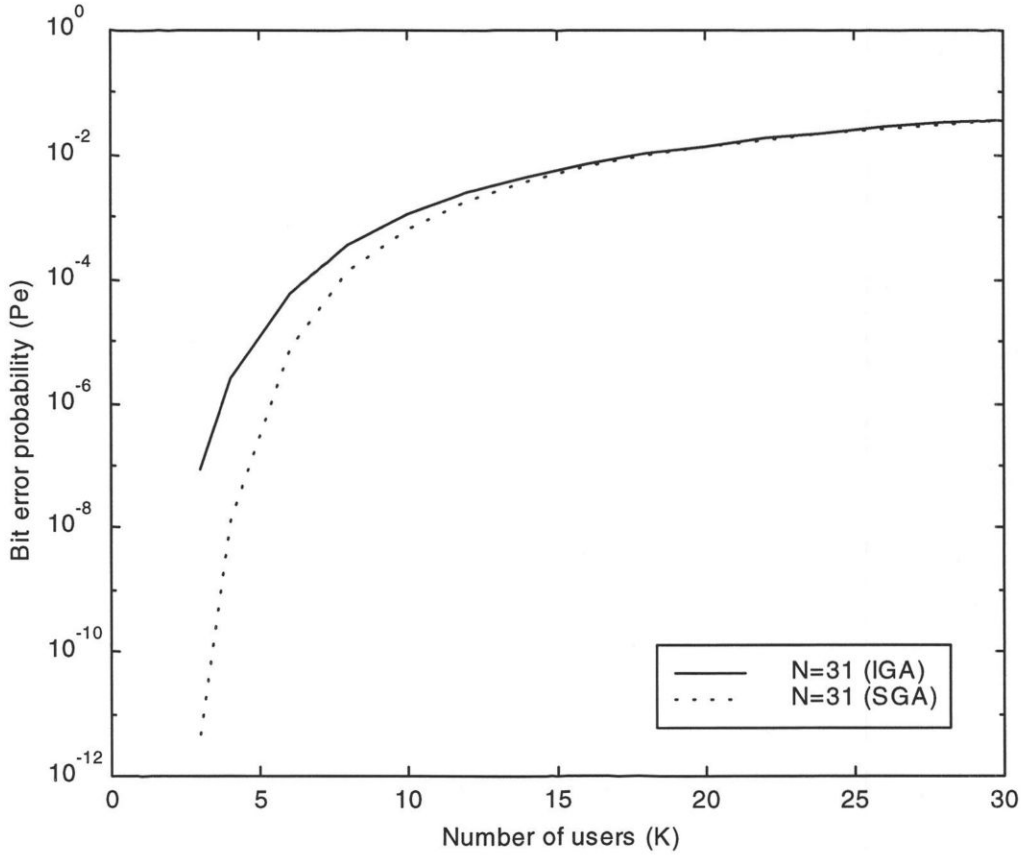

Figure 3.2 Probability of data bit error (Pe) as a function of number of users K (Spreading sequence length N =31)

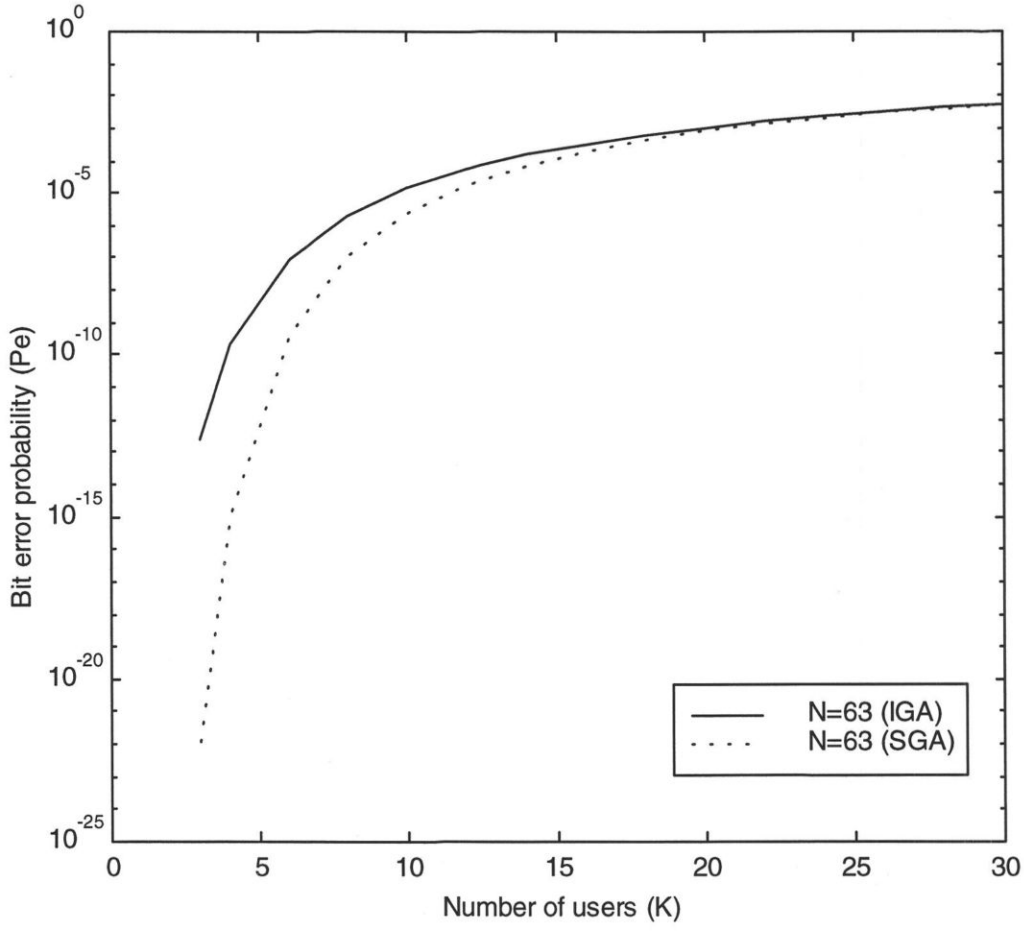

Figure 3.3 Probability of data bit error (Pe) as a function of number of users K (Spreading sequence length N=63)

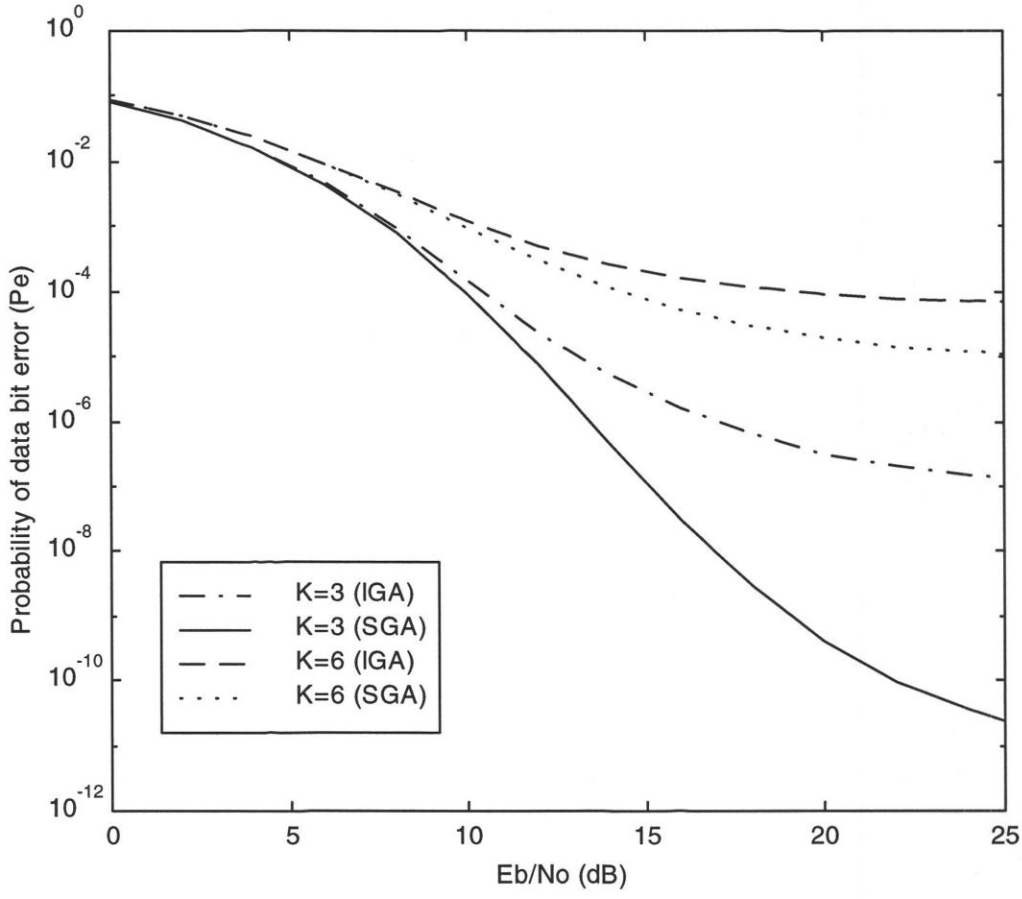

Figure 3.4 Probability of data bit error (Pe) as a function of E_b/N_o for number of users K =3 and 6 and spreading sequence length N = 31.

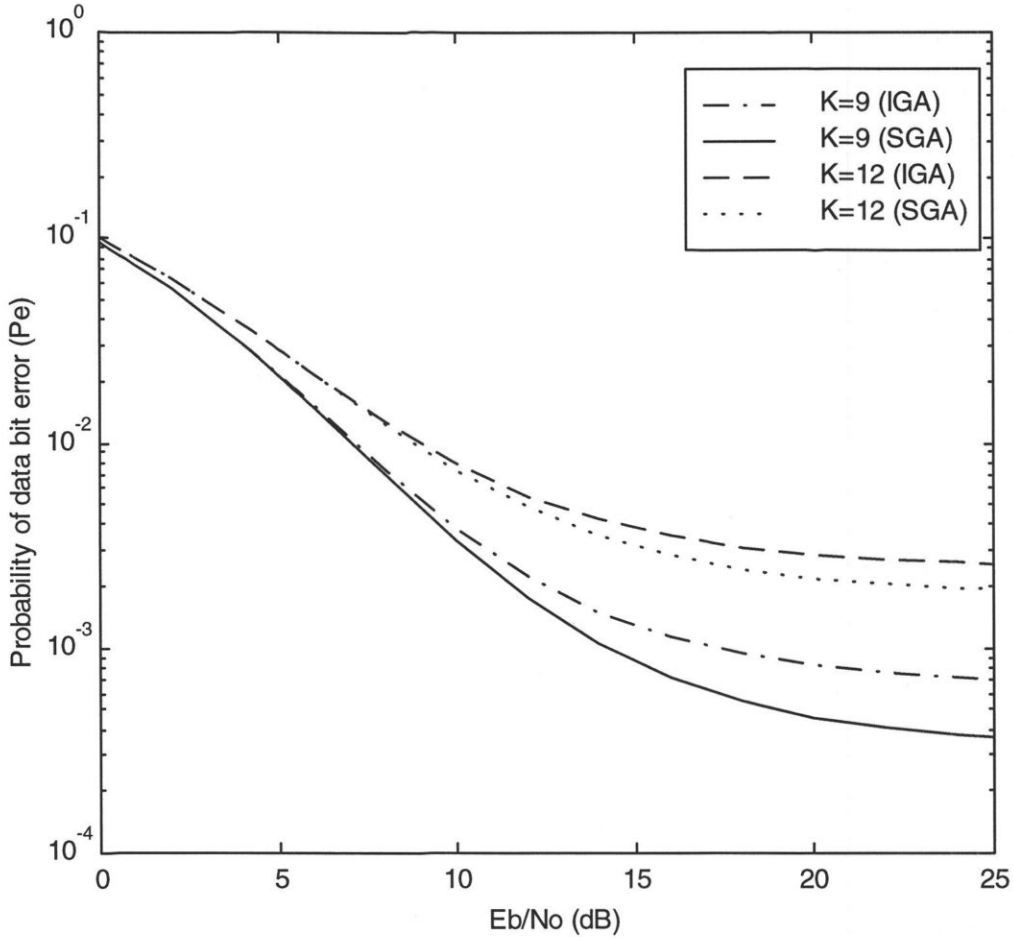

Figure 3.5 Probability of data bit error (Pe) as a function of E_b/N_o for number of users K=9 and 12 and spreading sequence length N =31.

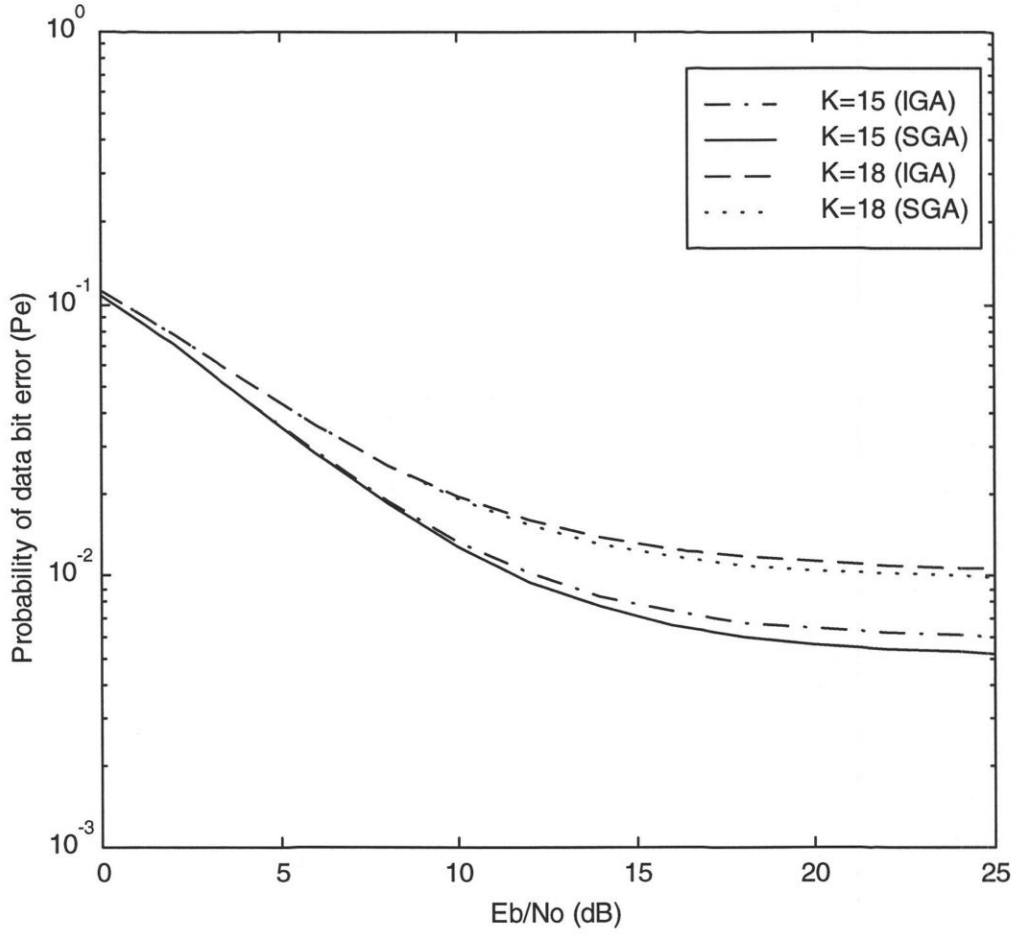

Figure 3.6 Probability of data bit error (Pe) as a function of E_b/N_o for number of users K =15 and 18 and spreading sequence length N =31.

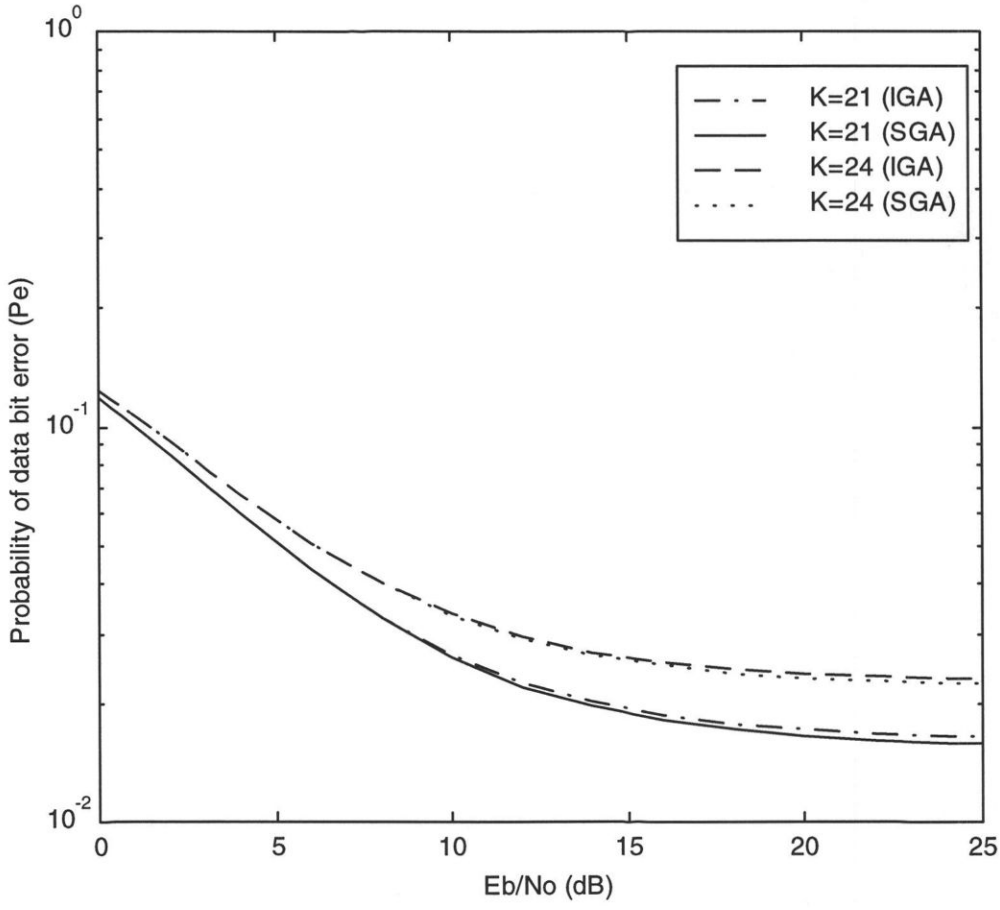

Figure 3.7 Probability of data bit error (Pe) as a function of E_b/N_o for number of users K =21 and 24 and spreading sequence length N=31

4. Effects of Filtering on the Performance of BPSK DS/CDMA Systems

4.1 Introduction

In the previous chapter, a computationally simple technique to approximate DS/CDMA bit error probability using standard Gaussian approximation and improved Gaussian approximation was applied. The results of chapter 3 are useful for assessing the performance of realistic DS/CDMA systems. However, the utility of the results of chapter 3 are limited because of some of the idealizations used there. For example, it is assumed that the information signal and the spreading signal have a unit amplitude and rectangular pulses which require a wide bandwidth for undistorted transmission. The need for a wide bandwidth is based on the fact that the frequency content of a rectangular pulse has a $\sin x/x$ shape in which tails decay very slowly, and hence a rectangular pulse requires a wide bandwidth for undistorted transmission. This assumption led to a disregard of the effect of band-limited channels, i.e., transmitter and receiver filters in chapter 3's analysis . In practical wireless systems, however, the presence of filters is essential to shape the in-band portion of the spectrum, to save bandwidth as much as possible, and to reject the out-of-band portion of the spectrum, to minimize the noise power.

In this chapter, the effect of a band-limited channels (i.e., filters) on the performance of BPSK DS/CDMA is analyzed. The system performance measures in this analysis are the signal to noise ratio (SNR) and bit error probability. Before the system analysis, different practical filter types and their characteristics will be considered. These filter types are described in section 4.3.

4.2 Filtering

In a variety of important applications it is of interest to change the relative amplitudes of the frequency components in a signal or perhaps eliminate some frequency components entirely, a process referred to as filtering. The word "filter", which is an associate word to filtering process, is used by electrical engineers to denote a circuit or system that exhibits some sort of frequency selective behavior.

Filters are devices which allow a certain range of desired frequencies to pass through with minimum attenuation while attenuating the undesired frequencies. Filters may be classified in several ways. One is as finite impulse response filters (FIR) and infinite impulse response filters (IIR). Another is as Butterworth, Chebyshev, elliptic-function or raised cosine response. Generally, they can also be classified as lowpass, bandpass, bandstop, and highpass. In Figure 4.1, the frequency responses of the last classification of ideal filters are shown.

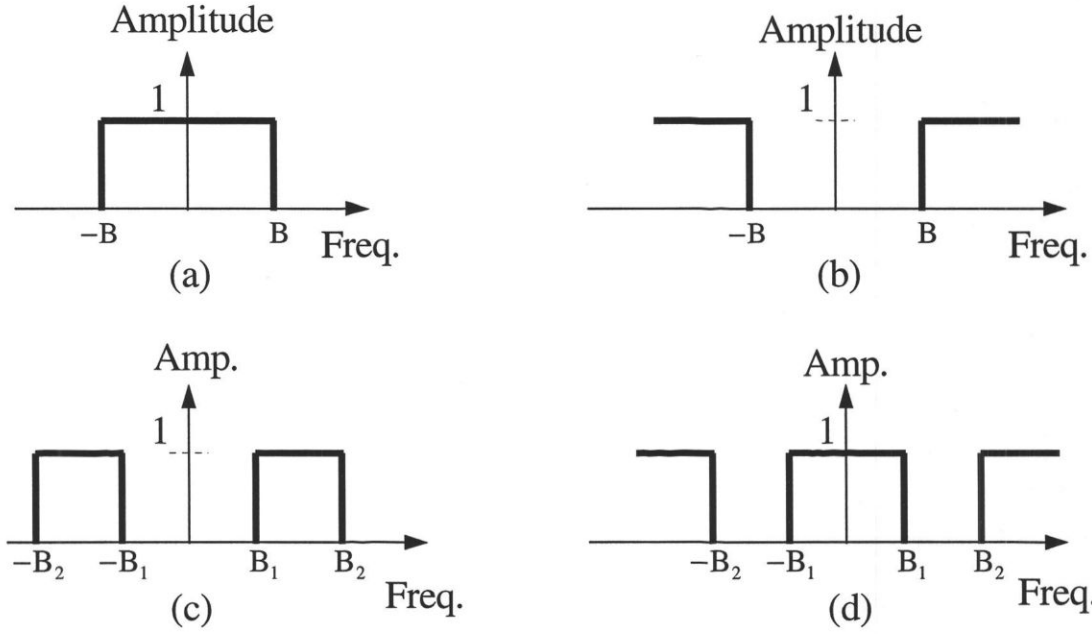

Figure 4.1 Magnitude functions of ideal filters: (a) lowpass; (b)highpass;

(c) bandpass; (d) bandstop

The fundamental parameter to represent a filter is the transfer function $H(s)$, which is a filter input-output relationship. Consider a filter transfer function written as a function of the Laplace transform variable s in the form [18]

$$H(s) = \frac{N(s)}{D(s)} , \tag{4.1}$$

where

$$N(s) = \sum_{l=0}^{m} a_l s^{\,l} = (s - z_1)(s - z_2).....(s - z_m) \tag{4.2}$$

and

$$D(s) = \sum_{l=0}^{n} b_l s^{\,l} = (s - p_1)(s - p_2).....(s - p_n) \tag{4.3}$$

are numerator and denominator polynomials in s of degrees m and n, respectively. The roots of $N(s)$, $z_1, z_2, ..., z_m$ are the zeros of $H(s)$ and the roots of $D(s)$, $p_1, p_2, ..., p_n$ are the poles of $H(s)$.The filter frequency response characteristics in (4.1), (4.2), and (4.3) are assumed to have 3-dB frequencies normalized to 1 rad/s. If a 3-dB cutoff frequency other than 1 rad/s is desired, s is replaced in (4.1) by

$$s' = \frac{s}{\omega_c} , \tag{4.4}$$

where ω_c is the new 3-dB cutoff frequency. FIR filters have only finite zeros, while IIR filters have either both zeros and poles or only poles.

4.3 Practical Filter Types

In real-time filtering applications, it is not possible to utilize ideal filters since they

are noncausal. In such applications it is necessary to use causal filters which are nonideal; that is, the transition from the passband to the stopband (and vice versa) is gradual. In particular, the magnitude functions of causal versions of lowpass, highpass, bandpass, and bandstop filters have gradual transitions from the passband to the stopband. Figure 4.2 shows the basic types of non-ideal filters.

In the SNR analysis in section 4.4, lowpass filters are considered for the DS/CDMA system structure. Therefore, some of practical lowpass filter types and their frequency response characteristics will be focused on. These include, Butterworth , Chebyshev , Elliptic-function filters (IIR filters) and raised cosine filters (FIR filters).

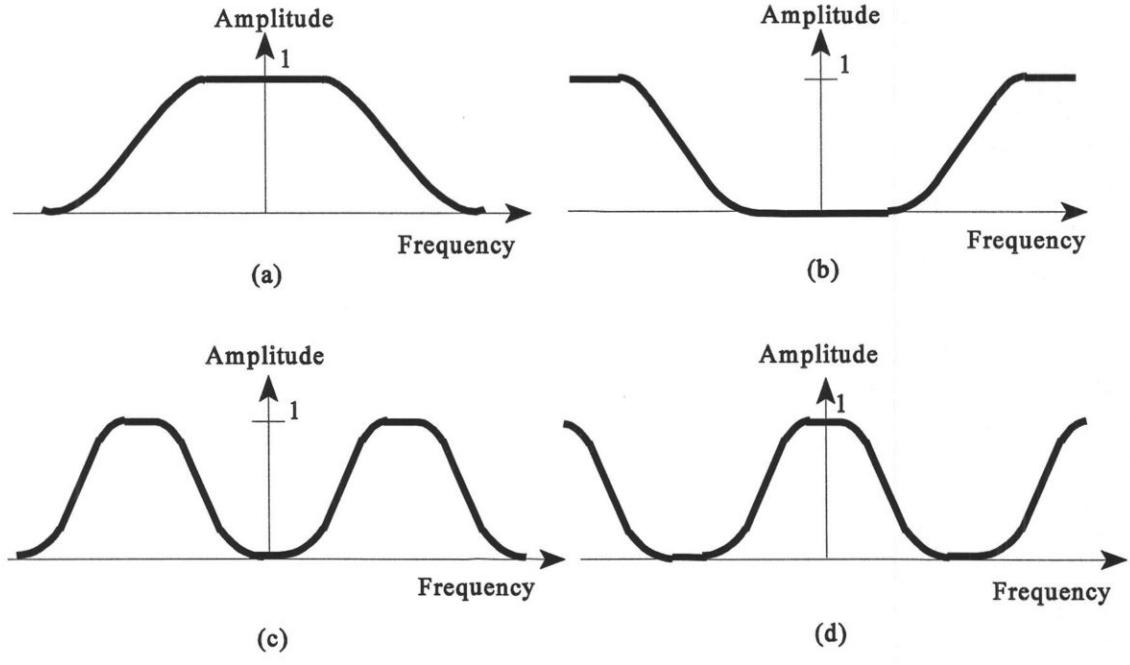

Figure 4.2 Magnitude functions of nonideal filters: (a) lowpass;

(b) highpass;(c) bandpass; (d) bandstop

4.3.1 Butterworth Filters

One of the simplest lowpass magnitude characteristics was first suggested by Butterworth in 1930 [28]. The Butterworth approximation to an ideal low-pass filter is based on the assumption that a flat response at zero frequency is more important than the response at other frequencies. That is why this type of filter is called maximally flat filter since the variation in the magnitude is as small as possible across the passband of the filter.

The Butterworth filter is an all-pole configuration with $N(s) = 1$. For filters of order 1-5, D(s) coefficients are given in Table 4.1 [18]. A magnitude function of Butterworth filter is shown in Figure 4.3.

The general form of the amplitude response $(A_{dB}(\Omega) = 20\log_{10}(|H(\omega_x)|)$, where $|H(\omega_x)| = \dfrac{1}{[1+(\omega_x/\omega_c)^{2n}]^{1/2}}$, of a Butterworth low-pass filter can be expressed by

$$A_{dB}(\Omega) = -10\log_{10}\left[1+(\Omega)^{2n}\right], \tag{4.5}$$

Table 4.1. Coefficients for the Denominator Polynomials of Butterworth filters of orders 1-5 (Unity 3-dB Cutoff Frequency)

Order	b_o	b_1	b_2	b_3	b_4	b_5
1	1	1				
2	1	$\sqrt{2}$	1			
3	1	2	2	1		
4	1	2.613126	3.414214	2.613126	1	
5	1	3.236068	5.236068	5.236069	3.236068	1

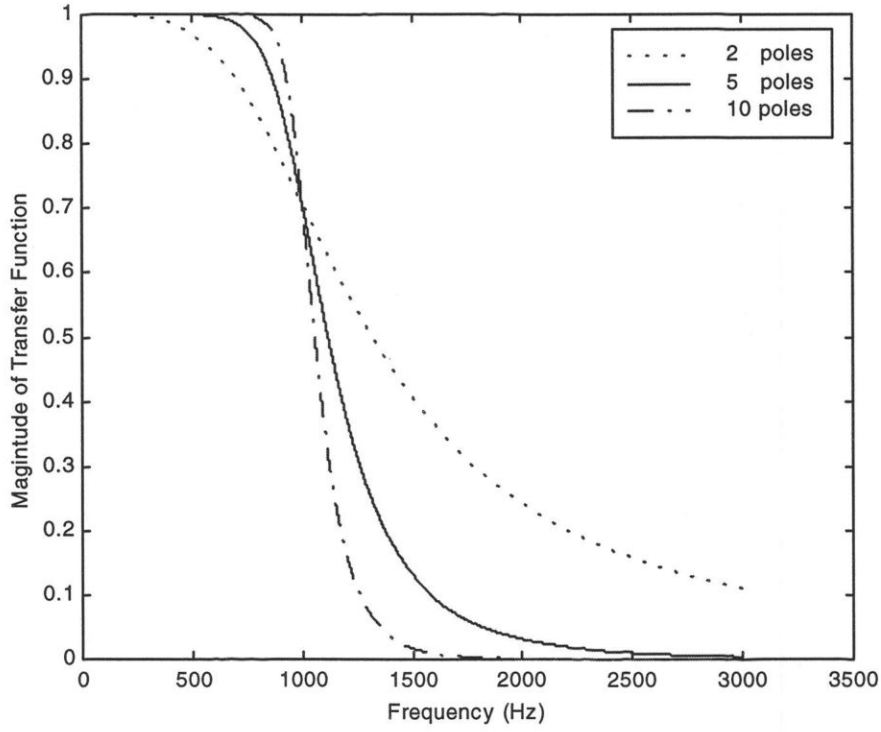

Figure 4.3 Magnitude function of Butterworth filters of different orders

where $\Omega = \omega_x / \omega_c$ is the ratio of the given frequency ω_x to the 3-dB cutoff frequency ω_c and n is the order of the filter. The poles of the unity cutoff filter can be computed from [18]

$$q_l = -\sin\frac{(2l-1)\pi}{2n} + j\cos\frac{(2l-1)\pi}{2n} \qquad for \quad l = 1,2,.....,n. \tag{4.6}$$

The Butterworth approximation results in a class of filters which have moderate attenuation steepness and acceptable transient characteristics. The rounding of the frequency response in the vicinity of cutoff may make these filters undesirable where a sharp cutoff is required [29].

As mentioned in the introduction of this chapter, a rectangular pulse requires a wide

band width for undistorted transmission. This can be illustrated by using MATLAB commands. The outputs of the Butterworth filter, for 10 rectangular pulses input, are shown in Figures 4.4 and 4.5. For sake of comparison, two cases of a filter bandwidth are considered: $BW = 2f_m$, $10f_m$, where $f_m = 1/T$ and T is the duration of the input rectangular pulse. As can be seen from the figures, the higher bandwidth filter has better output shape.

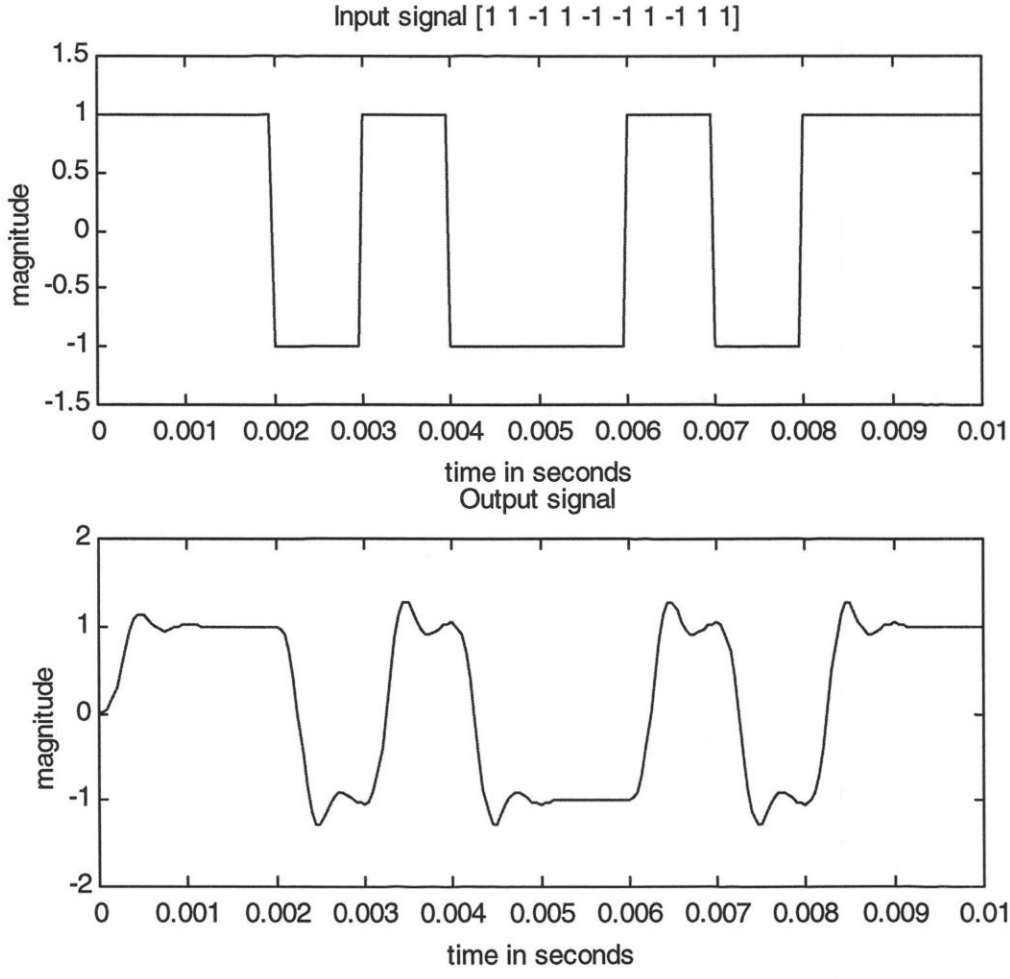

Figure 4.4 Input and output signals of Butterworth filter (BW=$2f_m$)

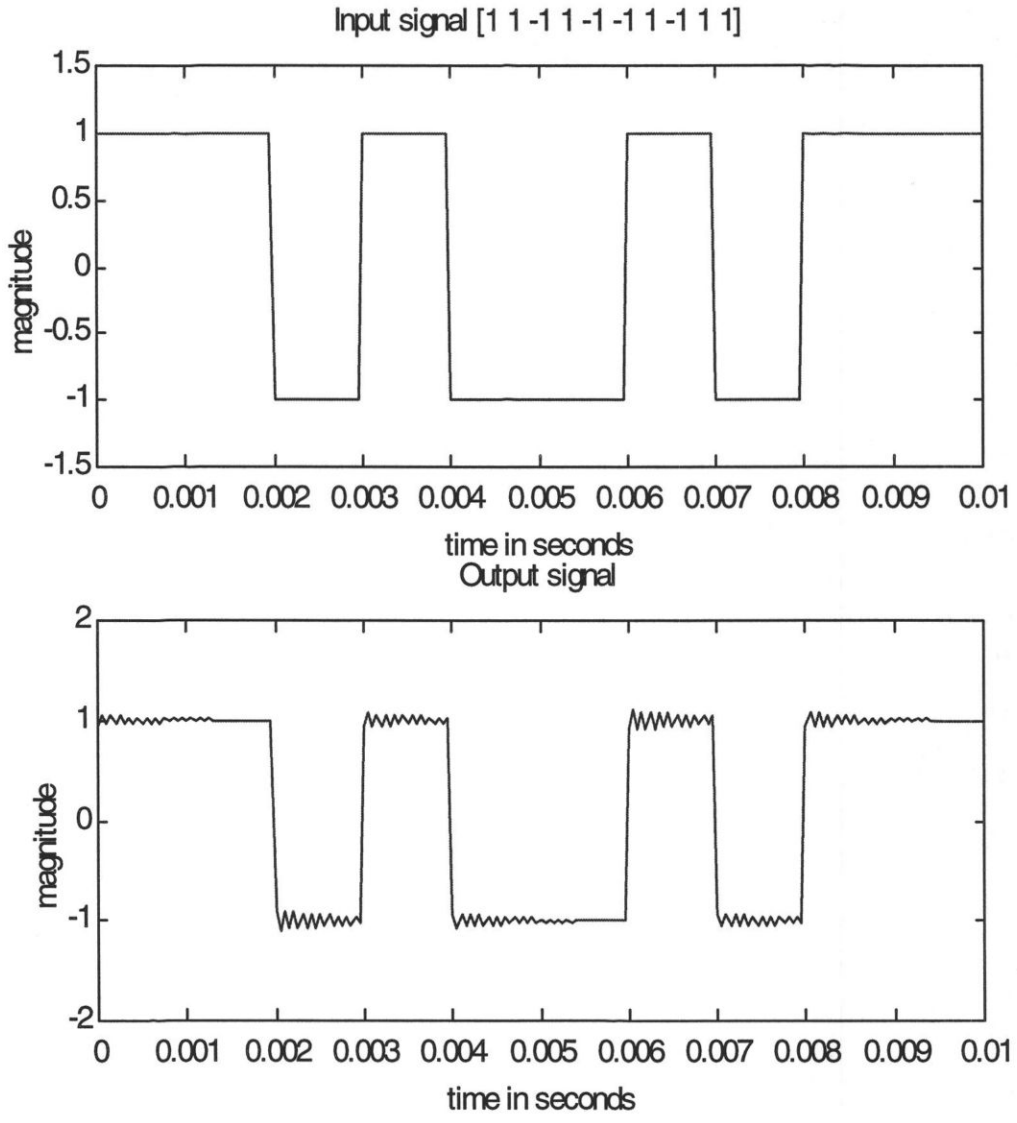

Figure 4.5 Input and output of Butterworth filter (BW=$10f_m$)

4.3.2 Chebyshev Filters

Another commonly used standard lowpass characteristics is the Chebyshev lowpass characteristics. The Chebyshev approximation to an ideal filter gives faster rolloff in the transition region than a Butterworth filter of the same order [18]. In other words, the Chebyshev approximation has a much more rectangular frequency response in the region

near cutoff than the Butterworth family of filters. This is achieved by allowing ripples in the passband region. The poles of a normalized Chebyshev filter are obtained by moving the poles of a normalized Butterworth response to the right by a factor [18]

$$R_c = \tanh A, \tag{4.7}$$

where

$$A = \frac{1}{n}\cosh^{-1}\frac{1}{\epsilon}, \tag{4.8}$$

in which

$$\epsilon = \sqrt{10^{R/10} - 1}, \tag{4.9}$$

and R is the passband ripple in decible. A magnitude function of Chebyshev filter is shwon in Figure 4.6.

The amplitude response function of Chebyshev filters can be expressed as

$$A_{dB}(\Omega) = -10\log_{10}\left[1 + \epsilon^2 C_n^2(\Omega)\right], \tag{4.10}$$

where $C_n(\Omega)$ is a Chebyshev polynomial of order n. Chebyshev polynomials of order 5 and less are tabulated in Table 4.2. A recursion relation for obtaining $C_n(\Omega)$ is [18]

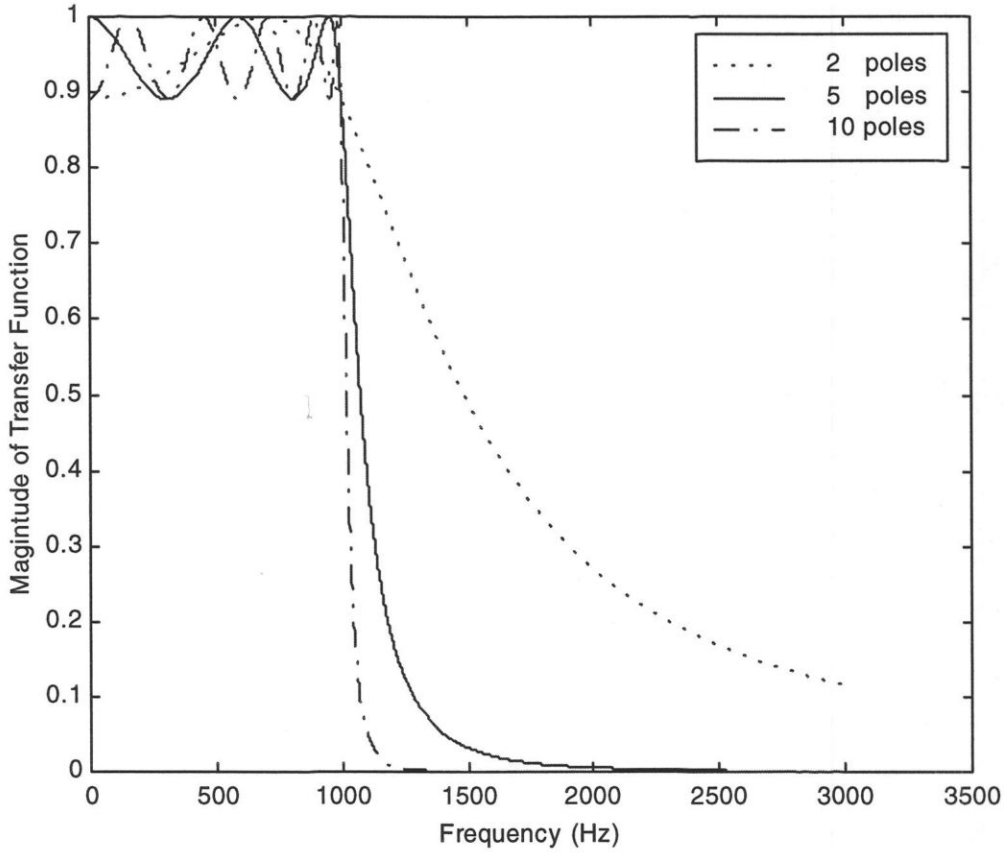

Figure 4.6 Magnitude function of Chebyshev filters of different orders

$$C_n(\Omega) = 2\Omega C_{n-1}(\Omega) - C_{n-2}(\Omega) \qquad for \quad n = 2,3,..... , \tag{4.11}$$

where $C_0(\Omega) = 1$.

Chebyshev filters have a narrower transition region between the passband and stopband than Butterworth filters but have more group delay variation in their passband. The rate of roll-off of this type of filters increases as the passband ripples is made larger, but the transient properties rapidly deteriorate. A Chebyshev filter degenerates to a Butterworth approximation type of filters if no ripples are permitted [29].

Table 4.2. Chebyshev Polynomials

Order	Chebyshev Polynomial
1	Ω
2	$2\Omega^2 - 1$
3	$4\Omega^3 - 3\Omega$
4	$8\Omega^4 - 8\Omega^2 + 1$
5	$16\Omega^5 - 20\Omega^3 + 5\Omega$

The Chebyshev function is useful where frequency response is the major consideration. It provides the maximum theoretical rate of roll-off of any all-pole transfer function for a given order, but it does not have the mathematical simplicity of the Butterworth family.

MATLAB commands are also used here to illustrate the outputs of the Chebyshev filter. Figures 4.7 and 4.8 show the outputs of two different bandwidths ($BW = 2f_m$, $10f_m$). As may be seen from the figures, the more bandwidth the filter has the better is the output shape.

4.3.3 Cauer Filters (Elliptic-Function Filters)

The previous two filter types, Butterworth and Chebyshev, are all-pole transfer function. Filters that have zeros as well as poles in the transfer function and equal-ripple variations in both the passband and stopband were first advanced by Professor Wilhelm Cauer in 1931 [28]. This type of filter characteristics is called Cauer (or elliptic-function) filters. The elliptic-function filter has a much more rapid rate of descent in the transition region than the previous two filter types. This improved performance is obtained at the expense of return lobes in the stopband region.

The following definitions apply to normalized elliptic-function lowpass filters and are illustrated in Figure 4.9:

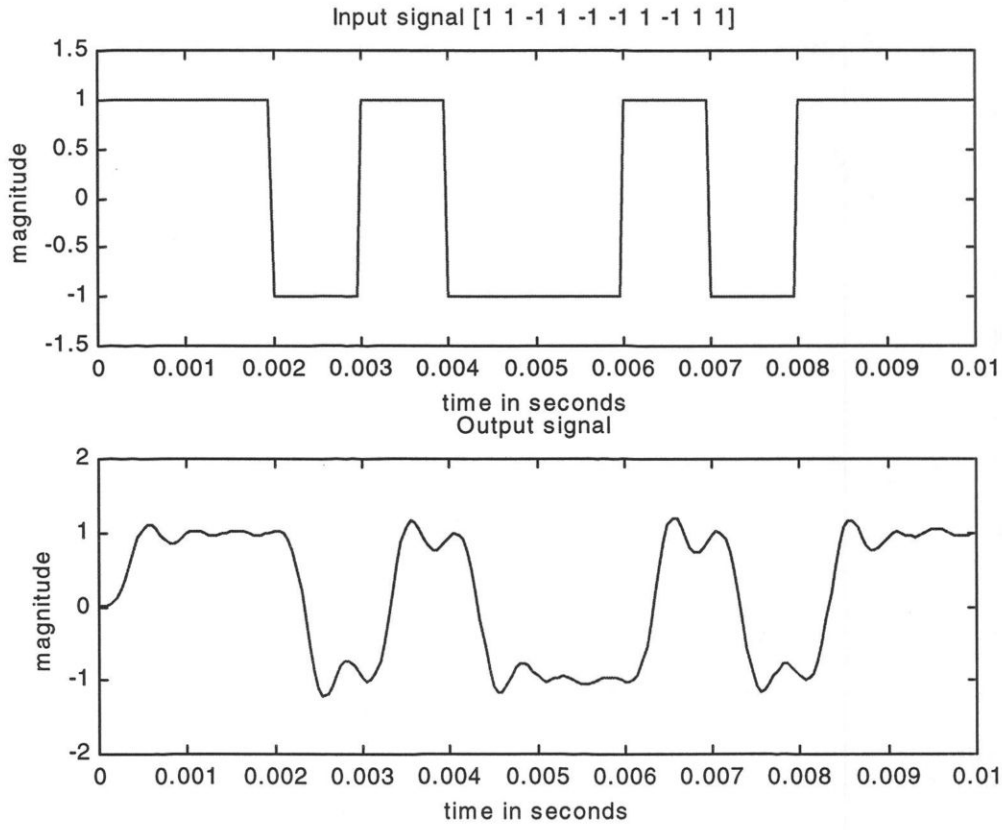

Figure 4.7 Input and output of a Chebyshev filter (BW= $2f_m$)

R_{dB} = passband ripple

$A_{\min}$ = minimum stopband attenuation in decibles

Ω_s = lowest stopband frequency at which $A_{\min}$ occurs

The attenuation of elliptic filters can be expressed as [29]

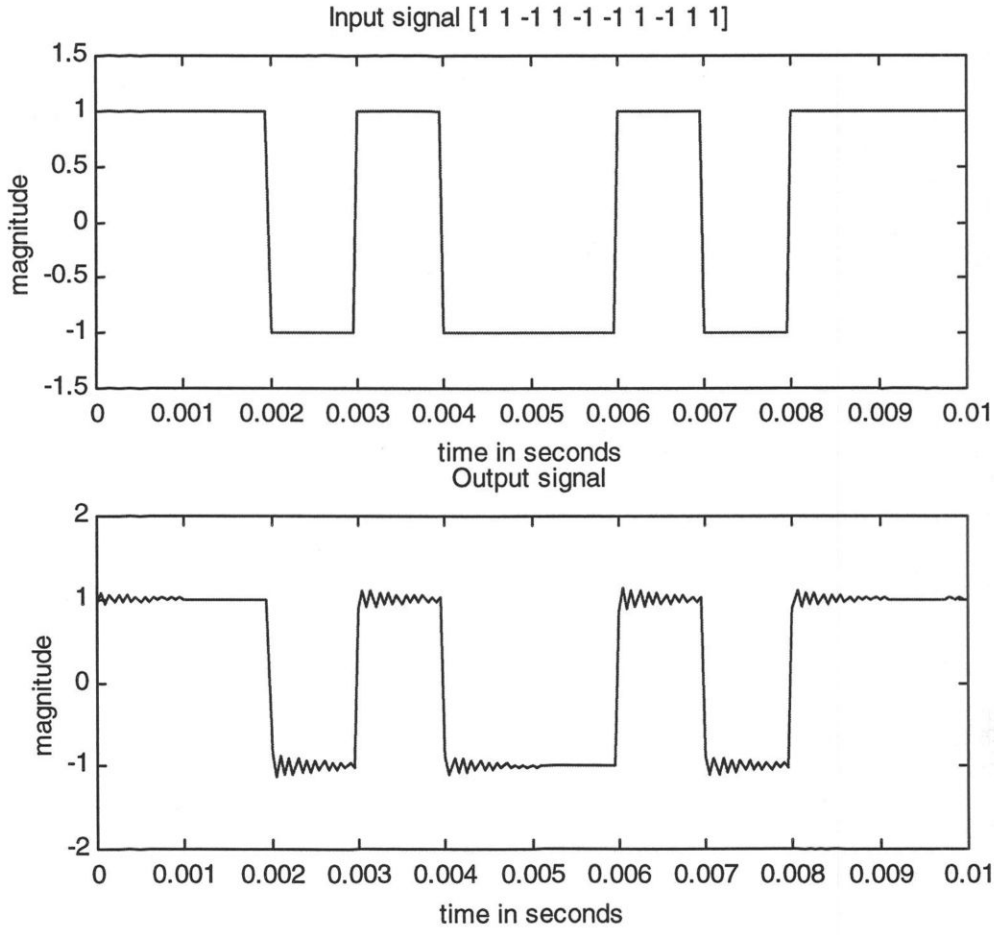

Figure 4.8 Input and output of a Chebyshev filter (BW= $10f_m$)

$$A_{dB} = -10\log_{10}[1+\epsilon^2 Z_n^2(\Omega)], \tag{4.12}$$

where ϵ is determined by the ripple (equation (4.9)) and $Z_n(\Omega)$ is an elliptic function of the

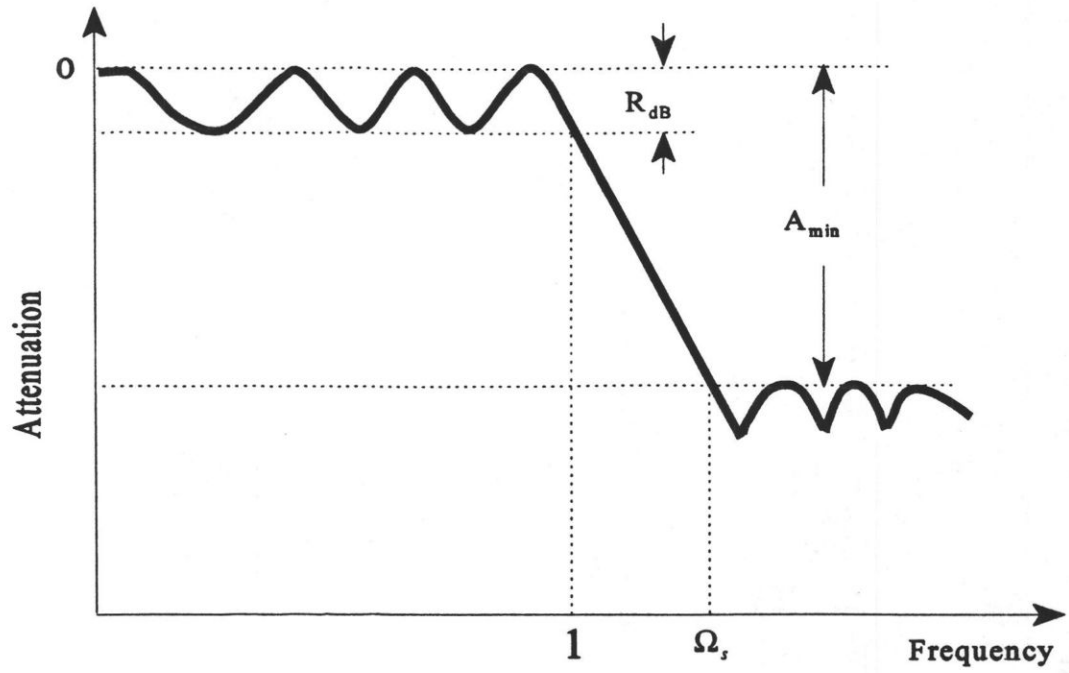

Figure 4.9 Normalized elliptic-function lowpass filter response

n^{th} order. Elliptic functions have both poles and zeros and can be specified as [29]

$$Z_n(\Omega) = \frac{\Omega(a_2^2 - \Omega^2)(a_4^2 - \Omega^2)\ldots(a_m^2 - \Omega^2)}{(1 - a_2^2\Omega^2)(1 - a_4^2\Omega^2)\ldots(1 - a_m^2\Omega^2)}, \tag{4.13}$$

where n is odd and $m = (n-1)/2$, or

$$Z_n(\Omega) = \frac{(a_2^2 - \Omega^2)(a_4^2 - \Omega^2)\ldots(a_m^2 - \Omega^2)}{(1 - a_2^2\Omega^2)(1 - a_4^2\Omega^2)\ldots(1 - a_m^2\Omega^2)}, \tag{4.14}$$

where n is even and $m = n/2$.

The zeros of Z_n are $a_2, a_4, \ldots, a_m$, whereas the poles are $1/a_2, 1/a_4, \ldots, 1/a_m$. The reciprocal relationship between the poles and zeros of Z_n results in equiripple behavior in both the stopband and the passband.

Elliptic-function filters are commonly classified using the following convention [29]:

$$C\, n\, \rho\, \theta,$$

where C represents Cauer, n is the filter order, ρ is the coefficient, and θ is the modular angle. The angle θ determines the steepness of the filter and is defined as

$$\theta = \sin^{-1} \frac{1}{\Omega_s}, \tag{4.16}$$

or alternatively it can be stated

$$\Omega_s = \frac{1}{\sin\theta}. \tag{4.17}$$

Table 4.3 gives some representative values of θ and Ω_s.

Table 4.3: Ω_s vs. θ

θ, degrees	0	20	40	60	80
Ω_s	∞	2.924	1.556	1.155	1.015

The parameter ρ, the reflection coefficient, can be derived from [29]

$$\rho = \sqrt{\epsilon^2/(1+\epsilon^2)}, \tag{4.18}$$

where ϵ is the ripple factor (see equation (4.9)). The passband ripple and reflection coefficient are related to each other by

$$R_{dB} = -10\log_{10}(1-\rho^2)\,. \tag{4.19}$$

It is important here to notice that, as the parameter θ approaches 90^o, the edge of the stopband Ω_s approaches unity. For θ's near 90^o extremely sharp roll-offs are obtained. However, for a fixed n, the stopband attenuation $A_{\min}$ is reduced as the steepness increases. For a given θ and order n, the stopband attenuation parameter $A_{\min}$ increases as the ripple is made larger [29].

Elliptic-function filters have an extremely steep rate of descent into the stopband because of transmission zeros. However, the delay variation in the passband is unacceptable when the transient behavior is of significance.

The outputs of the elliptic-function filter for the input of 10 rectangular pulses, are obtained using MATLAB commands to demonstrate the effect of this filter on rectangular pulses. Figures 4.10 and 4.11 show different outputs for different bandwidths ($BW = 2f_m$, $10f_m$).

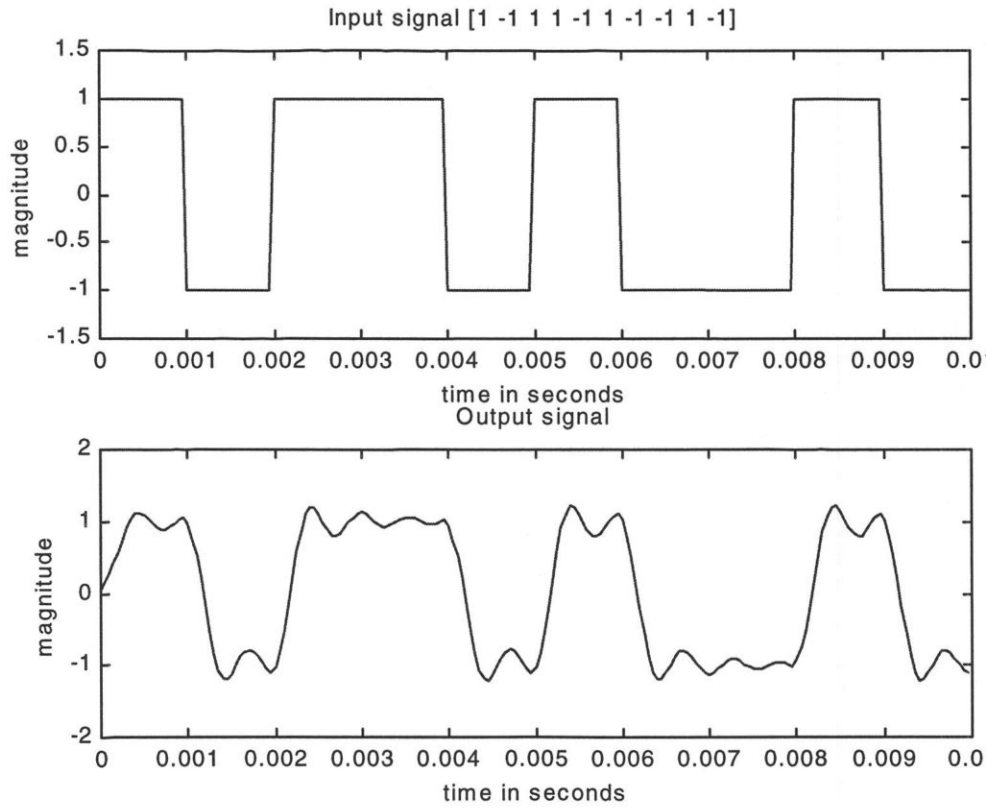

Figure 4.10 Input and output of an elliptic-function filter (BW= $2f_m$)

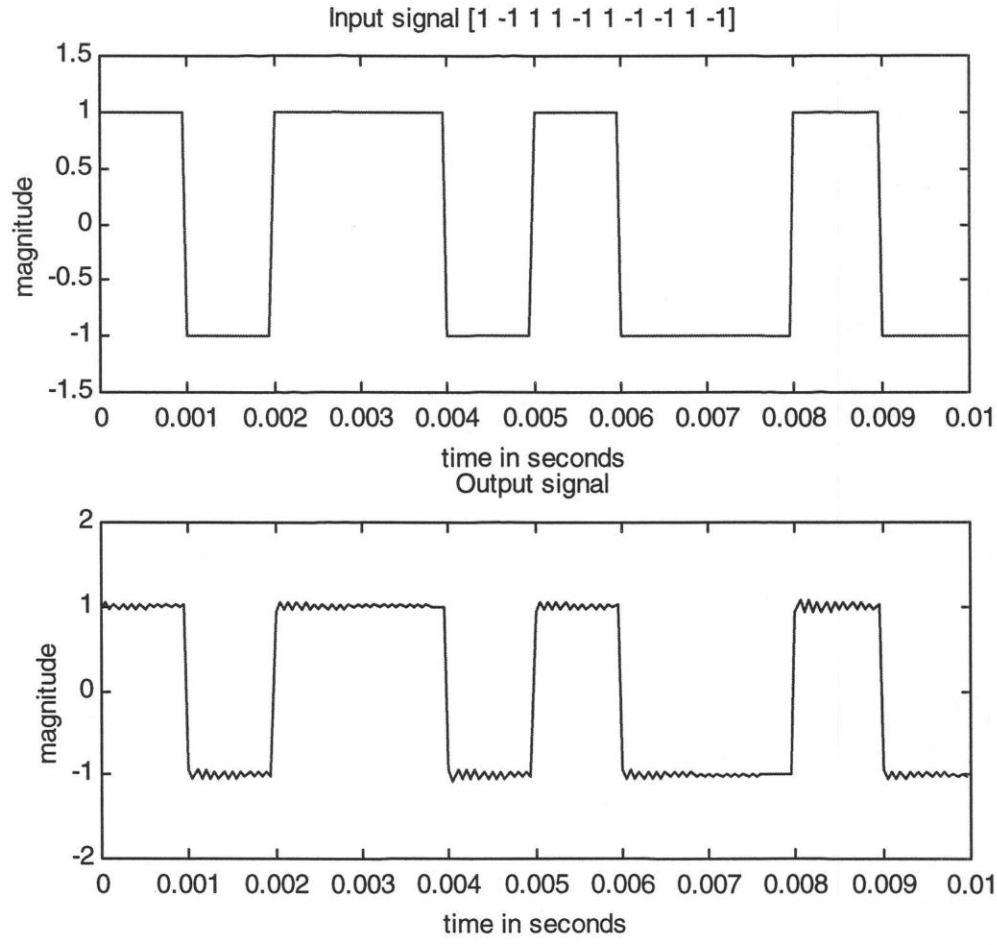

Figure 4.11 Input and output of an elliptic-function filter (BW= $10f_m$)

4.3.4 Raised Cosine Filters

As stated in the introduction of this chapter, the presence of a transmitter filter in practical radio systems is essential to save spectrum. However, such band-limitation could degrade the transmission performance due to intersymbol interference (ISI). Therefore, one has to reduce the signal bandwidth as much as possible without producing any ISI [10]. Nyquist was the first to solve the problem of overcoming ISI while keeping the transmission bandwidth low. The most popular pulse shaping filter used in mobile communications

which satisfy Nyquist criterion (see appendix D for more information about Nyquist criterion) is the raised cosine filter. A raised cosine filter belongs to the class of FIR filters.

The transfer function of a raised cosine filter is given by [3]

$$H(f) = \begin{cases} T & 0 \le |f| \le (1-\alpha)/2T \\ \dfrac{T}{2}\left[1+\cos\left(\dfrac{\pi|f| - 1/(2T)+\alpha}{2\alpha}\right)\right] & (1-\alpha)/2T < |f| \le (1+\alpha)/2T \\ 0 & |f| > (1+\alpha)/(2T), \end{cases} \tag{4.20}$$

where α is the rolloff factor which ranges between 0 and 1. This transfer function is plotted in Figure 4.12 for various values of α. When $\alpha = 0$, the raised cosine rolloff filter corresponds to a rectangular filter of minimum bandwidth [3]. As seen from Figure 4.12, as the rolloff factor α increases, the bandwidth of the filter also increases.

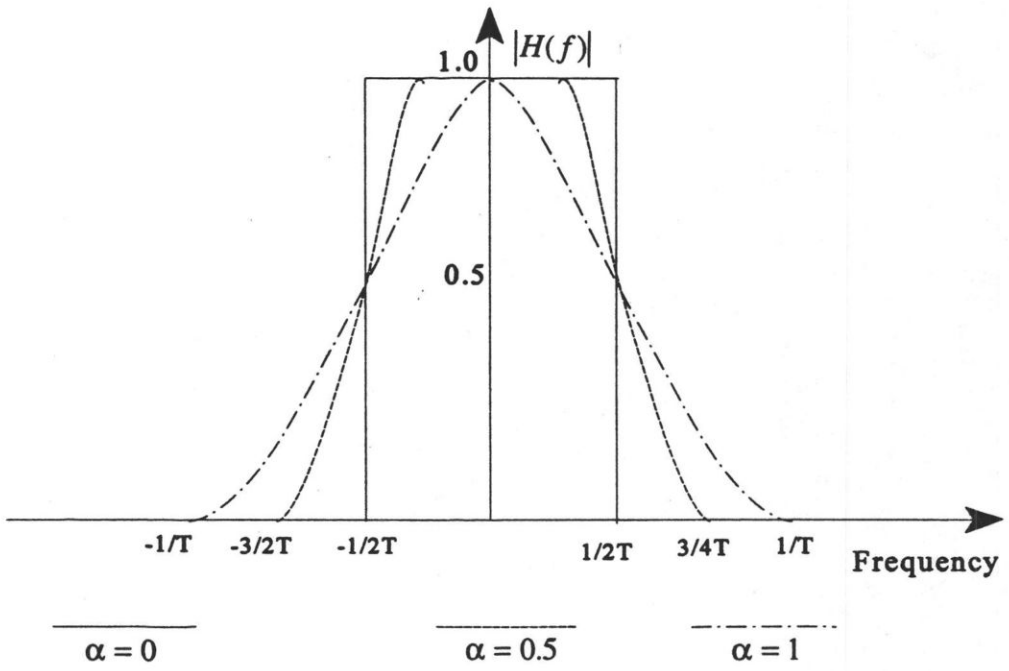

Figure 4.12 Magnitude transfer function of a raised cosine filter

The corresponding impulse response of the filter can be obtained by taking the inverse Fourier transform of the transfer function, and is given by [3]

$$h(t) = \left[\frac{\cos 2\pi\alpha t}{1-(4\alpha t)^2}\right]\left(\frac{\sin(\pi t/T)}{\pi t/T}\right). \tag{4.21}$$

This impulse response at baseband is shown in Figure 4.13 for various values of α. Notice that the impulse response decays much faster at the zero-crossing (approximately as $1/t^3$ for $t \gg T$) when compared to the ideal filter ($\alpha = 0$). The rapid time rolloff of the impulse response allows it to be truncated in time with little deviation in performance from theory [3]. This feature makes raised cosine filters (with $\alpha > 0$) satisfy Nyquist criterion and hence attractive in wireless communications applications.

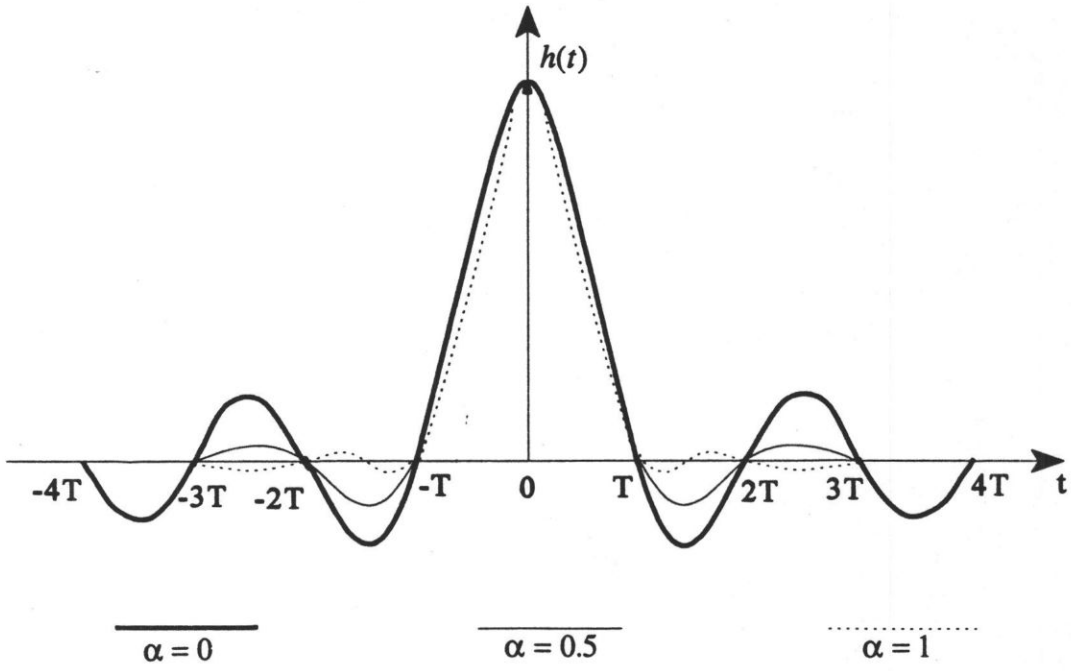

Figure 4.13 The impulse response of the raised cosine filter

Using MATLAB commands, the raised cosine filter outputs for an input of 10

rectangular pulses are obtained. For comparison, two cases of filter bandwidth are considered; $BW = 1.5f_m$, $1.9f_m$, where $f_m = 1/T$ and T is the duration of the input rectangular pulse. These are shown in Figures 4.14 and 4.15.

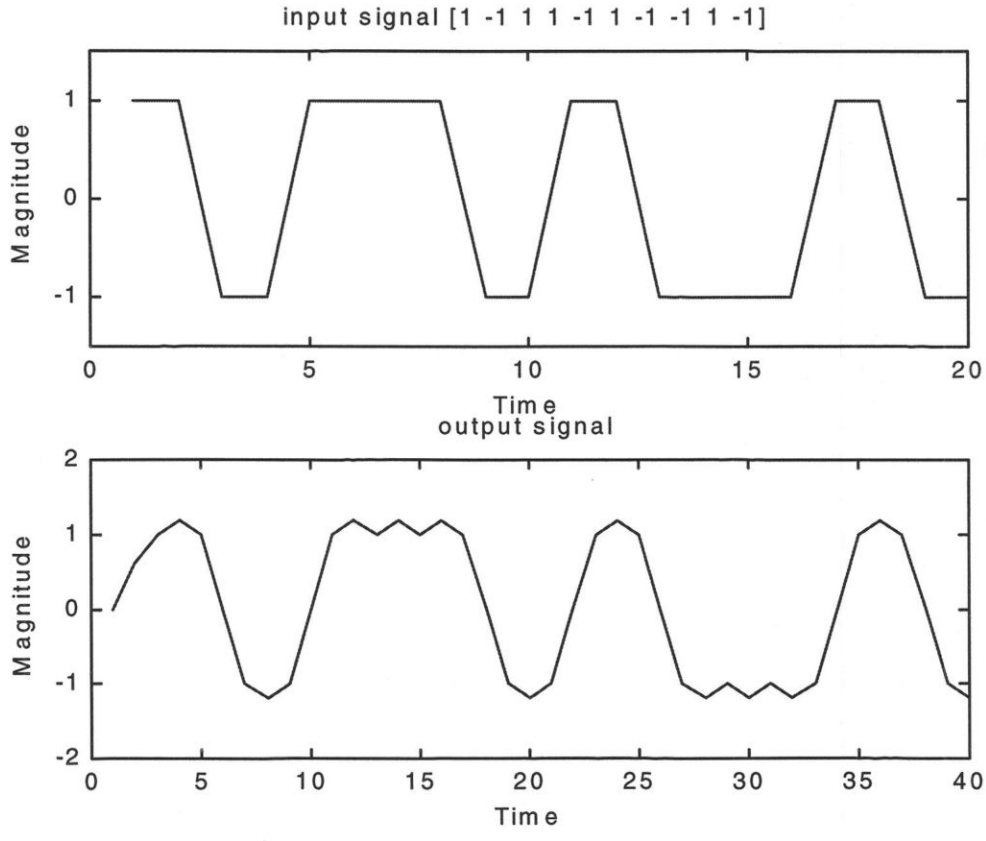

Figure 4.14 Input and output for a raised cosine filter ($\alpha = 0.5$; i.e., BW=$1.5f_m$)

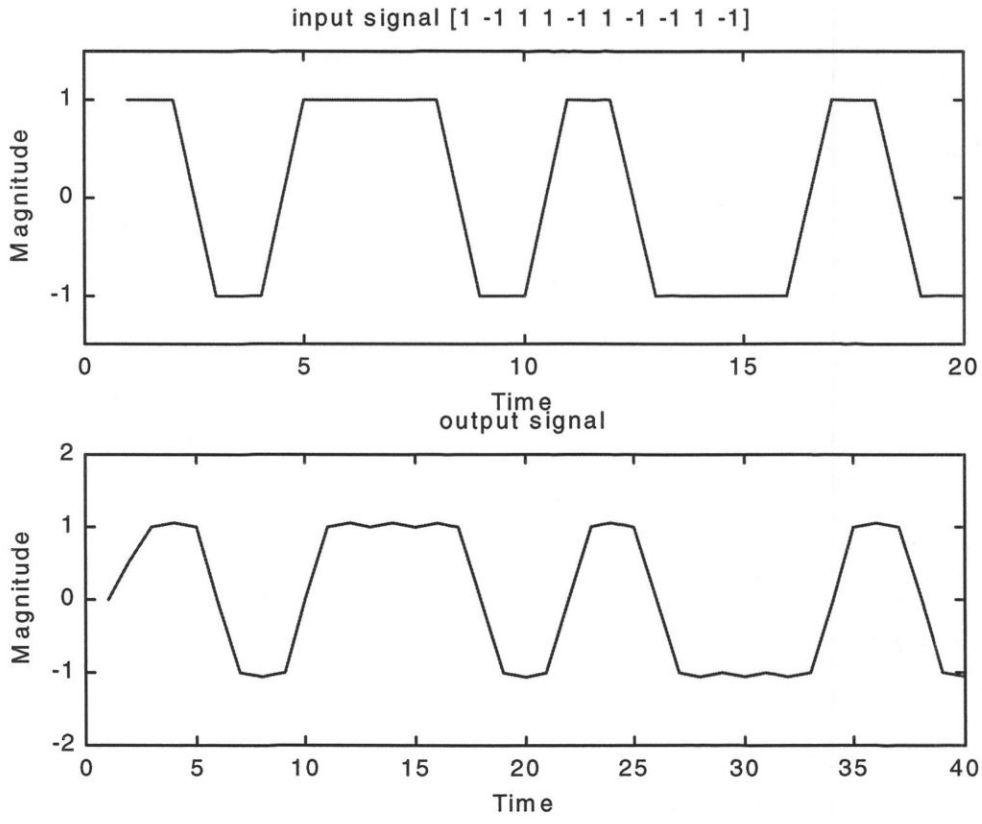

Figure 4.15 Input and output for a raised cosine filter ($\alpha = 0.9$; i.e., BW= $1.9f_m$)

4.4 Signal -to- Noise Ratio (SNR) Analysis

The system under consideration in this analysis is a wireless code division multiple access (CDMA) that supports K simultaneous and asynchronous users . The analysis reported in this section closely follows that in [30] with a difference of considering the BPSK modulation instead of quadrature phase-shift keying (QPSK) and minimum-shift keying (MSK). A block diagram of BPSK DS/CDMA system model is shown in Figure 4.16. The function that spreads the k^{th} user's signal, in the transmitter side, is denoted by $a(t)$. The chip widths of the binary (rectangular pulses) spreading function are generically

denoted T_c, where $T_c \ll T_b$(the data bit duration). As it is shown in Figure 4.16, the transmitter includes a low pass filter for the primary purpose of limiting the out-of-band signals. This filter can also be used to shape the in-band spectrum to minimize the effect of co-user interference [30].

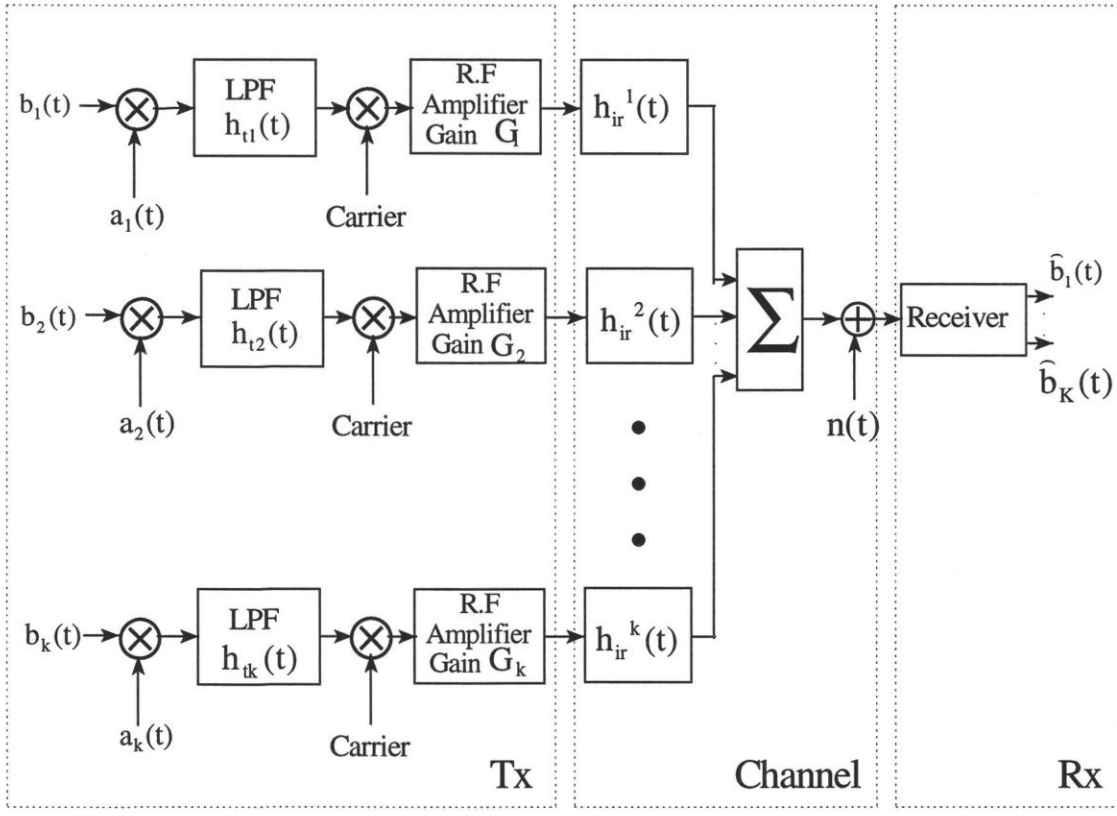

Figure 4.16 General structure for a BPSK DS/CDMA system

The lowpass equivalent impulse response of the channel for the k^{th} user is assumed to be

$$h_{ir}^{k}(t) = \sum_{l=1}^{L_k} \beta_{lk}\,\delta(t-\tau_{lk})\,e^{-j\phi_{lk}}, \qquad (4.22)$$

where l is an integer variable used to index the paths that link user k to the receiver (a single path is assumed in this thesis; i.e $l=1$) and β_{lk}, τ_{lk}, and ϕ_{lk} are the gain, delay, and phase of path l for the k[th] user. Throughout this analysis, it is assumed that the phase ϕ_{lk} is a uniform $[0, 2\pi)$ random variable independent of all gains and delays and all other phases. Delays τ_{lk} for $l=1, 2, \ldots L_k$ and $k=1, 2, \ldots K$ and the gain β_{lk} are also assumed to be independent random variables.

The structure of a generalized BPSK DS/CDMA receiver is shown in Figure 4.17. Since the received signal is in a complex form it should be multiplied by the complex conjugate of the channel phase to make it real. The filters in the receiver, denoted by $h_r(t)$, must have the same characteristics as the low pass filter in the transmitter for the receiver to be matched. To make sure the analysis holds for a practical situation where a simple receiver has a filter that does not perfectly match the filter in the transmitter, the effect of

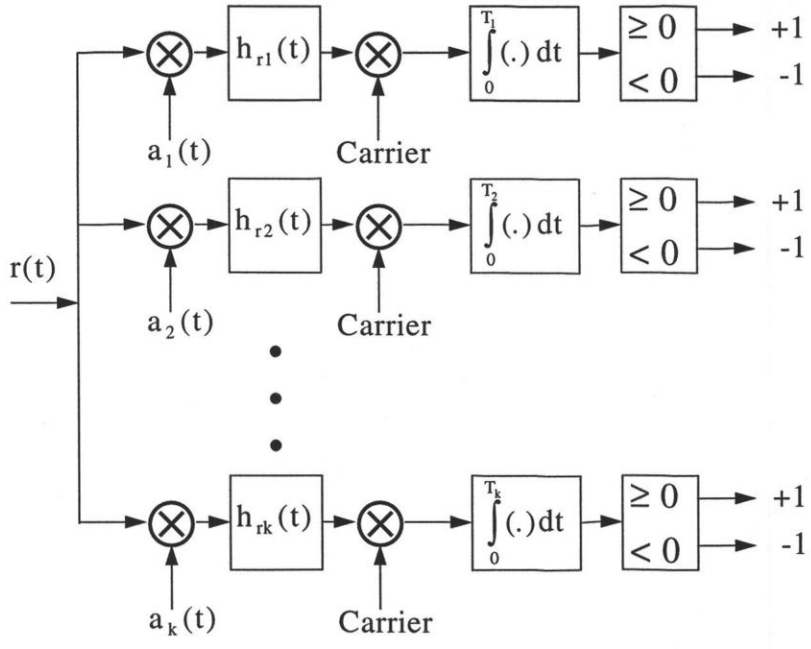

Figure 4.17 General structure for a BPSK DS/CDMA receiver

filters in the receiver and transmitter are considered separately in this analysis.

Without loss of generality, user 1 can be the reference user. The performance of user 1's receiver is now analyzed. The received signal may be given by

$$r_{tot}(t) = r(t) + n(t), \tag{4.23}$$

where $r(t)$ is component due to the transmission of the K users, while $n(t)$ is the component due to background and thermal noise. The component of the lowpass equivalent received signal may be expressed as [30]

$$r(t) = \sum_{k=1}^{K} G_k \beta_k e^{-j\phi_k} \int_{-\infty}^{\infty} [b_k(t - \tau_{lk} - \tau)]\,[a_k(t - \tau_{lk} - \tau)]\,[h_{tk}(\tau)]\,d\tau, \tag{4.24}$$

where $b_k(t)$ is the data signal waveform of the kth user and $h_{tk}(t)$ is the impulse response of the kth transmitter filter.

Perfect power control is assumed for this system . In other words, the power of each co-user is controlled so that the total received energy per bit is the same for every user. The power is controlled through the transmitter parameter G_k so that

$$G_k^2 \beta_k^2 = \mu\ R_k, \tag{4.25}$$

where μ is a constant and R_k is the rate of the user k. To reduce the number of symbols in the analysis, the constant μ is set to 1 second per bit which, in combination with the units of R_k (bits per second), leaves a unitless gain. In practical wireless systems, different users may have different data rates, R_k.

For sake of simplicity, the analysis focuses on the ability of the receiver to recover a particular bit. The bit is chosen at random which received via path j between times 0 and T_1. The expression for the received decision variable can be given by [30]

$$z_{jl} = \int_0^{T_1} [\Re\{r(t)\}\,(a_1(t) \star h_{rk}(t))]dt, \tag{4.26}$$

where $\Re\{.\}$ is operator that take the real part of a complex function and "$\star$" denotes convolution. Assuming the data bit is a 1, the signal component of z_{jl} can be given by [30]

$$\begin{aligned} z_{jls} &= G_1\beta_{jl}\int_0^{T_1}[a_1(t)\star h_{tl}(t)][a_1(t)\star h_{rl}(t)]\,dt \\ &= G_1\beta_{jl}\int_{-\infty}^{\infty}\int_{-\infty}^{\infty}\left\{\int_0^{T_1} a_1(t-\tau)a_1(t-\lambda)\,dt\right\}h_{tl}(\tau)h_{rl}(\lambda)\,d\tau\,d\lambda\,. \end{aligned} \tag{4.27}$$

The result of (4.27) is a random variable whose statistics depend on the product $G_1\,\beta_{jl}$ and also on the variation in the in-band power caused by the lowpass filtering of the spreading function. Since a perfect power is assumed in this analysis, the changes in the instantaneous power caused by lowpass filtering process would be the main factor that can affect the receiver decision variable given in (4.27).

The variation in the energy per bit due to filtering depends on the spreading gain and the filter bandwidth [30]. Consider the Fourier series representation of a PN-modulated data bit. The energy in this bit after filtering is the sum of the Fourier components inside the bandwidth. This can be explained by the following [31]:

If the input to a network (filter in this case) is a periodic signal with a spectrum given by

$$X(f) = \sum_{n=-\infty}^{n=\infty} c_n \delta(f - nf_o), \tag{4.28}$$

where $\{c_n\}$ are the complex Fourier coefficients of the input signal, the spectrum of the periodic output signal is

$$Y(f) = \sum_{n=-\infty}^{n=\infty} c_n H(nf_o)\,\delta(f - nf_o), \tag{4.29}$$

where $H(nf_o)$ and f_o are the transfer function and the cutoff frequency of the filter, respectively. Then the energy can be obtained by Parseval's theorem

$$E = \int_{-B}^{B} |Y(f)|^2 df, \tag{4.30}$$

where B is the filter's bandwidth.

Now, assuming a long PN sequence, the Fourier coefficients will vary from bit to bit depending on the segment of the PN sequence used to modulate the bit. Thus, the energy per bit is a random variable. Furthermore, the variation in the energy per bit will decrease as the number of the Fourier components inside the bandwidth increase due to the averaging effect. Based on the fact that the number of Fourier components is equal to the spreading gain, there should be relatively little variation for large spreading gains [30]. As explained in [30], the bandwidth of the system also affects the variation in energy per bit since decreasing the bandwidth increase the variation in Fourier components inside the bandwidth. The results in [30] shows a low values of the coefficient of variation were obtained for a high spreading gain and hence, for practical systems that have a high

spreading gain, this filter-induced variation will not have a significant effect on the SNR analysis. Therefore, the variation in received energy per bit due to filtering can be ignored.

The signal component of the decision variable of the path j receiver can be now expressed in terms of power spectra. The received energy per bit is simply given by T_1 times the power in the filtered process. Therefore, (4.27) can be rewritten as [30]

$$\begin{aligned} z_{j1s} &= T_1 G_1 \beta_{j1} [R^{(1)}(\tau)] \star h_{t1}(\tau) \star h_{r1}(-\tau)\big|_{\tau=0} \\ &= T_1 G_1 \beta_{j1} \frac{1}{2\pi} \int_{-\infty}^{\infty} [P^{(1)}(\omega)] H_{t1}(\omega) H_{r1}(-\omega) d\omega , \end{aligned} \tag{4.31}$$

where $R^{(k)}(\tau)$ is the auto-correlation function for user k's spreading function given by $R^{(k)}(\tau) = E[a_k(t) a_k(t-\tau)]$, $P^{(k)}(\omega)$ is the two-sided power spectral density of user k's spreading function, and $H_{tk}(\omega)$ and $H_{rk}(\omega)$ are the Fourier transforms of $h_{tk}(\tau)$ and $h_{rk}(\tau)$, respectively.

The decision variable of the receiver, which is the weighted output of the single path receiver, is given by

$$\begin{aligned} z_{1s} &= G_1 \beta_1 z_{j1s} \\ &= T_1 G_1^2 \beta_1^2 \frac{1}{2\pi} \int_{-\infty}^{\infty} [P^{(1)}(\omega)] H_{t1}(\omega) H_{r1}(-\omega) d\omega . \end{aligned} \tag{4.32}$$

Then, using (4.25), this becomes

$$z_{1s} = \frac{1}{2\pi} \int_{-\infty}^{\infty} [P^{(1)}(\omega)] H_{t1}(\omega) H_{r1}(-\omega) d\omega . \tag{4.33}$$

Similarly, the component of the path j receiver output due to co-users 2 through K

is expressed as [30]

$$z_{j1cu} = \sum_{k=2}^{K} G_k \beta_k \int_0^{T_1} [y_k(t)\cos\phi_k]\, dt\,, \tag{4.34}$$

where

$$y_k(t) = \int_{-\infty}^{\infty}\int_{-\infty}^{\infty} [b_k(t-\tau_{lk}-\tau)\, a_k(t-\tau_{lk}-\tau)]\,[a_1(t-\lambda)]\,[h_{tk}(\tau)h_{r1}(\lambda)]d\tau\, d\lambda. \tag{4.35}$$

As stated in [30], the random variable z_{j1cu} would be the integral of a stationary stochastic process. Then, the variance of z_{j1cu} may be given by [30]

$$\sigma_{jcu}^2 = T_1 \sum_{k=2}^{K} G_k^2\, \beta_k^2 \int_{-T_1}^{T_1} \left(1 + \frac{|\tau|}{T_1}\right) C_k(\tau)\, d\tau\,, \tag{4.36}$$

where $C_k(\tau)$ is the auto-covariance of the integral in (4.34) and given by

$$C_k(\tau) = \frac{1}{2} E[y_k(t)\, y_k(t-\tau)]\,. \tag{4.37}$$

As can be seen from (4.35), the statistical properties of the product of user k's data waveform and user k's spreading function would be the only factor that influence the expectation in (4.37). The effect of the data waveform on the statistics of the product

depends on the synchronization between user k's data and the spreading function used to spread the data. Assuming that the user k's spreading function is a random sequence of chips, where the chip rate is an integer multiple of the data rate, and the spreading function is phase synchronized to the data waveform so that the transitions in the data waveform coincide with chip boundaries. In this case, their will be no effect. That is because the product of user k's data and the spreading function used to spread the data is again a random sequence of chips for any data sequence [30]. Furthermore, there is a possibility that the data waveform and the spreading function are not synchronized. Having this, the phase difference between them is a random variable and hence they can be considered as independent stochastic process. It is also known that the auto-correlation function of user k's waveform is wider than that of user k's spreading function (assuming that the chip duration, T_c, « data bit duration, T_b). Thus, the auto-correlation function of the product is nearly the same as that of the spreading function [30].

For the above reasons, it can be assumed that the product of user k's spreading function and the data waveform $b_k(t)$ does not change the statistics. Then, using (4.35), the expectation in (4.37) is given by

$$E[y_k(t)\, y_k(t-\tau)] = [R^{(1)}(\tau) \star h_{rl}(\tau) \star h_{rl}(-\tau)]\, [R^{(k)}(\tau) \star h_{tk}(\tau) \star h_{tk}(-\tau)]\,. \qquad (4.38)$$

By taking advantage of some of the properties of practical spreading functions, it is possible to simplify (4.36). First, the auto-correlation of the spreading function used by all users is zero for $|\tau| \succ T_c$, where T_c is the chip duration, i.e., $R^{(k)}(\tau) = 0$ for $\tau \succ T_c$. Second, since the filtered spreading function has an auto-correlation function with its area concentrated near the origin in an interval that is much less than T_k for all k, the area under $C_k(\tau)$ is concentrated near the origin in an interval where $|\tau| \ll T_1$ (or $|\tau|/T_1 \ll 1$). Therefore, the $(|\tau|/T_1)\, C_k(\tau)$ term does not contribute significantly to the variance of z_{jlcu} in (4.34) and can be ignored (noting that $(|\tau|/T_1) \ll 1$ in the interval where $C_k(\tau)$ is concentrated) [30].

Using these simplification and substituting (4.38) into (4.37) and then into (4.36)

yields

$$\begin{aligned}\sigma_{jcu}^2 &= T_1 \sum_{k=2}^{K} G_k^2 \beta_k^2 \int_{-\infty}^{\infty} C_k(\tau)\, dt \\ &= \frac{T_1}{2} \sum_{k=2}^{K} G_k^2 \beta_k^2 \int_{-\infty}^{\infty} [R^{(1)}(\tau) \star h_{rk}(\tau) \star h_{rk}(-\tau)] \\ &\quad [R^{(k)}(\tau) \star h_{tk}(\tau) \star h_{tk}(-\tau)] d\tau.\end{aligned} \tag{4.39}$$

Based on the fact that the area under an autocorrelation is the dc value of the power spectral density, (4.39) can be expressed as [30]

$$\begin{aligned}\sigma_{jcu}^2 &= \frac{T_1}{2} \sum_{k=2}^{K} G_k^2 \beta_k^2 \frac{1}{2\pi} [P^{(1)}(\omega) H_{r1}(\omega) H_{r1}(-\omega)] \\ &\quad \star [P^{(k)}(\omega) H_{t1}(\omega) H_{t1}(-\omega)]\big|_{\omega=0} \\ &= \frac{T_1}{2} \sum_{k=2}^{K} G_k^2 \beta_k^2 \frac{1}{2\pi} \int_{-\infty}^{\infty} [P^{(1)}(\omega) H_{r1}(\omega) H_{r1}(-\omega)] \\ &\quad [P^{(k)}(\omega) H_{t1}(\omega) H_{t1}(-\omega)] d\omega\,,\end{aligned} \tag{4.40}$$

where $P^{(k)}(\omega)$ is the two-sided power spectral density of user k's spreading function. Assuming the spreading functions for all k users have the same power spectral densities denoted $P(\omega)$, and assuming $H_{rk}(\omega) = H_r(\omega)$ and $H_{tk}(\omega) = H_t(\omega)$ for all k, then using (4.25) the expression in (4.40) reduces to

$$\sigma_{jcu}^2 = \frac{T_1}{2} \sum_{k=2}^{K} R_k \frac{1}{2\pi} \int_{-\infty}^{\infty} P^2(\omega) |H_r(\omega)|^2 |H_t(\omega)|^2 d\omega\,, \tag{4.41}$$

which is the variance due to the co-users at the output of user 1's path j receiver prior to

weighting by $G_1\beta_1$.

The variance of the weighted output of the receiver is given by

$$\sigma_{cu}^2 = G_1^2 \beta_1^2 \sigma_{jcu}^2 \tag{4.42}$$

which, using (4.25), becomes

$$\sigma_{cu}^2 = R_1 \sigma_{jcu}^2 \tag{4.43}$$

and substituting for σ_{jcu}^2 from (4.41), gives

$$\sigma_{cu}^2 = \frac{1}{2} \sum_{k=2}^{K} R_k \frac{1}{2\pi} \int_{-\infty}^{\infty} P^2(\omega) |H_r(\omega)|^2 |H_t(\omega)|^2 d\omega \,. \tag{4.44}$$

From (4.33) and (4.44), the signal-to-noise ratio of the decision variable, considering only the co-user noise, is then expressed as [30]

$$SNR = \frac{z_{1s}^2}{\sigma_{cu}^2} = \frac{\frac{1}{\pi}\left[\int_{-\infty}^{\infty} P(\omega) H_t(\omega) H_r(-\omega) d\omega \right]^2}{\sum_{k=2}^{k} R_k \int_{-\infty}^{\infty} P^2(\omega) |H_r(\omega)|^2 |H_t(\omega)|^2 d\omega} \,. \tag{4.45}$$

It should be pointed out here that the SNR expression in (4.45) was developed under the assumption that the power received from each user is controlled in proportion to bit rate and does not depend on the absolute levels of the received signals.

The thermal noise, denoted by $n(t)$ in (4.23), normally has a lower spectral density

than the co-user noise [30]. In situations where it is significant, the thermal noise will be independent and can be added straight forward. Then, the system SNR can be given by

$$SNR_{sys} = \left[\frac{1}{SNR} + \frac{1}{SNR_{noise}} \right]^{-1}. \tag{4.46}$$

Using the approach that led to (4.44), considering a thermal noise instead of co-user noise, an equation for SNR_{noise} can be given by [30]

$$SNR_{noise} = \frac{\frac{T_1}{\pi}\left[\int_{-\infty}^{\infty} R_1 P(\omega) H_t(\omega) H_r(-\omega) d\omega \right]^2}{\int_{-\infty}^{\infty} P_{noise}(\omega) R_1 P(\omega) |H_r(\omega)|^2 d\omega}, \tag{4.47}$$

where $P_{noise}(\omega)$ and $R_1 P(\omega)$ are the lowpass equivalent power spectra of the thermal noise and user 1's signal at the input to the receiver, respectively.

The SNR expression given by (4.45) depends on the filter responses $H_r(\omega)$ and $H_t(\omega)$. By using Schwarz's inequality (see appendix E), it can be shown that, if the noise is either insignificant or has a white spectrum, then the frequency responses that maximize the system SNR are given by

$$H_r(\omega) = H_t(\omega) \tag{4.48}$$

and

$$|H_t(\omega)|^2 = \begin{cases} \dfrac{constant}{P(\omega)}, & |\omega| \le B \\ 0, & otherwise. \end{cases} \tag{4.49}$$

In other words, the filters should flatten or "whiten" the in-band portion of the spectrum of the spreading function. Substituting (4.49) into (4.45) produces an expression for the optimum SNR for receiver decision variable for K simultaneous users (see appendix E)

$$SNR_{opt} = \frac{4B}{\sum_{k=2}^{K} R_k}, \tag{4.50}$$

where B is the baseband bandwidth of the filtered spreading function, which translates to an RF bandwidth of $2B$. In the presence of white thermal noise with two-sided spectral density $N_o/2$, SNR_{opt} is [30]

$$SNR_{opt} = \left[\frac{\sum_{k=2}^{K} R_k}{4B} + \frac{No}{2E_b} \right]^{-1}, \tag{4.51}$$

where E_b is the received energy per bit.

Based on (4.51), it is possible to calculate the bit error probability by taking advantage of one of the spread spectrum properties. In spread spectrum, it can be assumed that B^{-1} is smaller than $1/R_k$ by a factor of the spreading gain (i.e., $B \succ R_k$). Therefore, for a large spreading gain (or large B) and one co-user, (4.51) may be simplified to

$$SNR_{opt} = \left(\frac{2E_b}{N_o} \right) \tag{4.52}$$

which has associated error probability $P_e = Q_f(2E_b/N_o)$ [24]. In general, for more than one co-user, the error probability will not be exactly $Q_f(SNR_{opt})$, but this is a good approximation for values of B and R_k of interest in practical systems. Thus, the error probability for the general case of (4.51) may also be expressed as

$$P_e \approx Q_f\left(\left[\frac{\sum_{k=2}^{K} R_k}{4B} + \frac{No}{2E_b}\right]^{-1}\right). \tag{4.53}$$

4.5 Computed results

The performance results for both the bit error rate and signal to noise ratio were computed using the analysis reported in section 4.4. These results are plotted in Figures 4.18 and 4.19 as a function of the channel bandwidth. The number of users, K, is once again treated as a parameter. The results were computed for different users data rates as this scenario is closer to the practical reality. For example in the CDMA cellular system standard IS-95, the user data rates of 1200, 2400, 4800, and 9600 bps are supported. Use of different data rate which depends on the speech activity of the digitized voice results in reducing the impact of the multiuser interference in a CDMA system. This reduction may be used to improve the system capacity. It may be seen from the Figure 4.18 that the SNR increases as the bandwidth increases. This is because of the fact that increasing the processing gain (i.e., increasing *N*), in a spread spectrum system, reduces the effect of multiuser interference which result in increasing signal to noise ratio (SNR). It can also be seen from Figure 4.18 that as the number of users increase the SNR performance degrades. It may be also noticed from Figure 4.19 that, the error probability improves as the bandwidth increases (i.e., as spreading gain increases). For the values of bandwidth less than 300 kHz, the error probability increases quite rapidly. For the values of bandwidth more than 300 kHz, this improvement is more gradual.

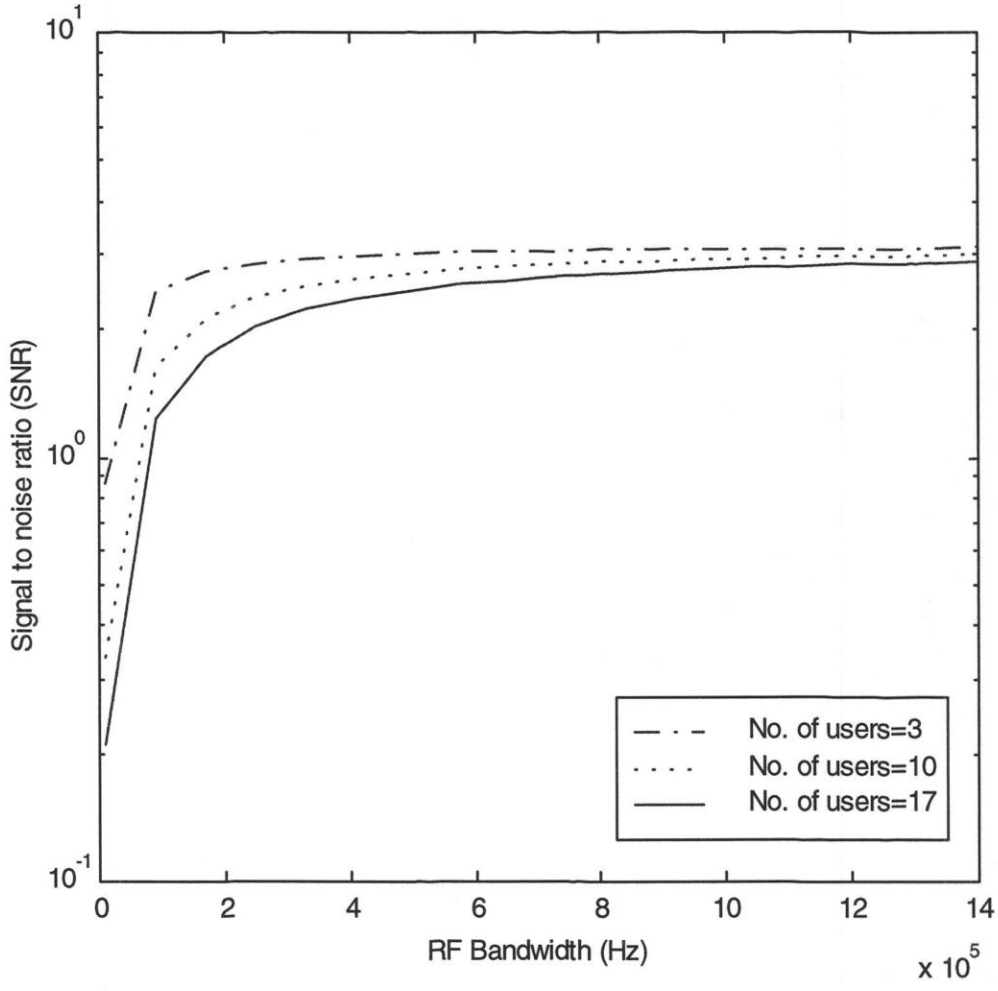

Figure 4.18 Signal to noise ratio (SNR) as a function of RF bandwidth

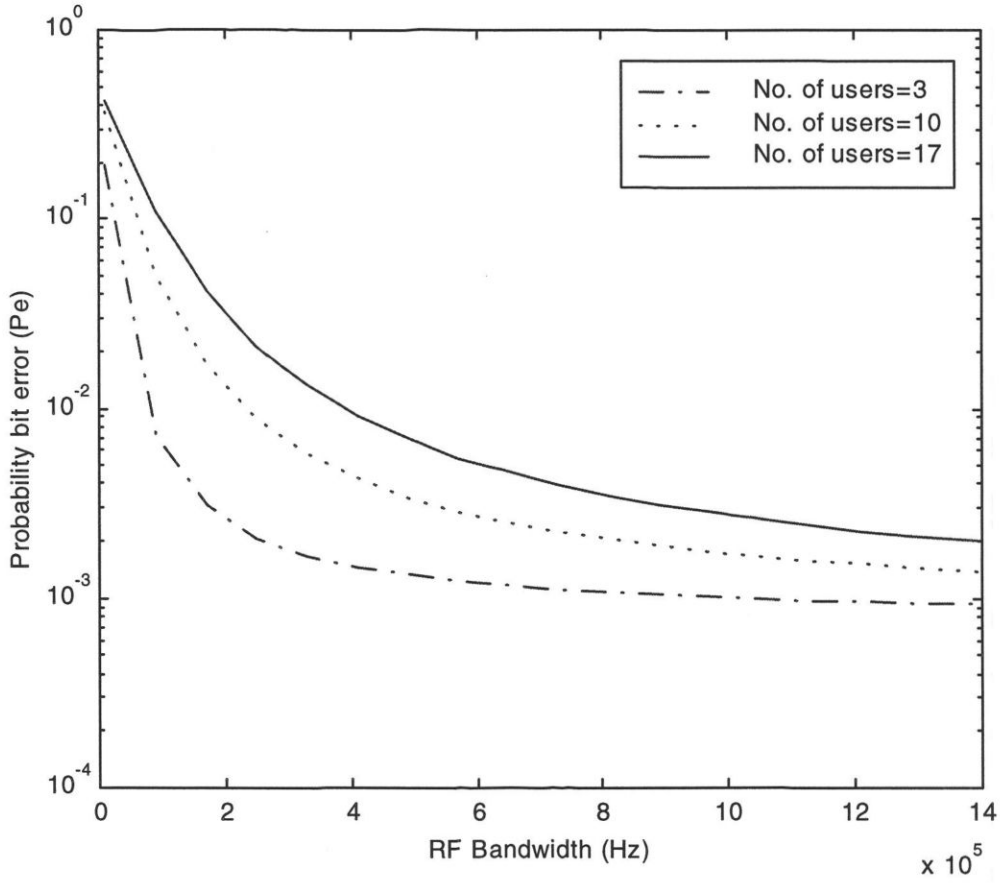

Figure 4.19 Probability bit error (Pe)as a function of RF bandwidth

5. BER Performance Simulation Results

5.1 Introduction

In chapters one to three, different issues of concern for wireless DS/CDMA communication systems were described. Spread spectrum, CDMA structure, and CDMA performance were among those issues of concern. In chapter four, the effects of filtering on the performance of DS/CDMA system were discussed. Some of practical filter types such as Butterworth, Chebyshev, elliptic-function, and raised cosine filters were explained in section 4.3, and the system model and the SNR analysis were described in section 4.4.

It is a common practice to estimate the performance of digital communication systems by computer-aided techniques (computer simulation). Simulation techniques allow one to accurately model complex systems and channels. In this chapter, time-domain simulation programs that model and simulate the lowpass equivalent signals of BPSK DS/CDMA communication system as well as the results obtained from these programs are presented. MATLAB software is used to develop the simulation programs. These programs are used to predict the bit error probability (Bit-Error-Rate, or BER) performance of CDMA receiver structures reported in previous chapters.

5.2 Simulation Methods for Estimating BER of a CDMA System

For a digital communication system, the relevant measure of performance is always one related to the system's error-producing behavior. The BER, namely, the fractional number of errors in a transmitted sequence, is one of these performance measures that indicates the basic reliability of a system. To estimate the BER of wireless BPSK CDMA/DS receivers using simulation, there are several methods that can be used [32]. In

this thesis Monte Carlo (MC) method is used to obtain BER estimation. Before introducing (MC), some basic information on the BER estimation is given below.

Consider a binary baseband communication system whose receiver is shown in Figure 5.1a [32]. The decision process can be described in terms of probability density function (pdf), $f_o(v;\tau)$ and $f_1(v;\tau)$, of the input $V(t)$ at the sampling instant τ, given that a "zero" or a "one" was sent, respectively. These densities are shown in Figure 5.1b. For a threshold-sensing decision, an error occurs when a "zero" is sent and there is an excursion of the input sufficient to exceed V_T, the threshold; or an error will occur when a "one" is sent and disturbances induce the input to drop below V_T [32].

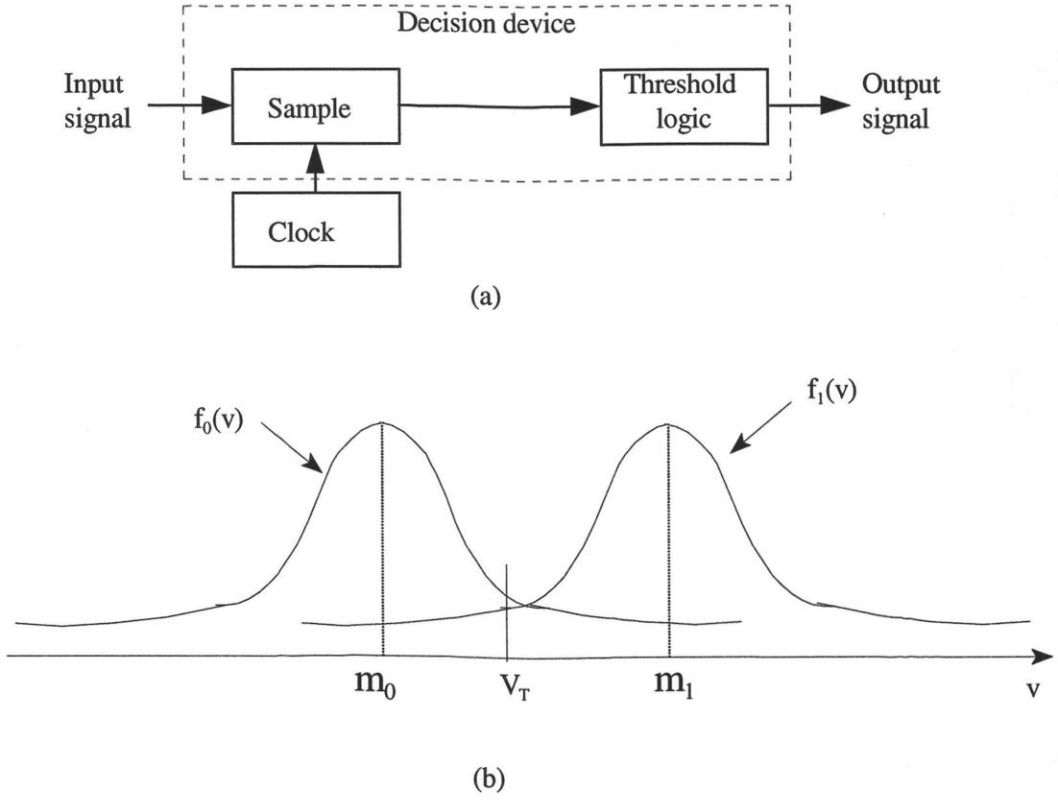

Figure 5.1 Illustration of some basic terms regarding BER estimation

(a) Typical decision mechanism in digital transmission

(b) Probability density functions

The probabilities of these occurrences are (omitting the τ-dependence for simplicity) [32]

$$P[error/one] \triangleq p_1 = \int_{-\infty}^{V_T} f_1(v)\, dv = F_1(V_T) \tag{5.1}$$

$$P[error/zero] \triangleq p_o = \int_{V_T}^{\infty} f_o(v)\, dv = 1 - F_o(V_T) \tag{5.2}$$

and the average probability of error is then

$$p_{av} = P_{e1}\, p_1 + P_{eo}\, p_o\,, \tag{5.3}$$

where P_{e1} and P_{eo} are the a priori probabilities of symbols (or bits) "one" and "zero", respectively (in most applications, the source statistics are considered to be equally likely, i.e., $P_{e1} = P_{eo} = ½$) [31]). The functions $F_1(.)$ and $F_o(.)$ are the cumulative distribution function (CDF) corresponding to $f_1(.)$ and $f_o(.)$, respectively.

As it mentioned above, Monte Carlo method is used to estimate BER of CDMA receivers in the simulation programs. "Monte Carlo" is simply a procedure of counting the number of successes (errors, in this context) and dividing by the number of trials [32]. In the applications where the source statistics are considered to be equally likely (the transmitted symbols are equally likely) and the channel is additive white Gaussian noise, the symbol error probability can be given by

$$p = \int_{-\infty}^{V_T} f_1(v)\, dv, \tag{5.4}$$

where $f_1(v)$ is the probability density function of sampled input at sampling period T given "1" was transmitted, and V_T is the threshold level for symbol decision. By defining the function

$$g(v) = \begin{cases} 1 & v \geq V_T \\ 0 & v < V_T, \end{cases} \tag{5.5}$$

(5.4) may be rewritten as

$$p = \int_{-\infty}^{\infty} g(v) f(v)\, dv. \tag{5.6}$$

Equation (5.6) is equivalent to

$$p = E[g(v)], \tag{5.7}$$

where E is expectation. Since an unbiased estimator $\hat{p}_M$ of the expectation in (5.7) is the sample mean, then $\hat{p}_M$ can be given by

$$\hat{p}_M = \frac{1}{N_M} \sum_{i=1}^{N_M} g(v_i), \tag{5.8}$$

where $v_i = v(t_i)$, t_i is the sequence of symbol-spaced instants at which decisions are made

, and N_M is the number of symbols in the sequence. From (5.8), one can see that $g(v_i)$ acts as an error detector and the summation is an error counter. Based on this equation, a simple estimator of the BER is the sample mean (if N symbols are processed through the system, out of which n are observed to be in error); i.e.

$$\hat{p}_M = \frac{n}{N_M}. \tag{5.9}$$

As $N_M \to \infty$, the estimator $\hat{p}_M$ tends to a normal distribution with mean p (i.e., $\hat{p}_M$ converges to p) and variance $(1-p)p/N_M$ [32]. This is referred to as the Monte Carlo (MC) method.

For finite N_M, the reliability of the estimator is quantified in terms of confidence intervals. Two numbers, y_- and y_+, which are functions of $\hat{p}_M$ are chosen such that with high probability, $y_+ \le p \le y_-$, and the confidence interval, $y_- - y_+$, is as small as possible. Then, the confidence level, $1-\alpha$, is defined by [33]

$$Prob[y_+ \le p \le y_-] = 1-\alpha. \tag{5.10}$$

For instance, at 95% (0.95) confidence level, a symbol size $N_M = 10/p$ (a popular rule-of-thumb is that N_M should be on the order of $10/p$ [32]) provides a confidence interval of $[1.8\,\hat{p}_M, 0.55\,\hat{p}_M]$ which has uncertainty factor of about 2 in the BER. If N_M is increased by a factor of 10, i.e., $N_M = 100/p$, then at a confidence level of 0.95, the confidence interval is narrowed to $[1.25\,\hat{p}_M, 0.8\,\hat{p}_M]$. This implies that to obtain a BER of 10^{-4}, 10^6 symbols should be processed. Thus, there is a trade-off between run time and the statistical variability.

5.3 System Model for Simulation

In order to simulate a wireless DS/CDMA system, the system elements have to be

simulated. These elements are multiple DS SS transmitters, channel, and receiver. The low-pass equivalent representation of the system is used in the simulation. The block diagram of the system used to simulate a DS/CDMA communication system is shown in Figure 5.2. Two cases are considered in the simulations: a BPSK DS/CDMA system without filters and a BPSK DS/CDMA system including filters. The system model consists of models for transmitter, channel, and receiver. Simulation is based on picking samples randomly as different input signals that model the random processes in a DS/CDMA radio system. To obtain BER estimates, the process is performed a number of times. In all of the simulations, six samples per spreading code chip are used.

The following assumptions are made in the system models for simulation:

- The data bits of the different users are independent.
- The different user transmissions are asynchronous in $[0, T_b]$, where T_b is the data bit duration.
- The channel parameters, delay and phase remain the same for a data bit duration.

Transmitter Model

As shown in Figure 5.2, the transmitter functions are represented by binary data source, spreading code, and asynchronous transmission. The data waveform and spreading code waveform are denoted as

$$b_k(t) = \sum_{i=-\infty}^{\infty} b_i^{(k)} \, p_{T_b}(t - iT_b) \tag{5.11}$$

and

$$a_k(t) = \sum_{j=-\infty}^{\infty} a_j^{(k)} \, p_{T_c}(t - jT_c), \tag{5.12}$$

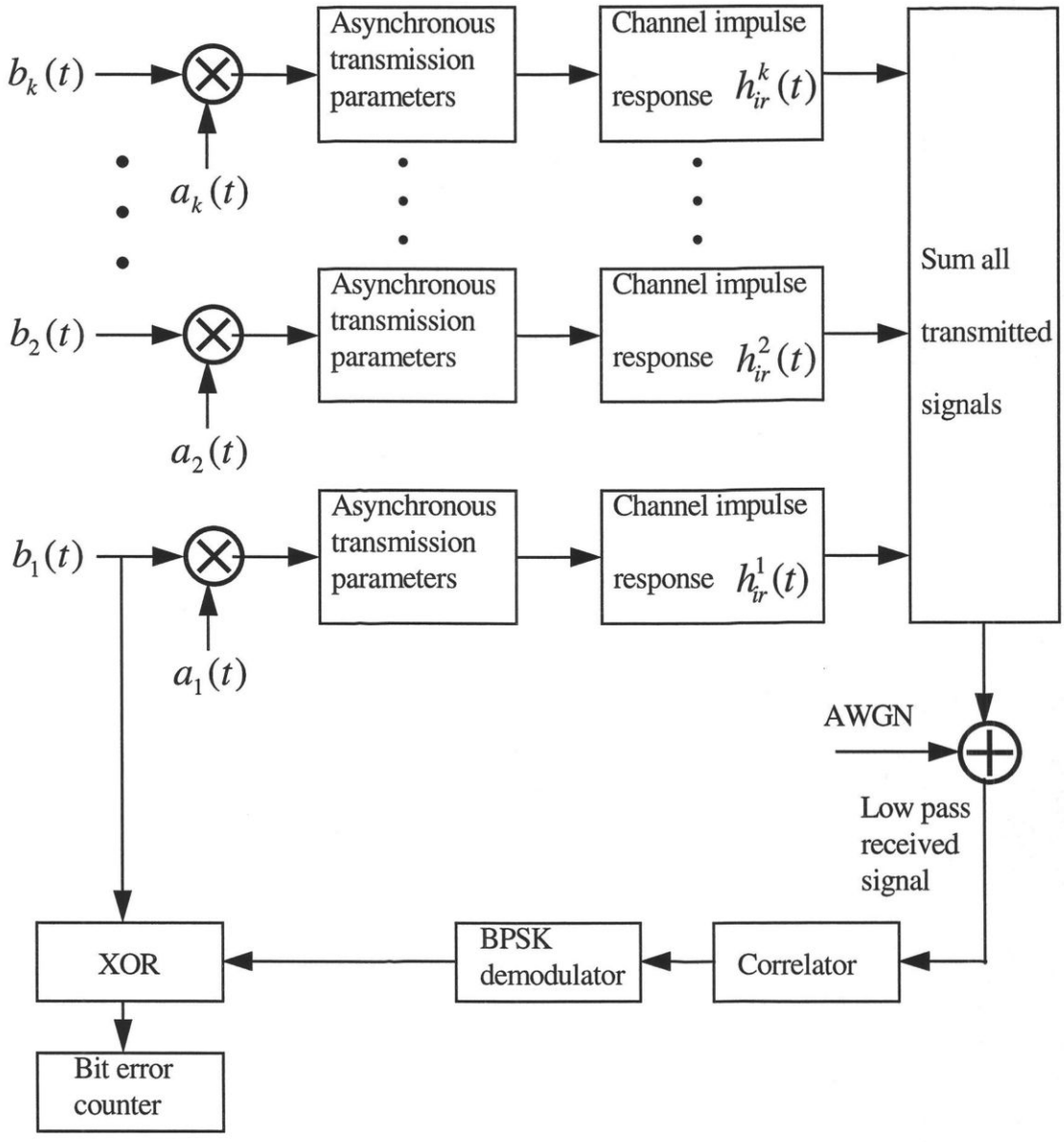

Figure 5.2 Low-pass equivalent of the CDMA system simulated to obtain the BER performance

respectively, where $b_i^{(k)} \in \{-1, +1\}$ is the i[th] data bit in the binary information sequence for user k, $a_j^{(k)} \in \{-1, +1\}$ is the j[th] chip of the k[th] user's signature sequence, and the rectangular pulse $p_{T_c}(t)$ is given by

$$p_{T_c} = \begin{cases} 1 & for\ 0 \le t \le T_c \\ 0 & otherwise. \end{cases} \tag{5.13}$$

The data bit duration T_b and the spreading code chip duration T_c are related to each other as $N = T_b / T_c$, where N is the period of the spreading code. To reduce the simulation time, $N = 31$ was used for all simulation programs. The users are assigned different spreading code sequences from a family of Gold code sequences with length of 31. It is assumed that the delay of the k[th] user's transmitter, τ_k, is an independent random variable and uniformly distributed over $[0, T_b]$. Since MATLAB software has built in functions to generate uniformly and Gaussian distributed random variables, τ_k and other needed random variables are generated using these functions. In the case of a CDMA system without filters, the spread signal is directly transmitted to the channel model, while for a CDMA system with filters , this signal is passed through a lowpass filter and then transmitted to the channel model. MATLAB functions are also used here for generating different filters to do the filtering process. These filters include Butterworth, Chebyshev, elliptic-function, and raised cosine filters.

Channel model

The complex low-pass equivalent impulse response of the channel is given by

$$h_{ir}^{k}(t) = \sum_{l=1}^{L_k} \beta_{lk} \delta(t - \tau_{lk}) e^{-j\phi_{lk}}, \tag{5.14}$$

where l is an integer variable used to index the paths that link user k to the receiver (a single path is assumed in this thesis; i.e $l = 1$), β_{lk}, τ_{lk}, and ϕ_{lk} is the gain, delay, and random phase of path l for the k[th] user. Phase ϕ_{lk} is a uniform $[0, 2\pi)$ random variable

independent of all gains and delays and all other phases. Delays τ_{lk} for $l = 1, 2, \ldots L_k$ and $k = 1, 2, \ldots K$ are also assumed to be independent random variables. The gain β_{lk} is also random variable and independent of all phases, all delays, and all other gains. However, with perfect power control assumption, the variation in the path gains are compensated through control of the R.F amplifier gain (see Figure 4.15).

Receiver model

The low-pass equivalent representation of a correlator receiver includes a correlator and a data decision stage for a CDMA system without filters , while the case of a CDMA system with filters includes a low-pass filter, correlator, and a data decision stage. To implement the function of the correlator in the simulation, the low-pass equivalent of the received signal is multiplied with a spreading code aligned with the signal. This is followed by a summation (summation is equivalent to integration) for the case of a CDMA system without filters and a summation after a filtering process in the case where filters are included. The same filter specification used in the transmitter, which is generated by MATLAB, is used in the receiver part. The hard decision stage takes a decision on the binary symbol by considering the polarity of the real part of the correlator output signal, a process equivalent to BPSK demodulation.

5.4 Program Structure

Program construction is shown in the flow chart in Figure 5.3. The first step , the initialization procedure, includes generating user spreading codes and random delays for all users as well as frame length definition in number of bits and the number of frames to be processed for obtaining BER estimates. The spreading codes are Gold code sequences of length 31 generated using two maximal length shift register (MLSR) sequences. In the second step, a loop is repeated for a sufficient number of times. This loop consists of a transmitter section, a channel section, and a receiver section. Following the receiver section, an error detector and counter stage detects and counts the number of bits in error. Based on MC simulations (section 5.2), the estimate of the BER is calculated by dividing the number

of errors by the number of bits processed.

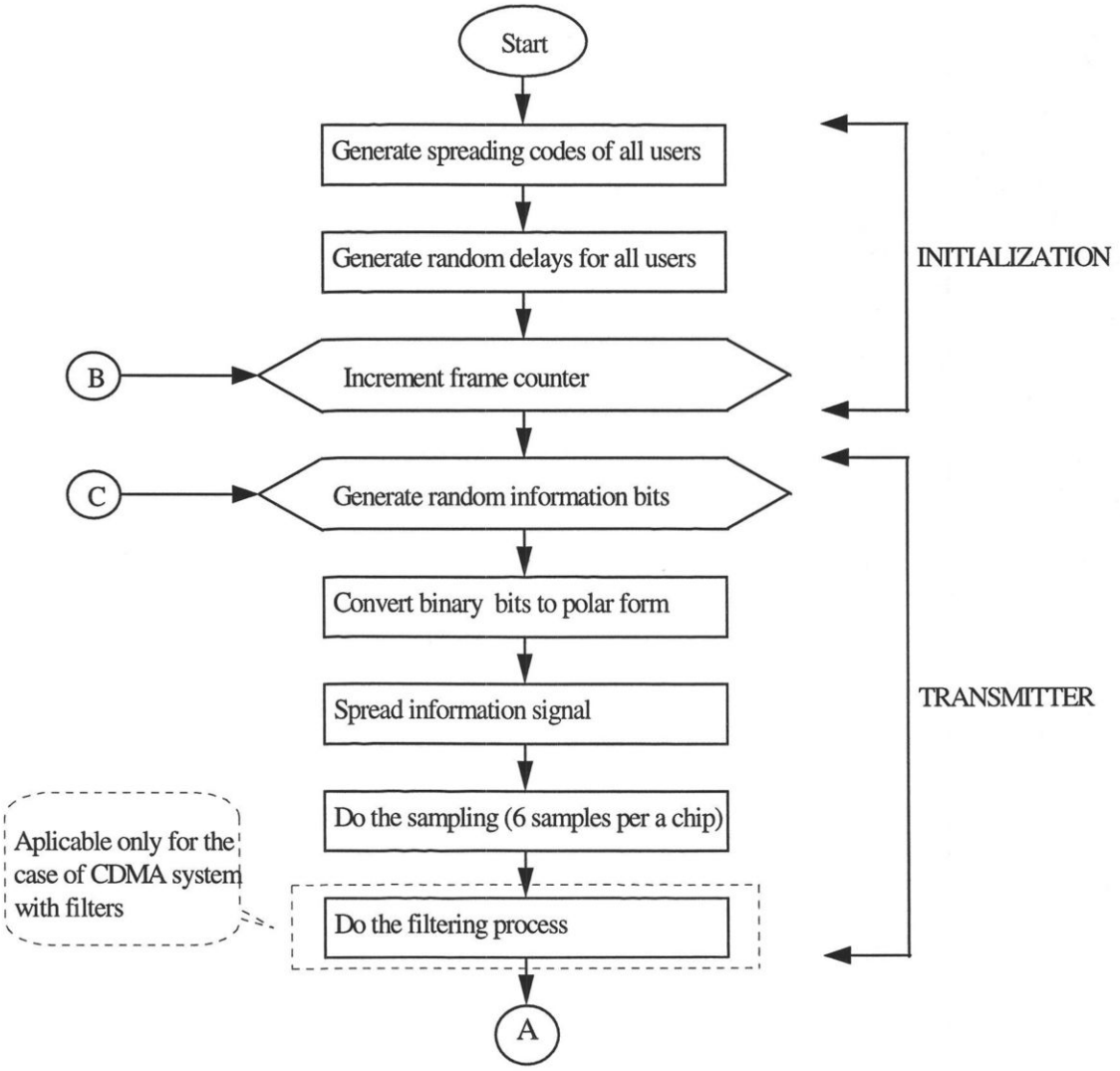

Continued ....

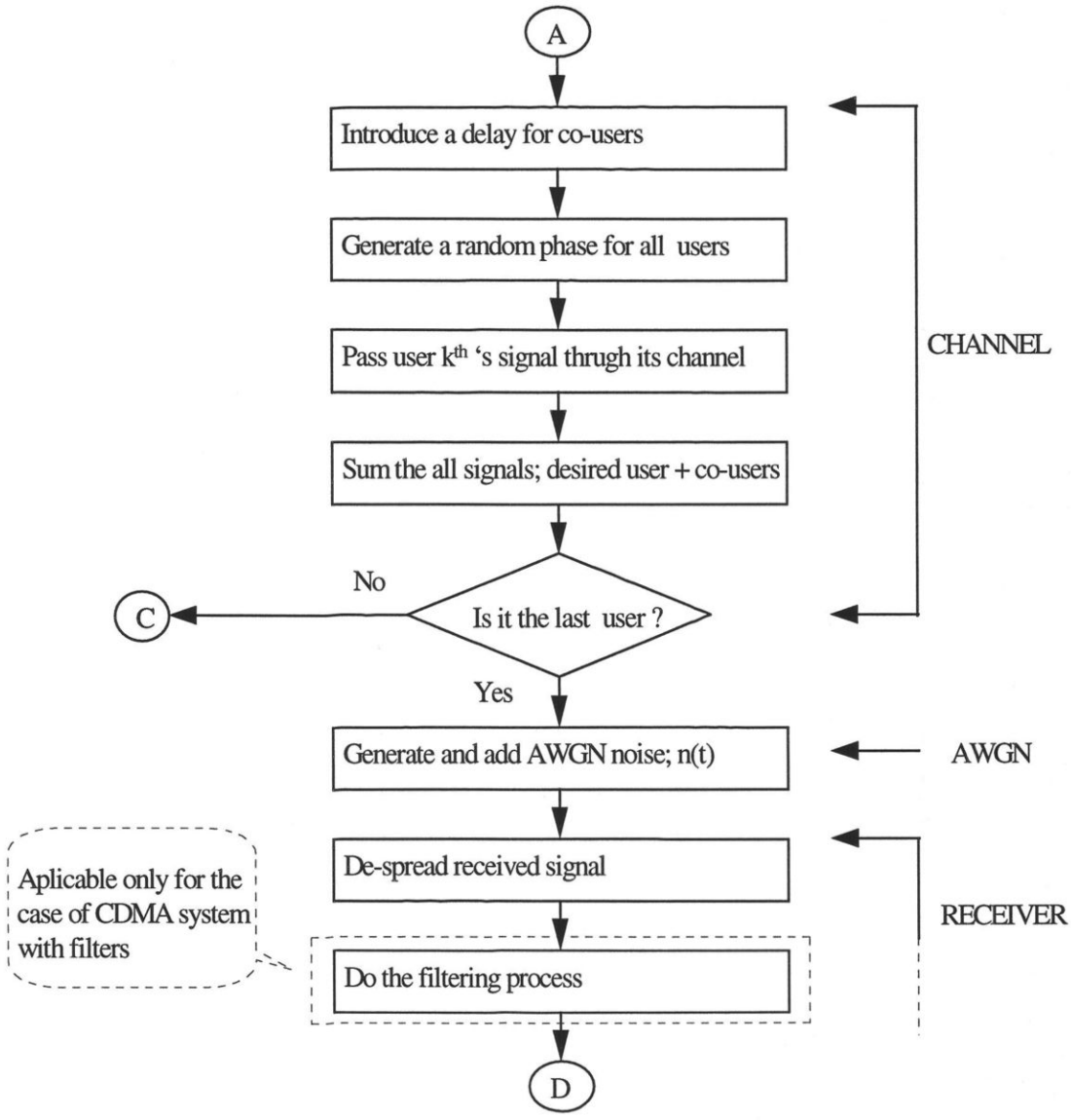
A
Introduce a delay for co-users
Generate a random phase for all users
Pass user k^th 's signal thrugh its channel
Sum the all signals; desired user + co-users
No
C
Is it the last user ?
Yes
CHANNEL
Generate and add AWGN noise; n(t)
AWGN
De-spread received signal
Aplicable only for the case of CDMA system with filters
Do the filtering process
RECEIVER
D

Continued ...

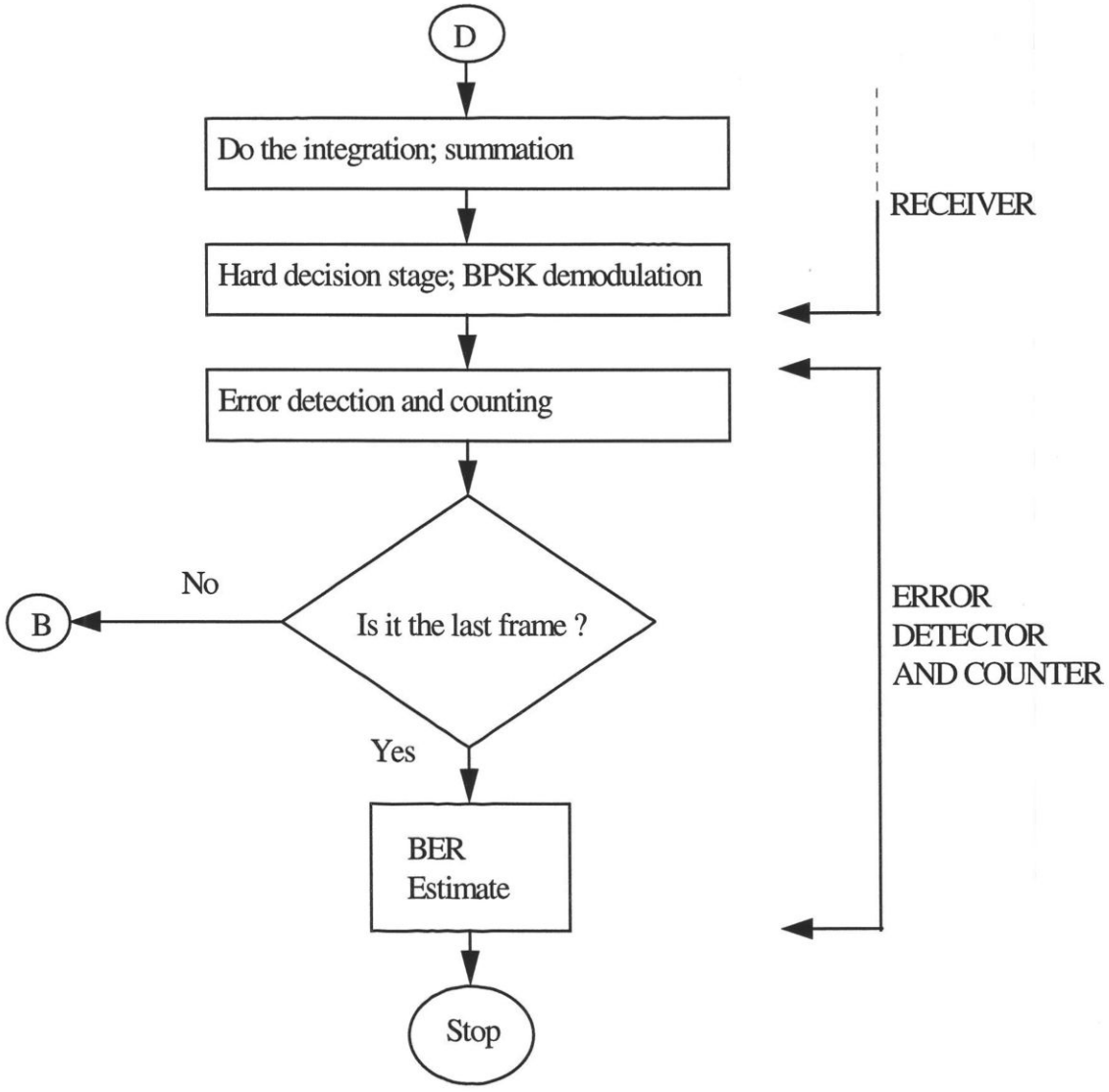

Figure 5.3 Flow chart of the simulation program for BER performance of a DS/CDMA receiver

In the transmitter section, random data frames are generated for each loop iteration, one frame each for all K users. A polar form (i.e. sequence of "1"s and "-1") of the data frame of each user is multiplied by a polar form of the corresponding spreading code sequence. This is followed by a sampling procedure where six samples per spreading code chip are used. In the case of a CDMA system with filters simulation, a filtering process is performed by passing the transmitted signals through a low-pass filter. Four different filter types are considered: Butterworth filter, Chebyshev filter, elliptic-function filter, and raised cosine filter.

In the channel section, the asynchronous nature of the user transmissions is taken into account by shifting the frames by an amount equal to their corresponding transmitter delay. A uniformly distributed phases for all K users are generated as well. White noise is also generated and added to the sum of the K user signals to obtain the total received signal at the receiver.

The received signal, in the receiver section, is passed through a correlator to reconstruct the transmitted information. The de-spreading procedure is done with the desired spreading code aligned with the received signal. This is followed by filtering process, in a CDMA system with filters case, summation and data hard decision. The hard decision stage decides in favor of a bit "1" if the real part of the correlator is positive and in favor of a bit "0" if the real part of the correlator is negative.

5.5 Simulation Results

The complete wireless CDMA system is simulated and the BER performance is evaluated using Monte Carlo (MC) technique. The MC simulation is used to obtain BER up to 10^{-3}. A symbol size of $10/p$, where p is the BER to be estimated, is selected for this. As stated in section 5.2, this symbol size provides a BER estimate in the confidence interval $[1.8p, 0.55p]$ at a 0.95 confidence level.

As mentioned in section 5.3, two cases of system simulations are considered in this chapter. The simulation results of these two cases are discussed below.

Case 1: CDMA system without filters

The simulated BER versus $\frac{E_b}{N_o}$ performance results are shown in Figures 5.4-5.7 for N=31 and various values of K, where $\frac{E_b}{N_o}$ is the SNR, N is the Gold code sequence length , and K is the number of users. The simulated BER results and BER results obtained using standard Gaussian approximation (SGA) and improved Gaussian approximation (IGA) analysis are compared. As evident in these figures, for $\frac{E_b}{N_o}$ values up to 9 dB, the SGA and IGA analytical BER results show good agreement with the simulated BER. The BER obtained using SGA and IGA lie within the confidence interval of the simulated BER estimate (Figures 5.4-5.7). This agreement between the simulated and analytical results justifies the approximations used in the analysis. One can also note that the SGA and IGA provide an almost identical BER for $\frac{E_b}{N_o}$ values up to 9 dB. At low values of BER (BER $\prec 10^{-3}$) and small number of users (figure 5.4 and 5.5), SGA provides optimistic BER compared to the simulated BER and the agreement gets poor. This may be attributed to the fact that the symbol size used in the simulations (10,000), based on MC symbol size of 10/p, needs to be increased to improve the agreement at BER values $\prec 10^{-3}$, which requires a long computational time. Furthermore, when the delays and phases of user transmissions are random, the number of users has to be large for the Gaussian approximation to be accurate. The SGA is inaccurate for small number of simultaneous users because of the inapplicability of the central limit theorem (on which the SGA is based) for this case [9, 25]. The results of simulated BER estimate presented in this chapter are consistent with the results presented in [8] even though the results presented here are lower than the one in [8]. The difference is because of the effect of the user self interference (the effect of signals' multipath) considered in [8] that degrade the BER performance.

Case 2: CDMA system with filters

The BER performance results of a BPSK CDMA receiver using MC simulation are shown in Figures 5.8-5.13. For comparison, the simulation results of a BPSK CDMA system without filters are also shown in these figures. In this BER simulation, three cases of filter bandwidth are considered: bandwidth = 0.5 f_m, f_m, 2 f_m, where $f_m = 1/T$ and T is

the duration of the input rectangular pulse. As evident in these figures, a filter bandwidth of $2f_m$ provides the closest BER performance compared to the BER in the case where no filters were included (case 1). This is valid for $\frac{E_b}{N_o}$ values up to 12 dB for K = 3 (especially raised cosine and Chebyshev filters) and up to 12 dB for K =10 (Figures 5.10 and 5.13). The agreement gets poor between the simulated BER of the two cases as the filter bandwidth decreases. This is expected because of the fact that a filter with larger bandwidth passes more signal energy and hence provides better BER performance. It can also be noted that, the simulated BER performance degrades when filters are included in the system (Figures 5.8-5.13). This shows the difference between BER performance of the case where infinite bandwidth is assumed (case 1) and band-limited case (case 2). As it can be seen from Figures 5.8-5.13, adding filters to a DS/CDMA system degrade the BER performance. In practice, however, the presence of filters is essential to shape the input signal for the benefit of using the spectrum efficiently and rejecting undesired signals at receiver side to improve the signal to noise ratio.

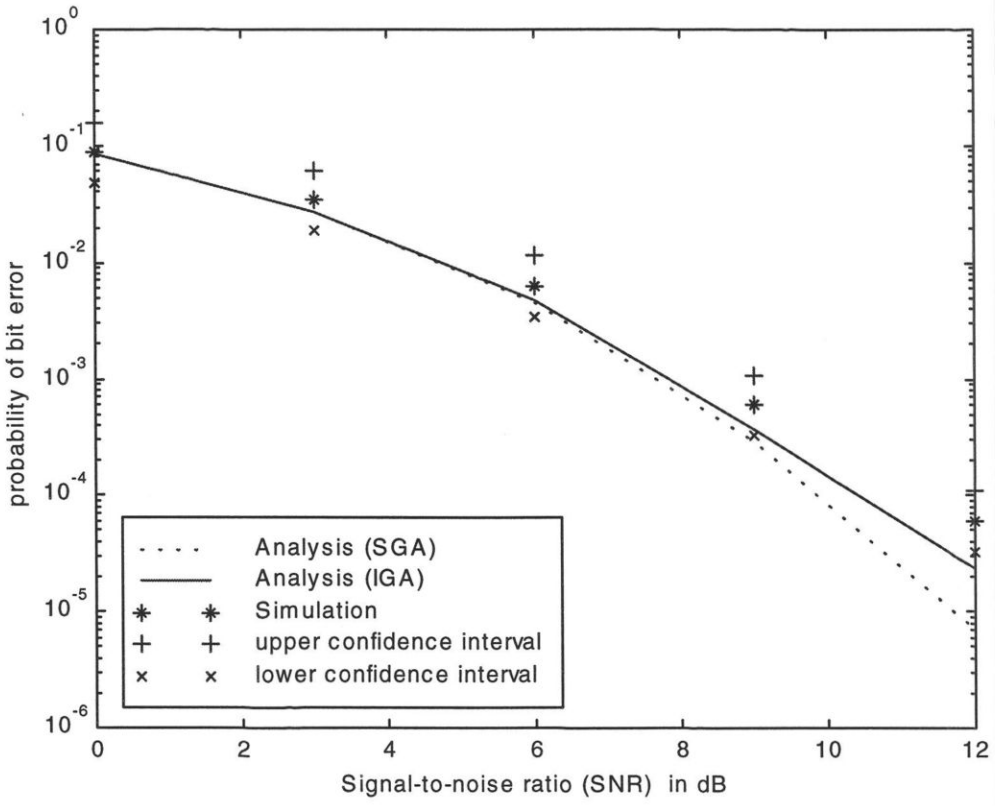

Figure 5.4 BER as a function of SNR results (analytical and simulation for a CDMA system without filters (No. of users K =3)).

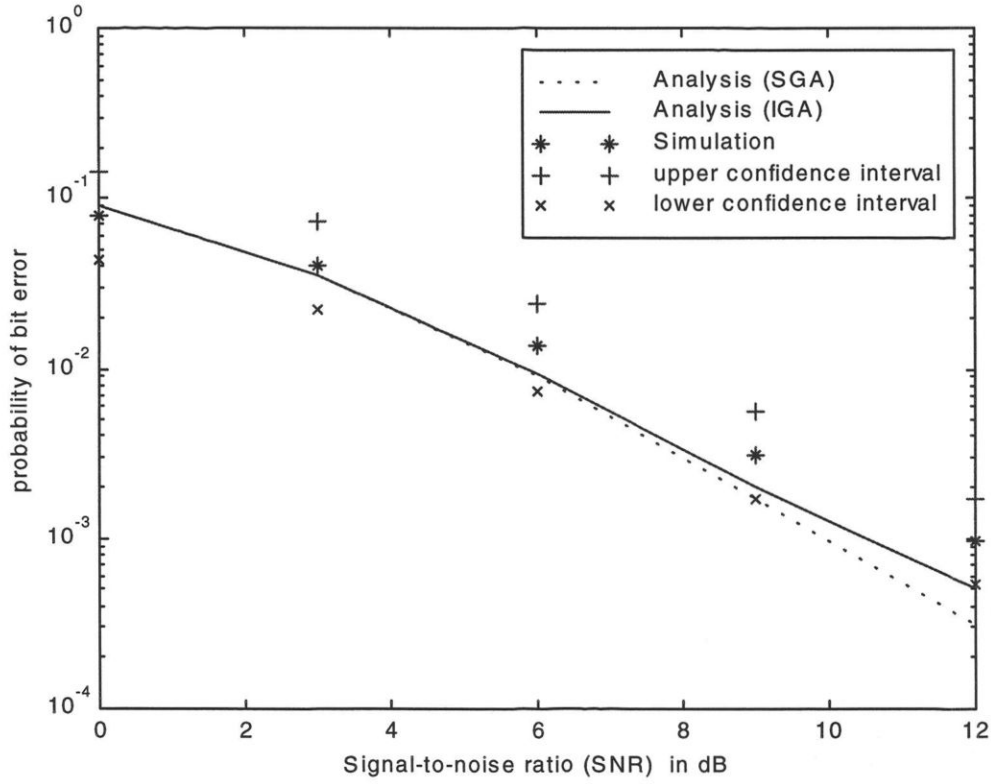

Figure 5.5 BER as a function of SNR results (analytical and simulation for a CDMA system without filters (no. of users K=6)).

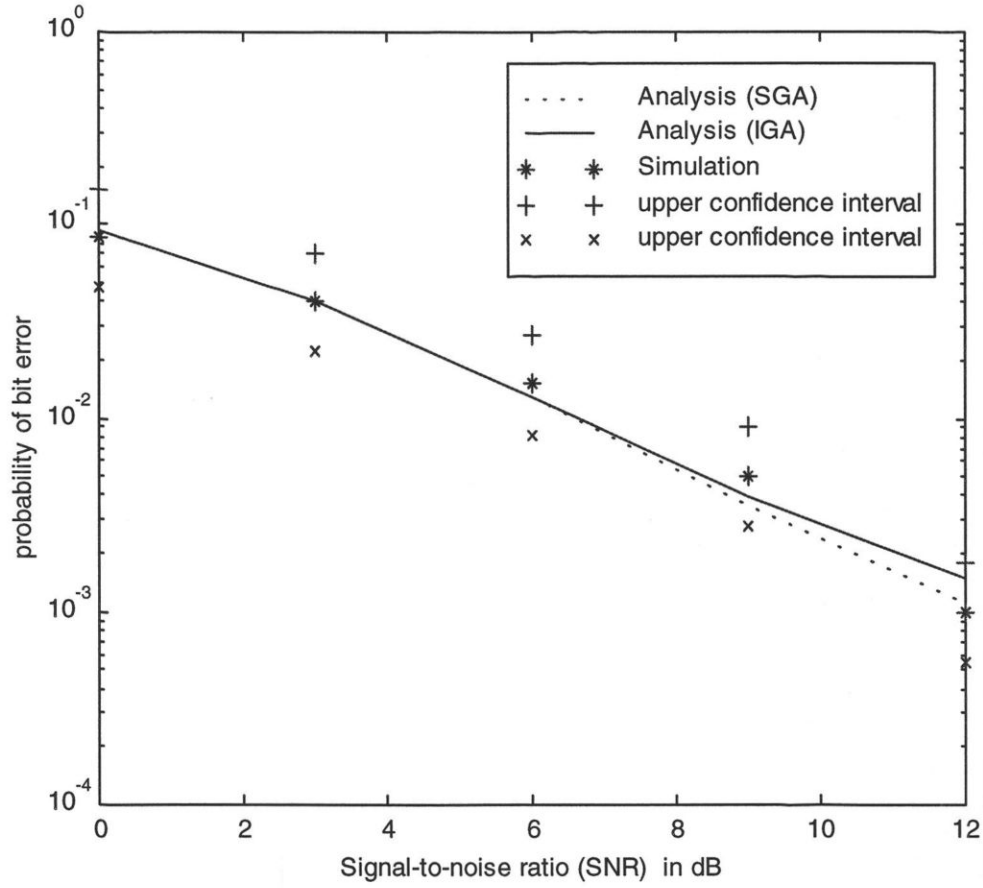

Figure 5.6 BER as a function of SNR results (analytical and simulation for a CDMA system without filters (no. of users K=8)).

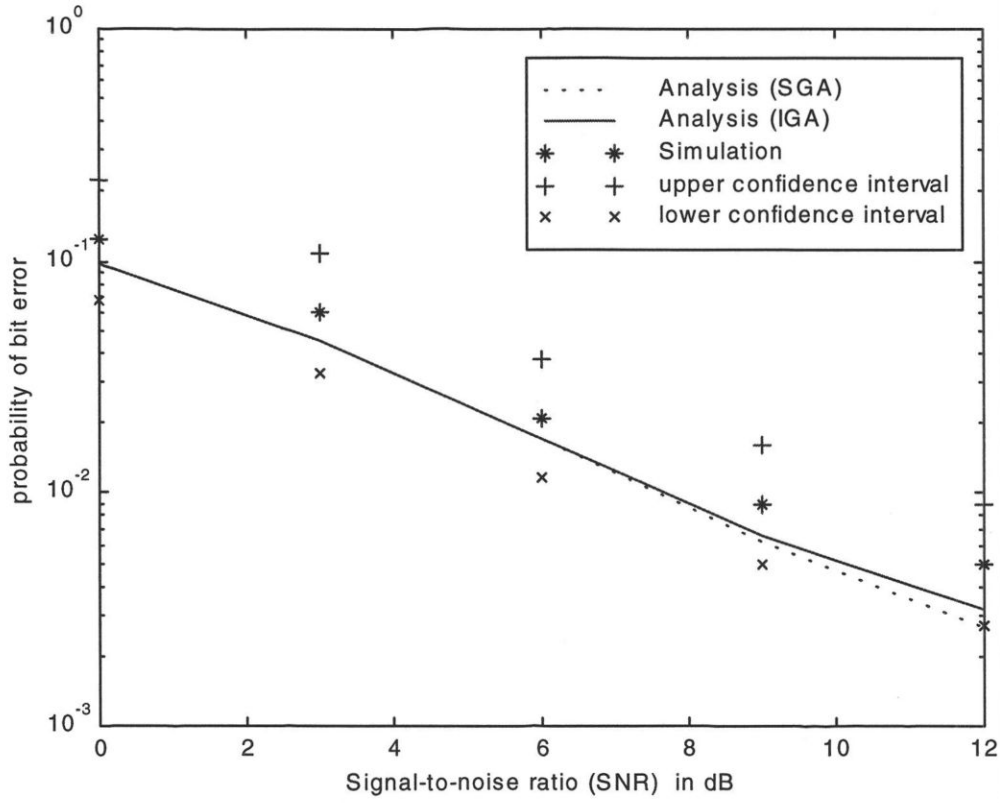

Figure 5.7 BER as a function of SNR results (analytical and simulation for a CDMA system without filters (no. of users K=10)).

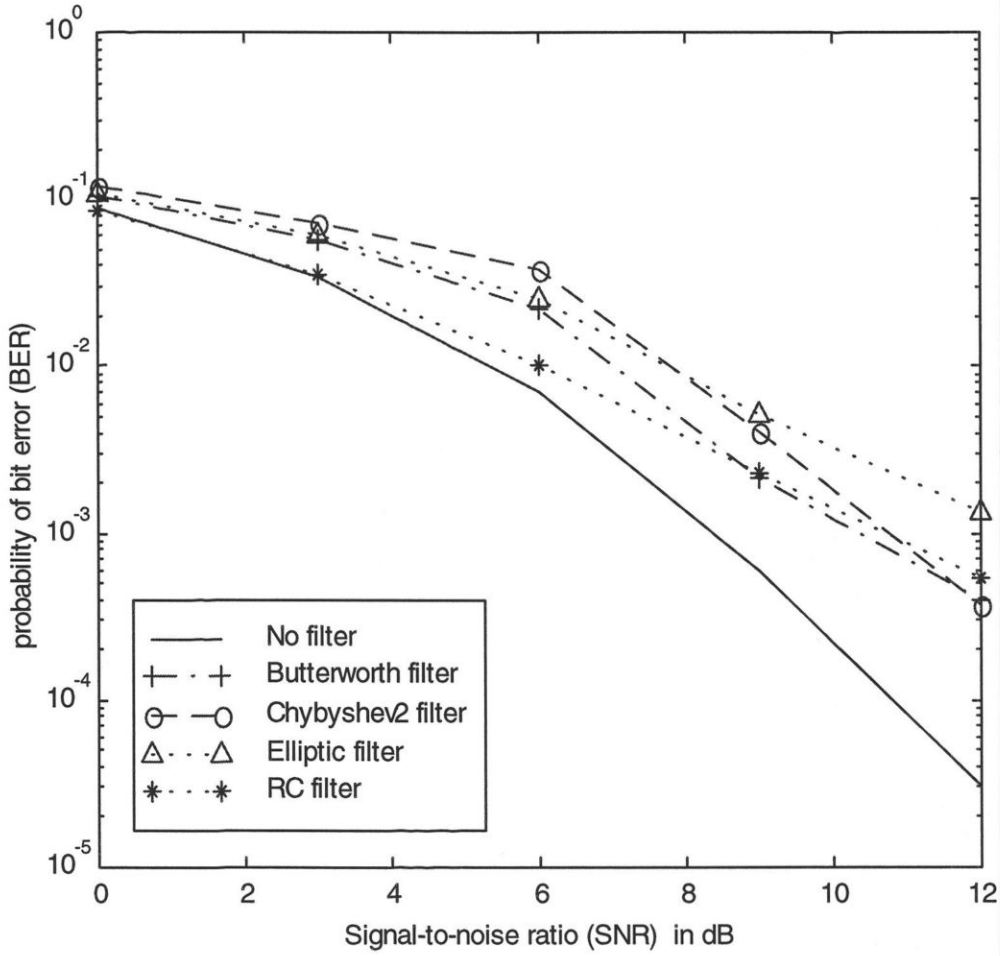

Figure 5.8 BER as a function of SNR results (simulation results for a CDMA system with and without filters); No. of users K =3, Bandwidth=$0.5f_m$

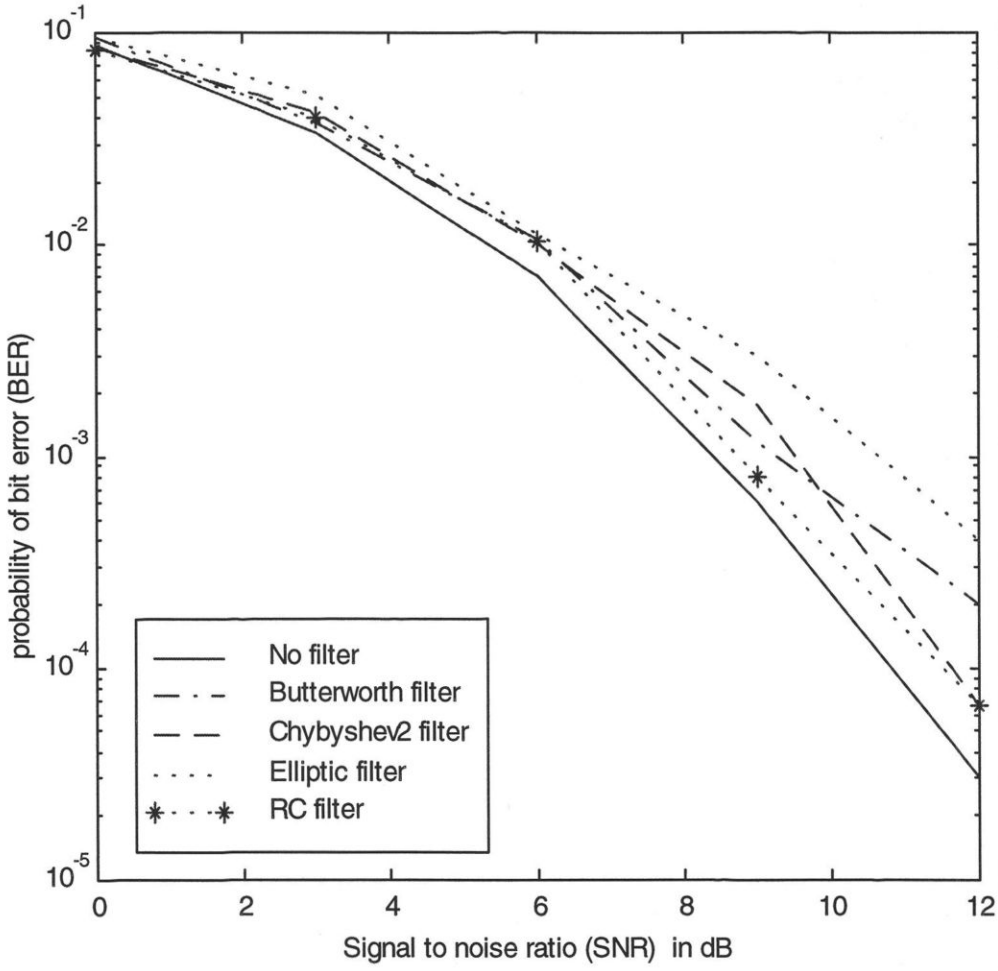

Figure 5.9 BER as a function of SNR results (simulation results for a CDMA system with and without filters); No. of users K =3, Bandwidth = f_m

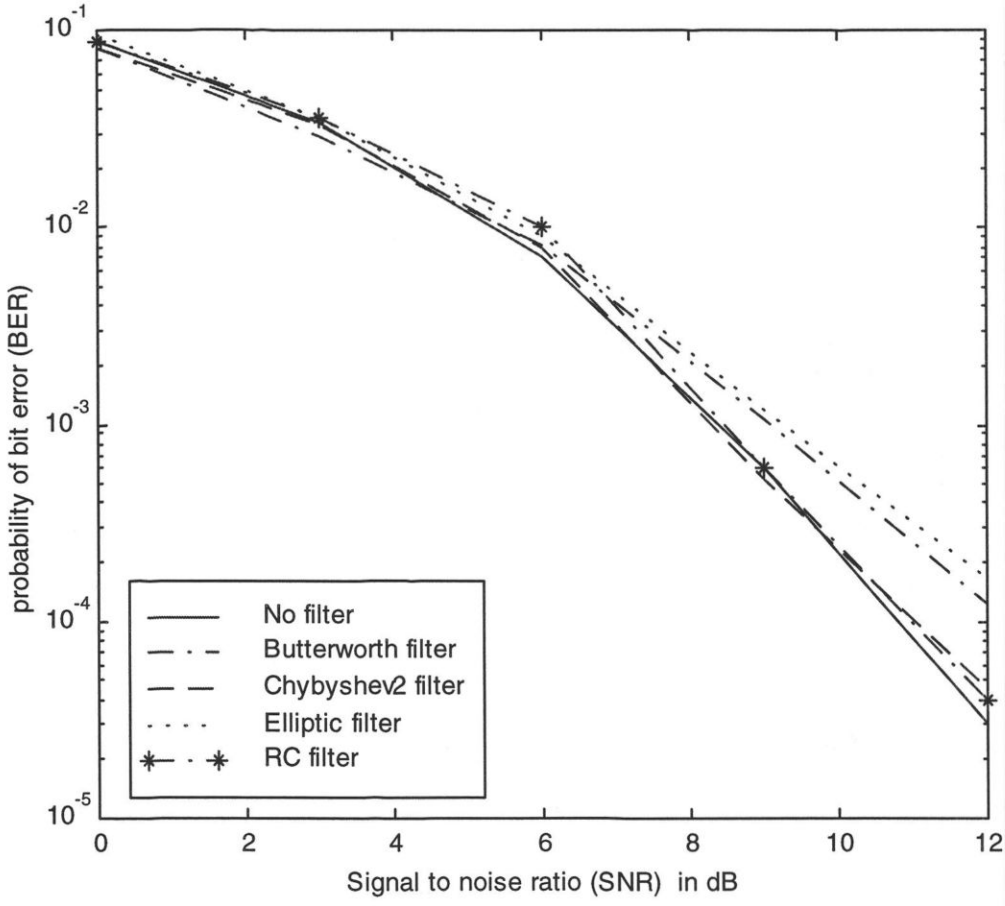

Figure 5.10 BER as a function of SNR results (simulation results for a CDMA system with and without filters); No. of users K =3, Bandwidth=$2f_m$

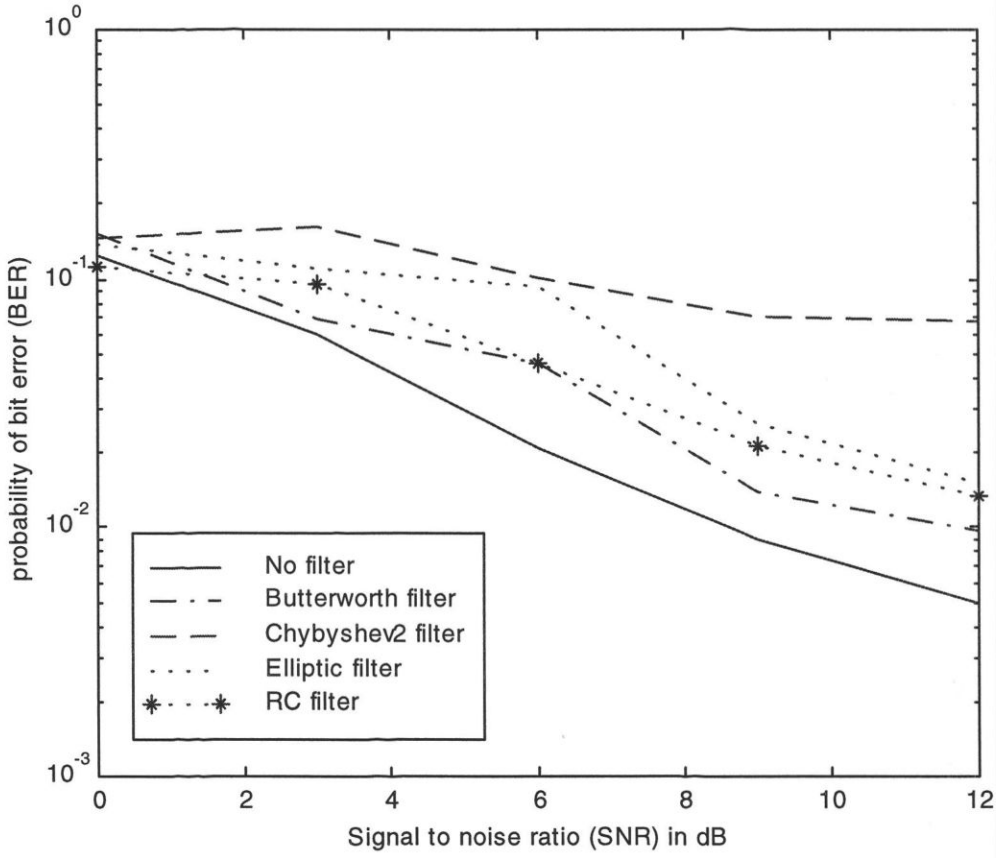

Figure 5.11 BER as a function of SNR results (simulation results for a CDMA system with and without filters); No. of users K =10, Bandwidth=0.5f_m

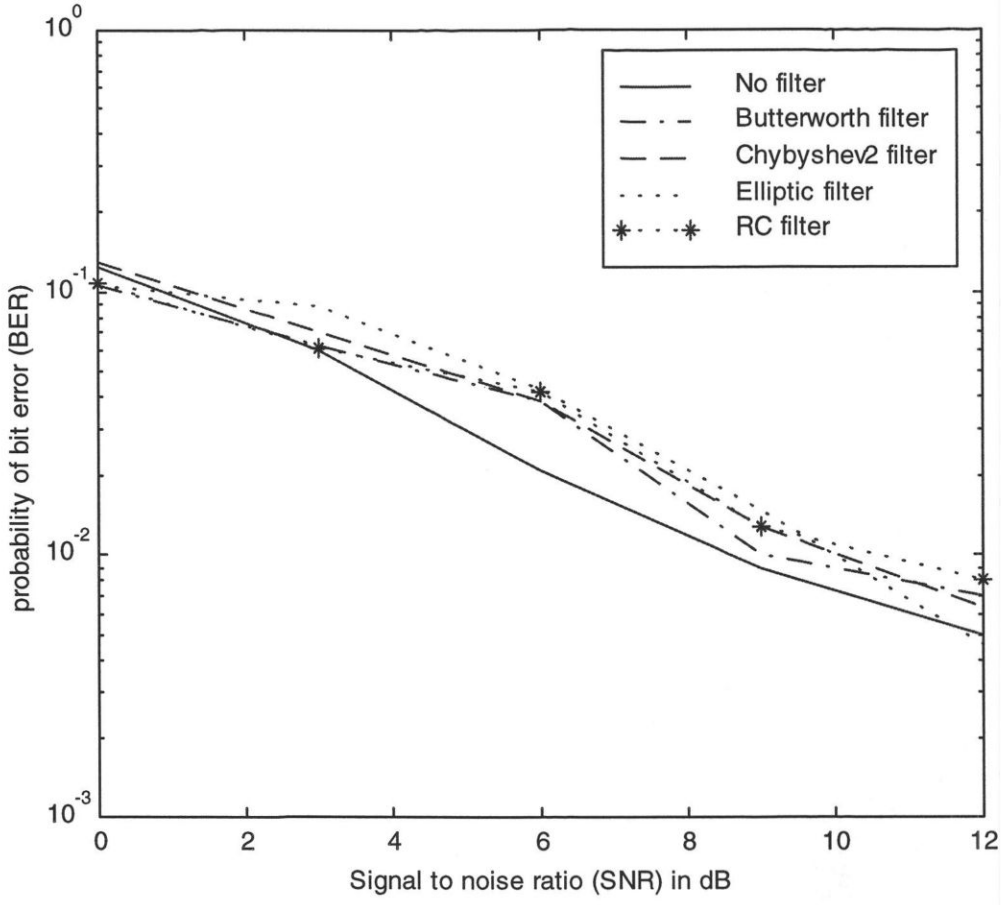

Figure 5.12 BER as a function of SNR results (simulation results for a CDMA system with and without filters); No. of users K =10, Bandwidth = f_m

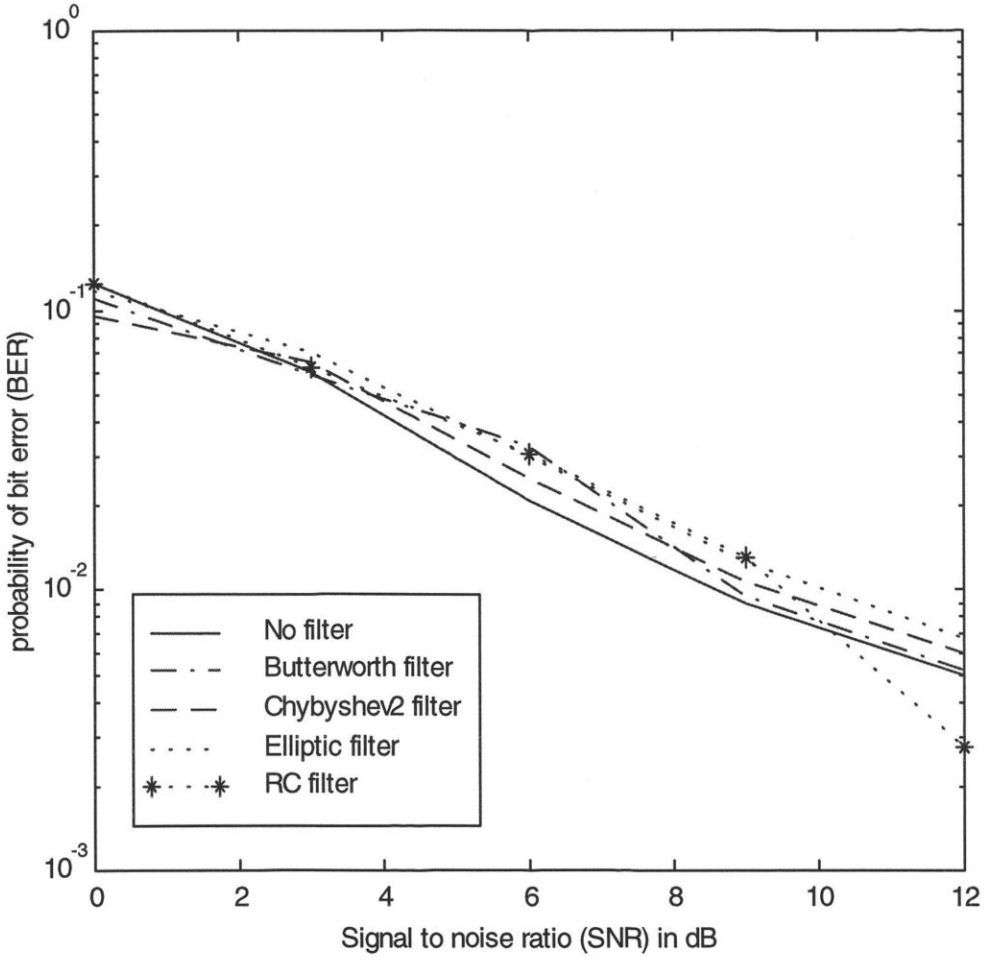

Figure 5.13 BER as a function of SNR results (simulation results for a CDMA system with and without filters); No. of users K =10, Bandwidth=$2f_m$

6. Summary, Conclusions, and Future Work

The following objectives of this thesis as stated previously in chapter one are:

1. Simulate a BPSK DS/CDMA communication system, in a wireless channel environment, using Monte-Carlo method for verifying the BER performance analyzed in [9].

2. Analyze the effect of filtering on the performance of BPSK modulation in DS spread spectrum using a correlator receiver. The system performance measures, in this analysis, are the signal-to-noise ratio (SNR) and the bit error probability (or BER).

3. Develop simulation programs using Monte-Carlo method to evaluate BER performance of DS/CDMA receiver, including filters, for investigating the effect of filters on the BER performance.

To reach the above objectives, an architecture for DS/CDMA system was developed and its performance analyzed. This has been done for two cases of DS/CDMA system: DS/CDMA system with and without filters. As well, simulation results based on the developed architecture were obtained using Monte-Carlo method. The contribution of this thesis are:

1. An expressions for the signal to noise ratio and its associated error probability that includes the effect of filtering of a BPSK modulation in DS/CDMA system were derived based on [24,30].

2. Simulation programs were developed to verify the analytical BER performance results obtained for a DS/CDMA system without filters (Chapter 5).

3. Simulation programs to investigate the effect of filtering on the BER performance of DS/CDMA receivers have been developed.

The work presented in this thesis shows that the above mentioned objectives have been realized. The overall conclusions are summarized as:

1. An expression for the bit error probability of a DS/CDMA correlator receiver without filters was derived. The BER was numerically computed for various combinations of factors in chapter 3. It is concluded that SGA analysis, for small number of simultaneous users, provides an optimistic results of BER values compared to IGA where in terms of complexity IGA is more complex than SGA. The optimistic results of SGA may be attributed to the inapplicability of central limit theorem (on which the SGA based) for small number of simultaneous users.

2. In the case of DS/CDMA system without filters, the SGA and IGA analytical BER results are in reasonable agreement with the simulated BER estimate for SNR values up to 12 dB and with a large number of users. For small number of users (K=3, 6), the agreement is reasonable for SNR values up to 9 dB and gets poor for SNR values greater than 9 dB. However, for BER in the range of 10^{-4} to 10^{-5} and K=3, Gaussian approximation results in a SNR difference of about 0.8-1.7 dB lower for a given value of BER.

3. An expression for the signal to noise ratio of a DS/CDMA correlator receiver was derived taking into account the effect of filtering. As well, a BER expression that based on this SNR expression was given. It is concluded from the analysis in chapter 4 that SNR is inversely proportional to the system capacity data rate, which is $\sum_{k=2}^{K} R_k$. Thus, the SNR can be maintained at a certain level by controlling the system data rate. Numerical results in chapter 4 also indicate that SNR and BER significantly improve by increasing the channel bandwidth (or increasing the spreading gain).

4. Based on simulation results of BER estimate, filter bandwidth of $2f_m$ provides a reasonable agreement with the results of BER estimate obtained for the DS/CDMA system with infinite bandwidth assumption.

5. Simulations results showed that, adding filters to a DS/CDMA system effect the BER performance negatively compared to a DS/CDMA system without filters. However, practically, the presence of filters is essential to shape the input signals for the benefit of using the spectrum efficiently and rejecting undesired signals at receiver side.

In this thesis, some assumptions were made to analyze the system. Some issues that could be considered in future research are:

- Deriving the bit error probability taking into account the effect of filtering.
- Investigate the effect of imperfect power control.
- Investigate the effect of the coding and interleaving on the bit error probability.
- Consider the effect of user self interference (multipath channel environment) in the analysis.
- Consider different modulation schemes, QPSK for instant, in the analysis.

References

[1] M. Madfors, K. Wallstedt, S. Magnusson, H. Olofsson, P. Backman, and S. Engstrom," High capacity with limited spectrum in cellular systems," *IEEE commun. Mag.*, Vol. 35 No. 8, pp. 38-45, August 1997.

[2] X. Lagrange, "Multitier Cell Design," *IEEE commun. Mag.*, Vol. 35 No. 8, pp. 60-64, August 1997.

[3] T. S. Rappaport, *Wireless Communications Principles and Practice*, Prentice Hall, Upper Saddle River, New Jersey 1996.

[4] M. D. Yacoub, *Foundation of Mobile Radio Engineering*, CRC Press, Inc., 1993.

[5] Y. Sanada, and M. Nakagawa, "A Multiuser Interference Cancellation Technique Utilizing Convolutional Codes and Orthogonal Multicarrier Modulation for Wireless Indoor Communications," *IEEE J. Select. Area Commun.,* Vol.14, No. 8, pp. 1500-1508, October 1996.

[6] W.C.Y Lee, "Overview of cellular CDMA," *IEEE Trans. On Veh. Technolo.,* Vol. 40, No.2, May 1991, pp. 291-301.

[7] TIA/EIA/IS-95 "Mobile Station-Base Station Compatibility Standard for Dual-Mode Wideband Spread Spectrum Cellular System," U.S Telecommunication Industry Association, July 1993.

[8] P.C. John Panicker , "Effect of System Imperfections on the Performance of CDMA Receivers with CCI Cancellation," Ph.D. Dissertation, University of Saskatchewan, Fall 1996.

[9] F. D. Simpson, "Direct Sequence Code Division Multiple Access Performance Analysis Methodologies," Ph.D. Dissertation, University of New Jersey, May 1992.

[10] S. Sampei, *Applications of Digital Wireless Technologies To Global Wireless Communications,* Prentice Hall, 1997.

[11] B.Sklar, *Digital Communications Fundamentals and Applications*, Prentice Hall, New Jersey 1988.

[12] F. Lau, "Spread Spectrum Code Synchronization Using Signal Transitions," M.Sc Thesis, University of Saskatchewan, Saskatoon, August 1991.

[13] D. Schilling, L. Milstein, R. Pickholtz, M. Kullback, and F. Miller, "Spread Spectrum for Commercial Communications," *IEEE Commun. Mag.,* Vol.29, No. 4, pp. 66-79, April 1991.

[14] K. Gilhousen, I. Jacobs, R. Padovani, A. Viterbi, L. Weaver, and C. Wheatley III, "On the Capacity of a Cellular CDMA System," *IEEE Trans. on Veh. Technolo.,* Vol. 40, No.2, pp. 303-312, May 1991.

[15] R. Pickholtz, L. Milstein, D. Schilling, "Spread Spectrum for Mobile Communications," *IEEE Trans. on Veh. Technolo.,* Vol. 40, No.2, May 1991, pp. 313-322.

[16] R. L. Pickholtz, D. L. Schilling, and L. B. Milstein, "Theory of Spread Spectrum communications - A Tutorial ," *IEEE Trans. on Commun.,* Vol.COM-30, pp . 855-884, May 1982.

[17] R. C. Dixon, *Spread Spectrum Systems*, 2nd edition, John Wiely & sons, Inc., 1984.

[18] R. Ziemer, and R. Peterson, *Digital Communications and Spread Spectrum systems*, Macmillan Publishing Company, 1985.

[19] D. V. Sarwate and M. B. Pursley, "Crosscorrelation Properties of Pseudorandom and Related Sequences," *Proc. IEEE*, vol. 68, pp. 593-619, May 1980.

[20] J. Proakis, *Digital Communications*, McGraw-Hill, Inc., 3rd edition, 1995.

[21] E. A. Geraniotis and M. B. Pursley, "Error Probability for Direct-Sequence Spread Spectrum Multiple-Access Communications--Part II:Approximations," *IEEE Trans. on Commun.*, Vol.COM-30, pp . 985-995, May 1982.

[22] J. S. Lehnert and M. B. Pursely, "Error probability for Binary Direct-Sequence Spread Spectrum Communications with random Signature Sequences," *IEEE Trans. on Commun.*, Vol.COM-35, pp. 87-98, Jan. 1987.

[23] B. Aazhang and H. Vincent Poor, "Performance of DS/SSMA Communications in Impulsive Channels---Part I: Linear correlation Receivers," *IEEE Trans. on Commun.*, Vol.COM-35, No. 11, pp . 1179-1188, November 1987.

[24] M. B. Pursley, "Performance Evaluation for Phase -Coded Spread-Spectrum Multiple Access Communications--Part I: System analysis," *IEEE Trans. on Commun.*, Vol.COM-25, pp. 795-799, Aug. 1977.

[25] R. K. Morrow, and J. S. Lehnert, "Bit-to-Bit Error Dependence in Slotted DS/SSMA Packet Systems with Random Signature Sequences ," *IEEE Trans. on Commun.*, Vol.COM-37, No. 10, pp . 1052-1061, Oct. 1989.

[26] J. M. Holtzman, "A simple, Accurate Method to Calculate Spread-Spectrum Multiple-Access Error Probabilities," *IEEE Trans. on Commun.*, Vol. 40, No. 3, pp. 461-464, March 1992.

[27] J. M. Holtzman , "On Using Perturbation Analysis to do Sensitivity Analysis: Derivative Versus Differences," *IEEE Trans. on Automatic Control.*, Vol. 37, No. 2, pp. 243-247, Feb. 1992.

[28] Kendall L. Su, *Analog Filters*, 1st ed.: Chapman & Hall, 1996.

[29] Arthur B. Williams and Fred J. Taylor, *Electronic Filter Design Handbook*, 3rd ed.: McGraw-Hill, Inc., 1995.

[30] J. Eric Salt, and Surinder Kumar, "Effects of Filtering on the Performance of QPSK and MSK Modulation in D-S Spread Spectrum Systems Using RAKE Receivers," *IEEE J. Select. Area Commun.*, Vol.12, No. 4, pp. 707-715, May 1994.

[31] Leon W. Couch II, *Digital and Analog Communication Systems*, 4th ed., Macmillan Publishing Company, 1993.

[32] Michel C. Jeruchim, Philip Balaban, and K. Sam Shanmugan, *Simulation of Communication Systems*, Plenum Press, New York, 1992.

[33] Michel C. Jeruchim, "Techniques for Estimating the Bit Error Rate in the Simulation of Digital Communication Systems," *IEEE J. Select. Area Commun.*, Vol. SAC-2, No. 1, pp. 153-170, January 1984.

[34] M. Kendall and A. Stuart, *Advanced Theory of Statistics*, 4th ed. New York: Macmillan Publishing Company, 1977.

Appendix A
Derivation of Equation (3.13)

In this appendix, the weighting factor, W_k, of the MAI term in equation (3.12) is calculated using the continuous-time partial cross-correlation functions (3.7 and 3.8).

It is assumed that the reference user and non-reference users use random signature sequences with a new sequence being selected for each consecutive data bit. In other words, the signature sequence may be assumed as an infinite sequence of rectangular pulses of duration T_c with amplitudes randomly selected from $\{-1, +1\}$. The time offset S_k of the k[th] user's sequence to the reference user is given by $S_k = \tau_k - lT_c$, where τ_k is uniformly distributed on [0, T_b) and $l = \lfloor \tau_k / T_c \rfloor$ is uniformly distributed on $\{0, 1, ..., (N-1)\}$. Taking $l = N-1$ implies that S_k is uniformly distributed on [0, T_c). Then (3.9) and (3.10) yields [9]

$$\begin{aligned} R_{k,1}(S_k) &= T_c C_{k,1}(-1) + [C_{k,1}(0) - C_{k,1}(-1)] S_k \\ &= (T_c - S_k) \sum_{j=0}^{N-2} a_{j+1}^{(K)} a_j^{(1)} + S_k \sum_{j=0}^{N-1} a_j^{(K)} a_j^{(1)} , \end{aligned} \tag{A.1}$$

and

$$\hat{R}_{k,1}(S_k) = (T_c - S_k) a_N^{(k)} a_{N-1}^{(1)} , \tag{A.2}$$

where $a_N^{(k)}$ is the first chip in data bit $b_0^{(K)}$, which is independent of $a_0^{(K)}$, the first chip in data bit $b_{-1}^{(K)}$. Using (A.1) and (A.2) in (3.6) yields [9]

$$\begin{aligned} B_{k,1}(S_k) &= (T_c - S_k) \left[\sum_{j=0}^{N-2} a_{j+1}^{(k)} a_j^{(1)} + a_N^{(k)} a_{N-1}^{(1)} \right] + S_k \sum_{j=0}^{N-1} a_j^{(k)} a_j^{(1)} \\ &= \sum_{j=0}^{N-2} a_{j+1}^{(k)} \left[(T_c - S_k) a_j^{(1)} + S_k a_{j+1}^{(1)} \right] + S_k a_0^{(k)} a_0^{(1)} + (T_c - S_k) a_N^{(k)} a_{N-1}^{(1)} . \end{aligned} \tag{A.3}$$

Since the signature sequence of the k[th] interfering sequence is random (i.e., the $a_j^{(k)}$'s are random), (A.3) does not depend on $b_{-1}^{(K)}$ and $b_0^{(K)}$. To simplify notation, introduce b as a symmetric Bernoulli trial, which has outcomes uniformly distributed on $\{-1, +1\}$ (so that b is zero mean and unit variance and each $a_j^{(k)}$ and the product of any two or more independent $a_j^{(k)}$ can be written as an appropriately subscripted b). Then conditioning on

the reference sequence $a_j^{(1)} = \hat{a}_j$ for $j \in \{0, 1, ..., (N-1)\}$ and using the fact that $(\hat{a}_j)^2 = 1$, $B_{k,1}(S_k)$ becomes [9]

$$B_{k,1}(S_k) = \sum_{j=0}^{N-2} b_{j+1}[(T_c - S_k) + S_k \hat{a}_j \hat{a}_{j+1}] + S_k b_0 + (T_c - S_k) b_N. \quad \text{(A.4)}$$

It is possible to make a further simplification by noting that $\hat{a}_j \hat{a}_{j+1} \in \{-1, +1\}$. Therefore, let

$$\alpha = \{j : \hat{a}_j \hat{a}_{j+1} = +1\}, \quad \text{(A.5)}$$

and

$$\beta = \{j : \hat{a}_j \hat{a}_{j+1} = -1\}, \quad \text{(A.6)}$$

for $j \in \{0, 1, ..., (N-2)\}$. Following this simplification, $B_{k,1}(S_k)$ can be expressed as

$$B_{k,1}(S_k) = L_k S_k + Q_k(T_c - S_k) + X_k T_c + Y_k(T_c - 2S_k), \quad \text{(A.7)}$$

where $L_k = b_0$ and $Q_k = b_N$ are uniformly distributed random variables on $\{-1, +1\}$, with

$$X_k = \sum_{j \in \alpha} b_j, \quad \text{(A.8)}$$

and

$$Y_k = \sum_{j \in \beta} b_j, \quad \text{(A.9)}$$

Assume A and B are the cardinalities of α and β, respectively, then X_k and Y_k are the sum of symmetric Bernoulli trials with densities as given in (3.14) and (3.15).

Now, from (7), W_k can be given by (assuming that the chip duration $T_c = 1$)

$$W_k = L_k S_k + Q_k(1 - S_k) + X_k + Y_k(1 - 2S_k), \quad \text{(A.10)}$$

Appendix B
Derivation of Mean and Variance of a Real Function of a Random Variable

In this appendix, the mean and variance of a real function h of a random variable ξ are derived using a Taylor series. Let $h(\xi)$ a real function of a random variable ξ. The expectation of this function is given by [34]

$$E[h(\xi)] = \int_{-\infty}^{\infty} h(\xi) f(\xi) d\xi, \tag{B.1}$$

where $f(\xi)$ is the probability density function of the random variable ξ. As it is known, $f(\xi)$ takes significant values in an interval near μ of the order of its standard deviation σ [29] (see Figure B.1).

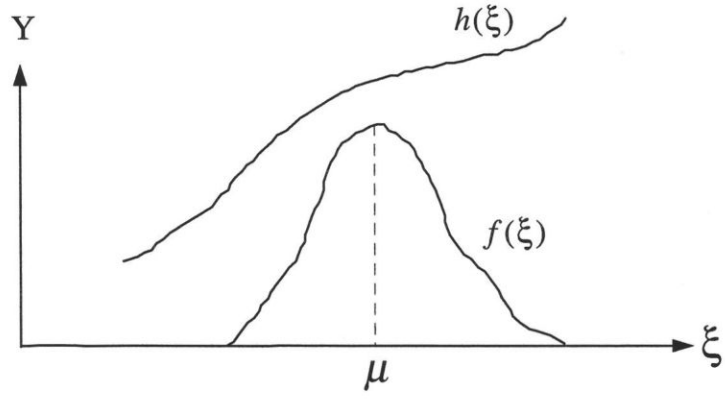

Figure B.1 A real function and probability density function of a random variable ξ

If in this interval $h(\xi)$ is "smooth" then

$$E[h(\xi)] \cong h(\mu) \int_{-\infty}^{\infty} f(\xi) d\xi \cong h(\mu) \tag{B.2}$$

since $\int_{-\infty}^{\infty} f(\xi) d\xi = 1$. This estimate is the beginning of a Taylor series expansion with

$$h(\xi) = h(\mu) + h'(\mu)(\xi - \mu) + h''(\mu)\frac{(\xi - \mu)^2}{2} + \ldots\ldots + h^{(n)}\frac{(\xi - \mu)^n}{n!} + \ldots\ldots \tag{B.3}$$

Inserting (B.3) in (B.1) yields

$$\begin{aligned} E[h(\xi)] &= \int_{-\infty}^{\infty} h(\mu) f(\xi)\, d\xi + \int_{-\infty}^{\infty} h'(\mu)(\xi - \mu) f(\xi)\, d\xi \\ &\quad + \int_{-\infty}^{\infty} h''(\mu)\frac{(\xi - \mu)^2}{2} f(\xi)\, d\xi + \ldots\ldots \\ &\cong h(\mu) + h''(\mu)\frac{\sigma^2}{2} + \ldots\ldots + h^{(n)}(\mu)\frac{\mu_n}{n!} + \ldots\ldots \end{aligned} \tag{B.4}$$

For $h(\xi)$ sufficiently smooth and retaining the first two terms, the following can be obtained

$$E[h(\xi)] = h(\mu) + h''(\mu)\frac{\sigma^2}{2} \tag{B.5}$$

which is the mean of the function $h(\xi)$.

The variance of $h(\xi)$ is given by

$$\sigma^2_{h(\xi)} = E[h^2(\xi)] - E^2[h(\xi)]. \tag{B.6}$$

Equation (B.5) can be used to evaluate $E[h^2(\xi)]$. Assume the following

$$g(\xi) = h^2(\xi), \tag{B.7}$$

$$g'(\xi) = 2h(\xi)h'(\xi), \tag{B.8}$$

and

$$g''(\xi) = 2\left[(h'(\xi))^2 + h(\xi)h''(\xi)\right]. \tag{B.9}$$

Then, using (B.5) and (B.9), $E[h^2(\xi)]$ can be expressed as

$$E\left[h^2(\xi)\right] = h^2(\mu) + \left[\left(h`(\mu)\right)^2 + h(\mu)h''(\mu)\right]\sigma^2. \tag{B.10}$$

Inserting (B.5) and (B.10) in (B.6) yields

$$\begin{aligned} \sigma^2_{h(\xi)} &= h^2(\mu) + \left[\left(h`(\mu)\right)^2 + h(\mu)h''(\mu)\right]\sigma^2 - \left(h(\xi) + h''(\xi)\frac{\sigma^2}{2}\right)^2 \\ &= \left(h'(\mu)\right)^2\sigma^2 + \left(h''(\mu)\frac{\sigma^2}{2}\right)^2. \end{aligned} \tag{B.11}$$

If one retain σ^2 power only, the variance of the function h is given by

$$Var[h(\xi)] \cong \left(h'(\mu)\right)^2\sigma^2. \tag{B.12}$$

Appendix C
Variance of Ψ

To find the variance of Ψ, which expressed in (3.45), one needs to find $E[Z^2]$ and $Cov(Z_j, Z_k)$. First, a derivation for equation (3.45) will be given.

As shown in (3.25), the Ψ is expressed as

$$\Psi = \sum_{k=2}^{K} Z_k. \tag{C.1}$$

Then σ^2 of (C.1) can be given by

$$\sigma^2 = E\left[\left(\sum_{k=2}^{K} Z_k\right)^2\right] - E^2\left[\left(\sum_{k=2}^{K} Z_k\right)\right]. \tag{C.2}$$

The first part of the RHS of (C.2) can be simplified as

$$\begin{aligned} E\left[\left(\sum_{k=2}^{K} Z_k\right)^2\right] &= E\left[\sum_{j=2}^{k}\sum_{k=2}^{K} Z_j Z_k\right] \\ &= E\left[(K-1)[Z_k^2] + (K-2)(K-1)[Z_j Z_k]\right] \\ &= (K-1)\left[E[Z_k^2] + (K-2)E[Z_j Z_k]\right] \\ &= (K-1)\left[E[Z_k^2] + (K-2)Cov(Z_j, Z_k)\right] \qquad for\ j \neq k \end{aligned} \tag{C.3}$$

and the second part of the RHS of (C.2) can be simplified as

$$\begin{aligned} E^2\left[\left(\sum_{k=2}^{K} Z_k\right)\right] &= \sum_{k=2}^{K} E^2[Z_k] \\ &= (K-1)E^2[Z_k]. \end{aligned} \tag{C.4}$$

Substituting (C.3) and (C.4) in (C.2) yields (assuming $Z = Z_k$)

$$\sigma^2 = (K-1)\left[E[Z^2] - E^2[Z] + (K-2)Cov(Z_j, Z_k)\right] \qquad for\ j \neq k, \tag{C.5}$$

which is the same as (3.45).

The derivations for $E[Z^2]$ and $Cov(Z_j, Z_k)$ are now given. The expected value of Z^2 can be expressed as [9]

$$\begin{aligned} E[Z^2] &= E\left[E[Z^2|B]\right] \\ &= E\left[\left(1+\cos(2\varphi)\right)^2\left((2B+1)(S^2-S)+N/2\right)^2\right]. \end{aligned} \tag{C.6}$$

Squaring each term, expanding the product, and noting that $E[S^2-S] = -1/6$, $E[(S^2-S)^2] = 1/30$ for S uniformly distributed on [0, 1], $E[\cos(2\varphi)] = 0$, and φ, B, and S are independent, (C.6) is given by

$$E[Z^2|B] = \frac{3N^2}{8} - \frac{N(2B+1)}{4} + \frac{(2B+1)^2}{20}. \tag{C.7}$$

Taking the expectation of (C.7) yields (noting that $E[B] = (N-1)/2$ and $E[B^2] = N(N-1)/4$ [9])

$$\begin{aligned} E[Z^2] &= \frac{15N^2 + (8-20N)(N-1)/2 + 8E[B^2] + 2 - 10N}{40} \\ &= \frac{7N^2 + 2N - 2}{40}. \end{aligned} \tag{C.8}$$

The $Cov(Z_j, Z_k)$ can be expressed as [9] (see next page)

$$
\begin{aligned}
Cov(Z_j, Z_k) &= E[U_j V_j U_k V_k] - (E[Z])^2 \\
&= E\Big[(1+\cos(2\varphi_j))(1+\cos(2\varphi_k))((2B+1)(S_j^2 - S_j) + \\
&\quad N/2)((2B+1)(S_k^2 - S_k) + N/2)\Big] - \\
&\quad \Big(E[1+\cos(2\varphi)]E[2B+1]E[S^2 - S] + N/2\Big)^2 \\
&= E^2[1+\cos(2\varphi)]\Big\{E[(2B+1)^2]E^2[S^2 - S] + N^2/4 + \\
&\quad NE[2B+1]E[S^2 - S]\Big\} - \\
&\quad \Big\{E^2[1+\cos(2\varphi)]E^2[2B+1]E^2[S^2 - S] + N^2/4 + \\
&\quad NE[1+\cos(2\varphi)]E[2B+1]E[S^2 - S]\Big\} \\
&= E^2[S^2 - S]\Big(E[(2B+1)^2] - E^2[2B+1]\Big) \\
&= \frac{Var[2B+1]}{36} \\
&= \frac{Var[B]}{9} \\
&= \left(\frac{1}{9}\right)\left(\frac{N-1}{4}\right).
\end{aligned}
\tag{C.9}
$$

Appendix D
Nyquist Criterion for Intersymbol interference (ISI) Cancellation

Nyquist was the first to solve the problem of overcoming intersymbol interference (ISI) while keeping the transmission bandwidth low [3]. He observed that the effect of (ISI) could be completely nullified if the overall response of the communication system (including transmitter, channel, and receiver) is designed so that at every sampling instant at the receiver, the response due to all symbols except the current symbol is equal to zero. In other words, the effects of ISI can be completely negated if it is possible to obtain a received pulse shape, $h_r(t)$, with the property [18]

$$h_r(nT) = \begin{cases} 1 & n = 0 \\ 0 & n \neq 0, \end{cases} \tag{D.1}$$

where T is the symbol period and n is an integer. This condition guarantees zero ISI. Nyquist derived transfer function $H_r(f)$ which satisfy the condition of equation (D.1).

There are two important consideration in selecting $H_r(f)$ which satisfy equation (D.1). First, $h_r(t)$ should have a fast rate of decay with a small magnitude near the sample values for $n \neq 0$. Second, it should be possible to realize or closely approximate shaping filters at both the transmitter and receiver to produce the desired $H_r(f)$. A family of spectra, $H_r(f)$, that satisfy the Nyquist pulse-shaping criterion is the raised cosine family, which is defined by [18]

$$H_r(f) = \begin{cases} T & 0 \le |f| \le (1-\alpha)/2T \\ \dfrac{T}{2}\left[1 + \cos\left(\dfrac{\pi|f| - 1/(2T) + \alpha}{2\alpha}\right)\right] & (1-\alpha)/2T < |f| \le (1+\alpha)/2T \\ 0 & |f| > (1+\alpha)/(2T). \end{cases} \tag{D.2}$$

The spectra given by (D.2) are illustrated in Figure D.1 for several values of the rolloff

factor α. Note that the bandwidth of $H_r(f)$ lies between $1/2T$ and $1/T$ hertz depending on the value of α.

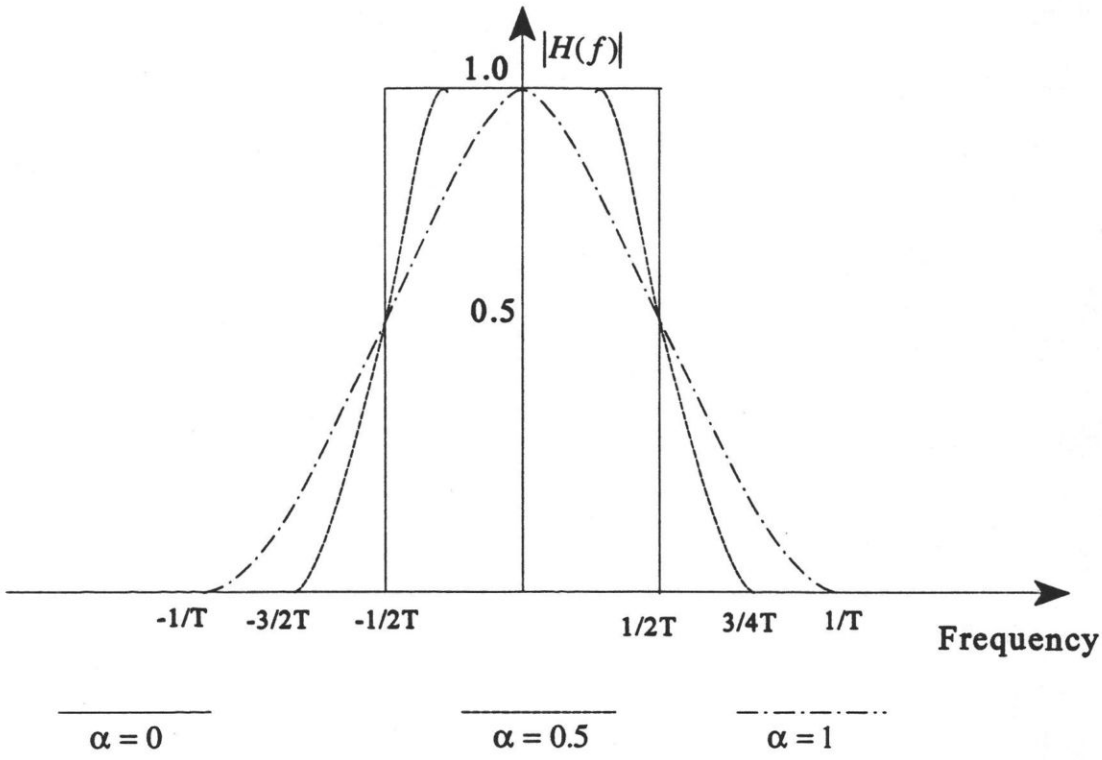

Figure D.1 Magnitude transfer function of a raised cosine filter

The inverse Fourier transform of $H_r(f)$ can be shown to be

$$H_r(t) = \frac{\cos 2\pi\alpha t}{1-(4\alpha t)^2}\ sinc\left(\frac{t}{T}\right), \qquad \text{(D.3)}$$

which is graphed in Figure D.2 for several values of α. Note that larger bandwidth for $H_r(f)$ result in pulse shapes that decay faster.

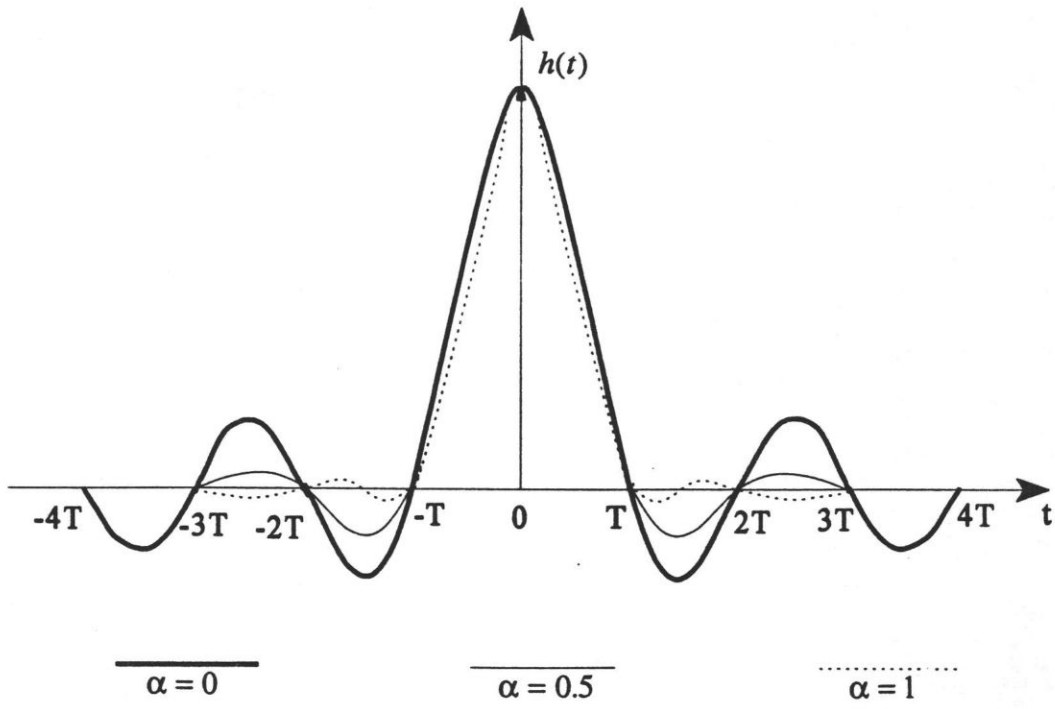

Figure D.2 Pulses with raised cosine spectra

Appendix E
Schwarz's Inequality

In this appendix, Schwarz's inequality will be discussed (based on [18]) and then applied in (4.45) to get (4.50). It is a generalization of the inequality involving the dot product of two vectors $\bar{A}$ and $\bar{B}$, which is

$$|\bar{A}\bullet\bar{B}| = |\bar{A}|\,|\bar{B}|\,|\cos\theta| \le |\bar{A}|\,|\bar{B}|\,, \tag{E.1}$$

where θ is the angle between them and $|\bar{A}|$ denotes the magnitude of $\bar{A}$. That (E.1) holds is obvious, since $|\cos\theta| \le 1$. Furthermore, since $|\cos\theta| = 1$ if, and only if, $\theta = n\pi$, where n is an integer, it follows that equality holds in (E.1) if, and only if, $\bar{A} = k\bar{B}$, where k is a constant (i.e., if $\bar{A}$ and $\bar{B}$ are collinear).

The generalization of (E.1), which is one form of Schwarz's inequality, occurs if $\bar{A}$ is replaced by $X(f)$, $\bar{B}$ is replaced by $Y(f)$, and the dot product is replaced by

$$\int_{-\infty}^{\infty} X(f)\,Y^{\star}(f)\,df\,, \tag{E.2}$$

where " $\star$ " denotes a complex conjugate (both $X(f)$ and $Y(f)$ may be complex functions). Then the inequality analogous to (E.1) is

$$\left|\int_{-\infty}^{\infty} X(f)\,Y^{\star}(f)df\right|^2 \le \int_{-\infty}^{\infty} |X(f)|^2\,df \int_{-\infty}^{\infty} |Y(f)|^2\,df \tag{E.3}$$

with equality if, and only if, $X(f) = kY^{\star}(f)$, where k is a constant. (E.3) is known as Schwarz's inequality.

To maximize (4.45), let $X(f) = 1$ and $Y^{\star}(f) = P(\omega)H_t(\omega)H_r(-\omega)$, then (E.3) becomes

$$\left| \int_{-\infty}^{\infty} P(\omega) H_t(\omega) H_r(-\omega)\, d\omega \right|^2 \le \int_{-\infty}^{\infty} |1|^2\, d\omega \int_{-\infty}^{\infty} |P(\omega) H_t(\omega) H_r(-\omega)|^2\, d\omega \,. \qquad \text{(E.4)}$$

Substituting (E.4) into the numerator of (4.45) yields

$$SNR \le \frac{K_c \int_{-\infty}^{\infty} |1|^2\, d\omega \int_{-\infty}^{\infty} |P(\omega)|^2 |H_t(\omega)|^2 |H_r(-\omega)|^2\, d\omega}{\sum_{k=2}^{K} R_k \int_{-\infty}^{\infty} |P(\omega)|^2 |H_t(\omega)|^2 |H_r(-\omega)|^2\, d\omega}, \qquad \text{(E.5)}$$

where $K_c = 1/\pi$. Assuming $H_r(f)$ and $H_t(f)$ are zero for frequencies outside the interval [-B, B], it can be shown that

$$SNR \le \frac{4B}{\sum_{k=2}^{K} R_k}. \qquad \text{(E.6)}$$